Spheroidisation of Steel Designed for Nanostructured Bainite

Danyi Luo

Cambridge University

2012

Preface

This dissertation is submitted for the degree of Master of Philosophy in Physics (Material Science) at the University of Cambridge. The work described was carried out under the supervision of Professor H. K. D. H. Bhadeshia in the Department of Material Science and Metallurgy, University of Cambridge, between April 2011 and March 2012.

Except where acknowledgement and suitable references are made to previous work, this work is, to the best of my knowledge, original. Neither this, nor any substantially similar dissertation has been submitted for any degree, diploma or qualification at any other university or institution. This dissertation does not exceed 15,000 words in length.

Some of this work will be presented in publications in the future.

Danyi Luo

May 2011

Acknowledgements

First of all I would like to sincerely thank my supervisor, Professor H. K. D. H. Bhadeshia, for his constant guidance and encouragement on my research work, it is always enjoyable working with him.

I am grateful to all the people in the Phase Transformations Group for the happy memories we shared and for their support with various sections of my work. Especially Yanpei, Steve Ooi, Hanzheng Huang and Mathew, who gave me so much help with the use of MTDATA and the experimental devices. I also want to express my great thanks to Professor Yin for his constructive suggestions and expansions whenever I was having any confusion or detailed questions about my project.

At last, I would like to take this opportunity to express my gratitude to my family and Hao Chen for their reassurance and love as always.

Abstract

Superbainitic steel forming at temperatures as low as 200 °C or less possesses extreme strength combined with ductility and extraordinary resistance to fatigue, which represents a significant engineering achievement. The steel can be manufactured in bulky quantities and be made large in all directions, without the need for deformation or rapid processing.

The nanostructured bainite may be suitable for bearing applications over the traditional alloys which are used mostly in the quenched and tempered condition. However, one essential attribute of the structure is that its hardness is extremely high (up to 700 HV) in its transformed state and it is important to machine the steel in a softened state, which can be done by spheroidisation. Although a spheroidisation heat treatment can be completed in many ways, to do this effectively without incurring large costs it is necessary to use the concept of a “divorced eutectoid transformation” (DET). In this, the steel is annealed at a high temperature where only austenite and cementite exist, and then cooled slowly to allow eutectoid decomposition, but not into lamellar pearlite, rather into a mixture of spheroidised cementite in austenite. The exploration of this method in the context of the superbainite is the major aim of this thesis.

To complete this work systematically requires the development of a mathematical model so that any heat treatments can be optimised for specific chemical compositions. The proper amount of carbon was determined by MTDATA and added to the original superbainitic steel to produce two hypereutectoid steels. A variety of spheriodisation processes for the two steels were investigated and comprehensive microstructural examination and hardness measurements were carried out. The changes in microstructure and hardness of these alloys after isothermal heat treatments intended to produce the bainite have also been studied.

The experimental results showed that, by adopting an appropriate heat treatment condition, both steels can be successfully spheroidised. The existence of proeutectoid cementite was found to promote spheriodisation process. Finally an optimal spheroidisation heat treatment was proposed as the conclusion of the study.

Contents

Chapter 1
Introduction

SAE 52100 is a traditional high-chromium bearing-steel that is used widely in the manufacture of mechanical parts, such as ball bearings, rollers and rings. In the final application, the steel has to be very hard (>700 HV) but during manufacture it is necessary to soften it in order to reduce costs during forming and machining [1].

The structure of hot rolled SAE 52100 steel usually consists of lamellar pearlite, often with proeutectoid cementite at the prior austenite grain boundaries, Fig.1a [1]. As a result, this has a hardness in excess of 300 HV [2] and a low ductility which makes it difficult to process into the shapes required, and does not give good machinability. The microstructure needs to be spheroidised in order to make the alloy more amenable to large scale manufacture, Fig.1b [3]; spheroidisation involves the thermally induced break up of pearlite lamellae into spherical particles of cementite in a ferrite matrix, a process akin to coarsening in the sense that it involves a reduction in the total interfacial area per unit volume [4, 5].

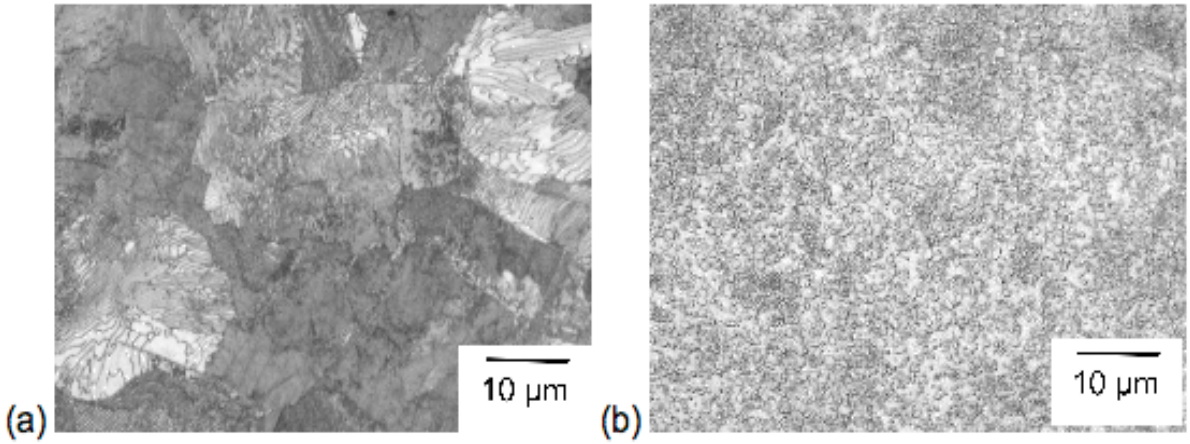

Figure 1: (a) Microstructure of 52100 steel as supplied by the manufacturer, in a hot-rolled condition. (b) The microstructure after spheroidisation. Micrographs courtesy of W. Trojahn [1].

Such a heat treatment is theoretically possible using many time and temperature combinations. In general, both isothermal and continuous annealing can take a long period of time to complete,

normally between 10 to 16 h because the driving force for spheroidisation is rather small [5]. This is inefficient from an industrial point of view so an alternative, fast spheroidisation method has been widely studied. The method actually involves phase transformation during the evolution of cementite as austenite is cooled. The aim is to prevent the development of a common transformation front between austenite and ferrite+cemenite, a scenario that leads to the lamellar pearlite which is not desired in the present context. Instead, a *divorced* eutectoid transformation (DET) is stimulated [6], in which spheroidal particles of proeutectoid cementite present within the austenite, simply grow and absorb the excess carbon as the austenite transforms into ferrite. As a consequence, the time required to generate the final structure of only spheroidal cementite in ferrite is dramatically reduced.

Referring to the principle of the divorced eutectoid, the process requires the existence of proeutectoid cementite particles within the austenite, prior to the decomposition of the latter below the eutectoid temperature. Superbainite, however, is designed to be fully austenitic at normal austenitisation temperatures, and hence is not amenable to spheroidisation via the divorced eutectoid route. The purpose of the work presented in this thesis was to alter the composition of the superbainite such that proeutectoid cementite particles can exist, and to see whether divorced pearlite is obtained along with the accompanying softening. This is important because superbainite is now being proposed for bearing applications.

Chapter 2
Literature Review

This section includes a review of relevant literature on spheroidisation and isothermal treatment. The discussion involves a historical understanding of spheroidisation and isothermal treatment, case studies, factors that influence the process and the bainitic microstructure.

2.1 Spheroidisation

Spheroidising annealing is a heat treatment that is used to achieve a microstructure with a mixture of spheroidised cementite surrounded by ferrite, which can be achieved through a "divorced eutectoid transformation". It is driven by the reduction in the interface energy per unit volume. The primary objective is to reduce hardness to enable fabrication prior to the final hardening. It has been reported [2] that spheroidisation reduced the hardness of the steel supplied to a bearing manufacturer to about 230HV.

Hewitt argued that spheroidal carbides included in the microstructure with ferrite allow good machinability of bearing steels [5]. Gupta and Sen found that the type and quantity of alloying elements influence the microstructure resulting in a wide range of properties [7]. Alloying elements can be classified as those that do not easily form carbides in steel such as Ni, Si, Co, Al, Cu and N, and others that do, such as Cr, Mn, Mo, W, V, Ti, Zr and Nb. The normal compositions of carbon/chromium bearing steel, for example, are illustrated in Table 2.1 below. Mechanical properties such as reduction of strength and increase in ductility are achieved by spheroidisation. For 52100 steel, the yield and ultimate tensile strengths in this condition are 455 and 635 MPa respectively, with an elongation of 36% [8]. However, full spheroidisation, which is preferred for optimum machinability, requires long and expensive heat treatment cycles [5].

Table 2.1

Typical compositions of high-carbon bearing and spring steels [5]

Grade	Type	Composition (wt%)				
		C	Si	Mn	Cr	Mo
BS 970-534A99	Carbon/chromium bearing steel	1.0	0.25	0.4	1.4	-
DIN 100CrMo7.3	Carbon/chromium molybdenum bearing steel	1.0	0.25	0.35	1.9	0.3
BS 970-070A78	Carbon spring steel	0.8	0.25	0.7	-	-
BS 970-060A96	Carbon spring steel	0.95	0.25	0.6	-	-

2.2 The spheroidisation process

Spheroidisation is conventionally achieved by long-time annealing at temperatures depending on the type of steel and desired mechanical properties. Heron [9] described spheroidisation accomplished by heating a high carbon chromium steel (1 C, 1.4 Cr wt%) to a temperature within the austenite and cemnetite phase field, holding it at that temperature for the complete solution of pearlite, and then cooling at a controlled rate so that the austenite can transform into ferrite and spheroidal cementite (Fig. 2.1). The time of heating up to austenising temperature was not found to have influence on the final structure; on the other hand, an undesirable structure containing pearlite and/or very fine spheroids can result from rapid rate of cooling from the austenitising temperature. The austenitising temperature, transformation temperature and time influence the size and uniformity of spheroids. With a high austenitising temperature or a long soak at a lower temperature, more carbides dissolve into austenite, resulting in less nuclei available for precipitation of the carbides at the transformaion temperature. This condition tends to produce larger spheroids. However, too high an austenitising temperature can be detrimental as the available time to finish the transformation under normal cycle conditions is so short that some pearlite will be produced. Similarly, when the austenitising temperature is too low and/or the soaking time is too short, some of the primary lamellar pearlite remains (not dissolved), which results in an unsatisfactory microstructure (Fig. 2.1b).

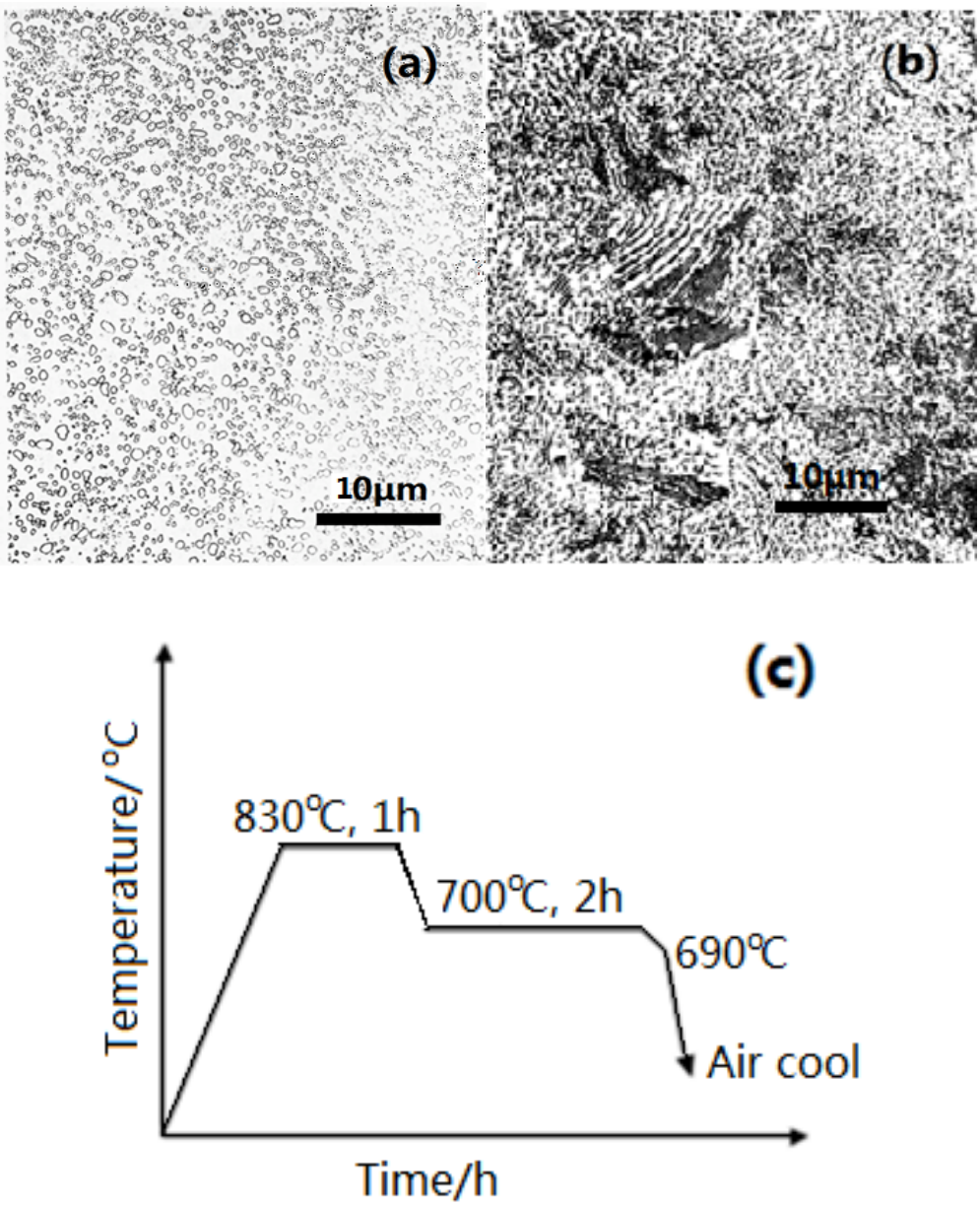

Figure 2.1: (a) Fully spheroidised microstructure; (b) primary pearlite; (c) spheroidising process curve [9].

The spheroidisation of carbides is achieved by prolonged heat treatment processes with controlled temperatures and cooling rates. According to Hewitt, close control of processes within tight ranges of temperatures and cooling rates produces satisfactory results for machinability following the spheroidising treatment, for a microstructure which contains fully spheroidised carbides in a ferritic matrix [5]. In other words, reasonably large cementite particles with a size in the range 0.5-3 μm and a small number density lead to less wear on the tools for machining [1]. The spacing of cementite particles is estimated to be 0.5-4 μm [10] and the ferrite grain size is about 15-25 μm [11]. It also should achieve a hardness of around 230 HV in this condition [2], which will

help to obtain a machined surface with lower roughness [2].

However, a lack of control can result in a non-spheroidised microstructure. A eutectoid pearlite is the two-phase lamellar structure observed in steels used for spheroidisation. Austenitisation of high-carbon steel followed by subsequent cooling below the eutectoid temperature or isothermal treatment (Fig. 2.2) transforms the austenite into lamellar pearlite which then spheroidises.

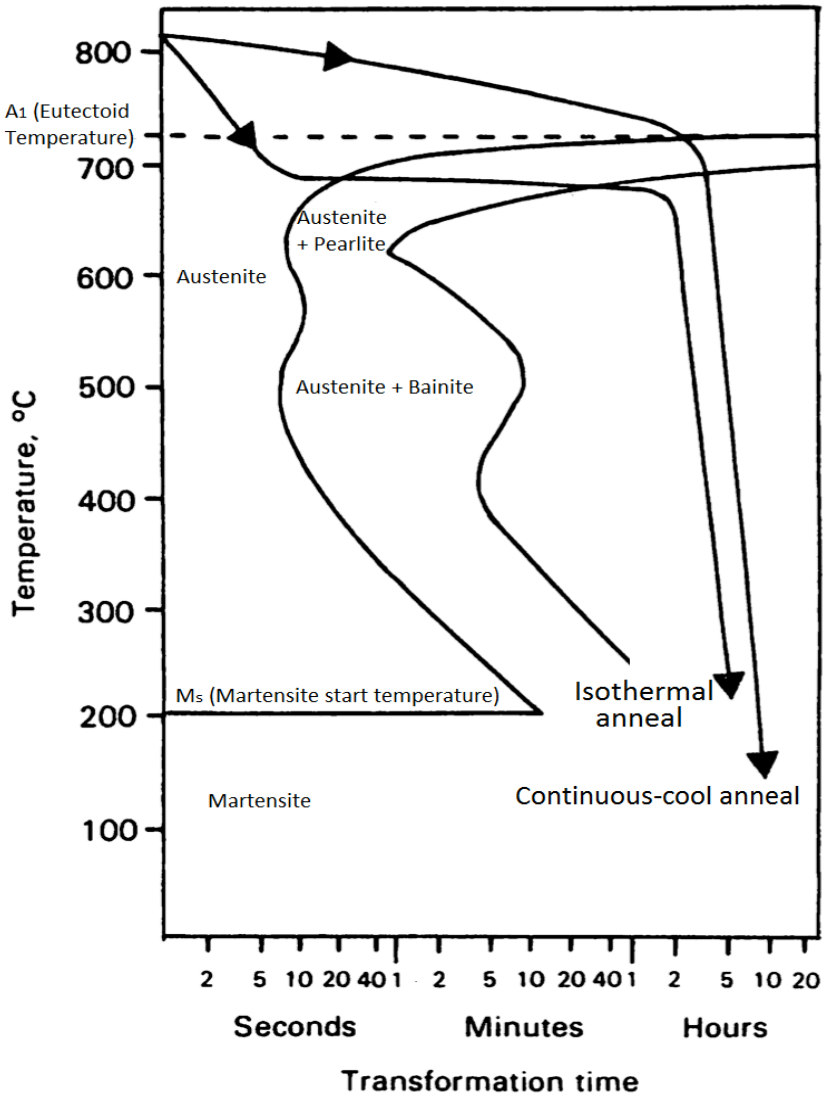

Figure 2.2: Typical process curves for continuous-cool and isothermal spheroidise-annealing treatments on the time-temperature-transformation diagram for 534A99 bearing steel that is listed in Table 1 [5].

Hewitt [5] has proposed two classical processes for the soft-annealing of the 52100 type steels: continuously cool and isothermal annealing (Fig. 2.3). The spheroidising occurs between 680 ˚C and

730 ˚C. Cooling is carried out at less than 25 ˚C h^{-1} from 830 ˚C to 750 ˚C and at less than 10˚C h^{-1} between 750 ˚C and 690 ˚C for the former method; quenching the hot-rolled material to temperatures below 620 ˚C followed by air cooling before spheroidisation could necessarily accelerate this treatment [12]. Rapid cooling to a temperature less than that at which austenite starts to form (700 ˚C) is carried out for isothermal spheroidal annealing and held at this temperature for more than two hours [5]. One aim of continuous annealing is to avoid the formation of lamellar pearlite [1], and this treatment has been proved to be more suitable for hypereutectoid steels since it reduces the proeutectoid cementite layers at the prior austenite grain boundaries into spheres [13].

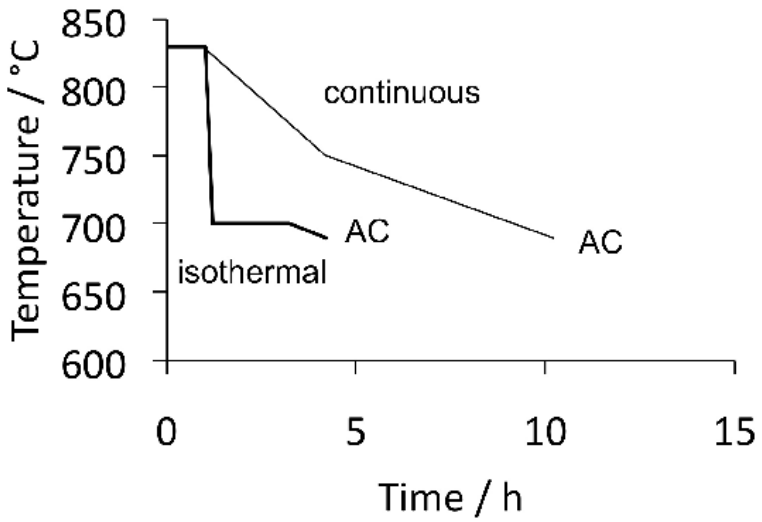

Figure 2.3: The two common process cycles for spheroidisation heat treatment of hot-rolled 52100 steel. Air cooling (AC) is adopted at the final stages of the process. Data from [5] and curve from [1].

It is well established [14] that spheroidisation of steels with pearlite changes cementite lamellae into spherical particles, with a speed that depends on the temperature and the cementite-ferrite interfacial energy per unit area. The total area of the interface per unit of volume is minimised through spheroidisation, assuming that the interfacial energy is isotropic. Spheroidisation occurs at a faster rate if the initial microstructure is fine.

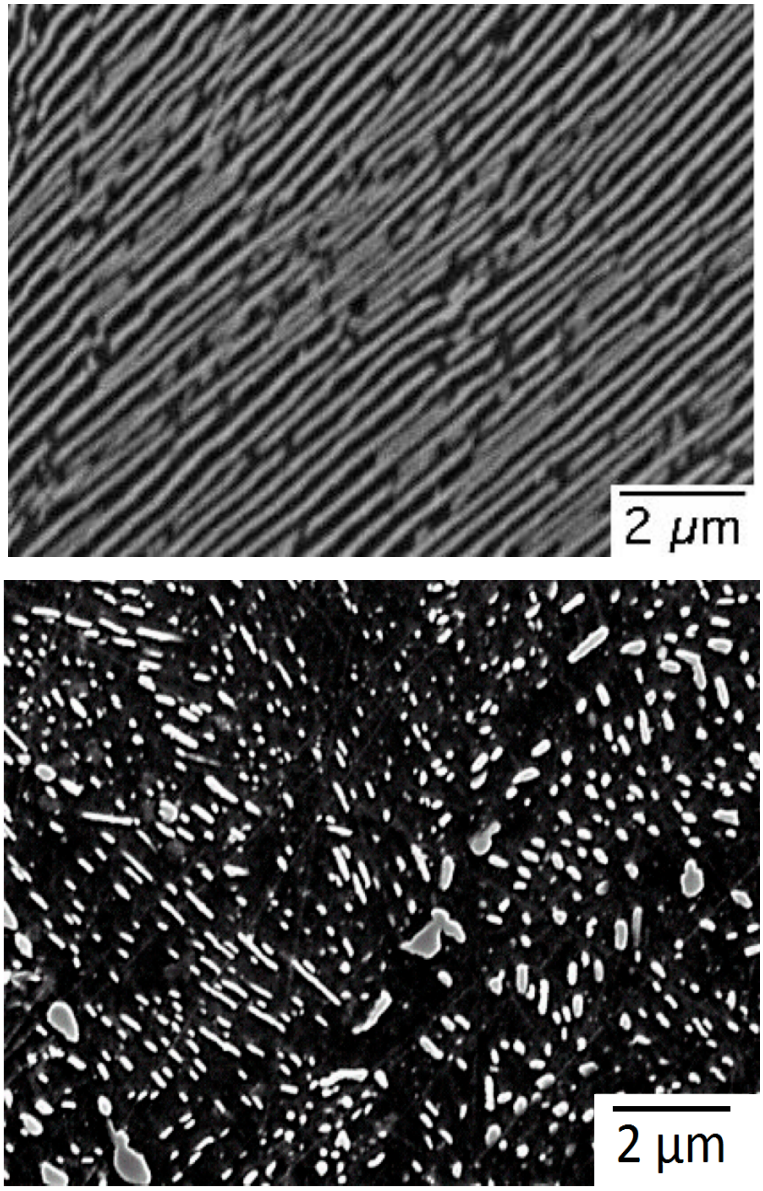

Figure 2.4: (a) Pearlite with 0.23 μm inerlamellar spacing. (b) Microstructure after spheroidisation for 1.5 h at 750 °C [14].

2.3 Case studies

Lyashenko [4] investigated the spheroidisation process of 52100 type bearing steel in order to shorten the annealing time. It was found that spheroidisation depends mainly on the annealing temperature, holding time, cooling rate in the temperature range from 800 to 650 ˚C and the initial microstructure. The results indicated that the process could be significantly accelerated by beginning with rapidly cooled raw material. The spheroidisation mechanism in general can be hastened by using a fine initial structure. However, the desired structure and hardness can only be achieved after long

holding times (Fig. 2.5). The following simple annealing treatment was found to reduce the hardness of the steel to a sufficiently low level: isothermal annealing at 780-750 ˚C for 3 h followed by slow cooling to 650 ˚C at 30 ˚C h^{-1}, then air cooling to room temperature.

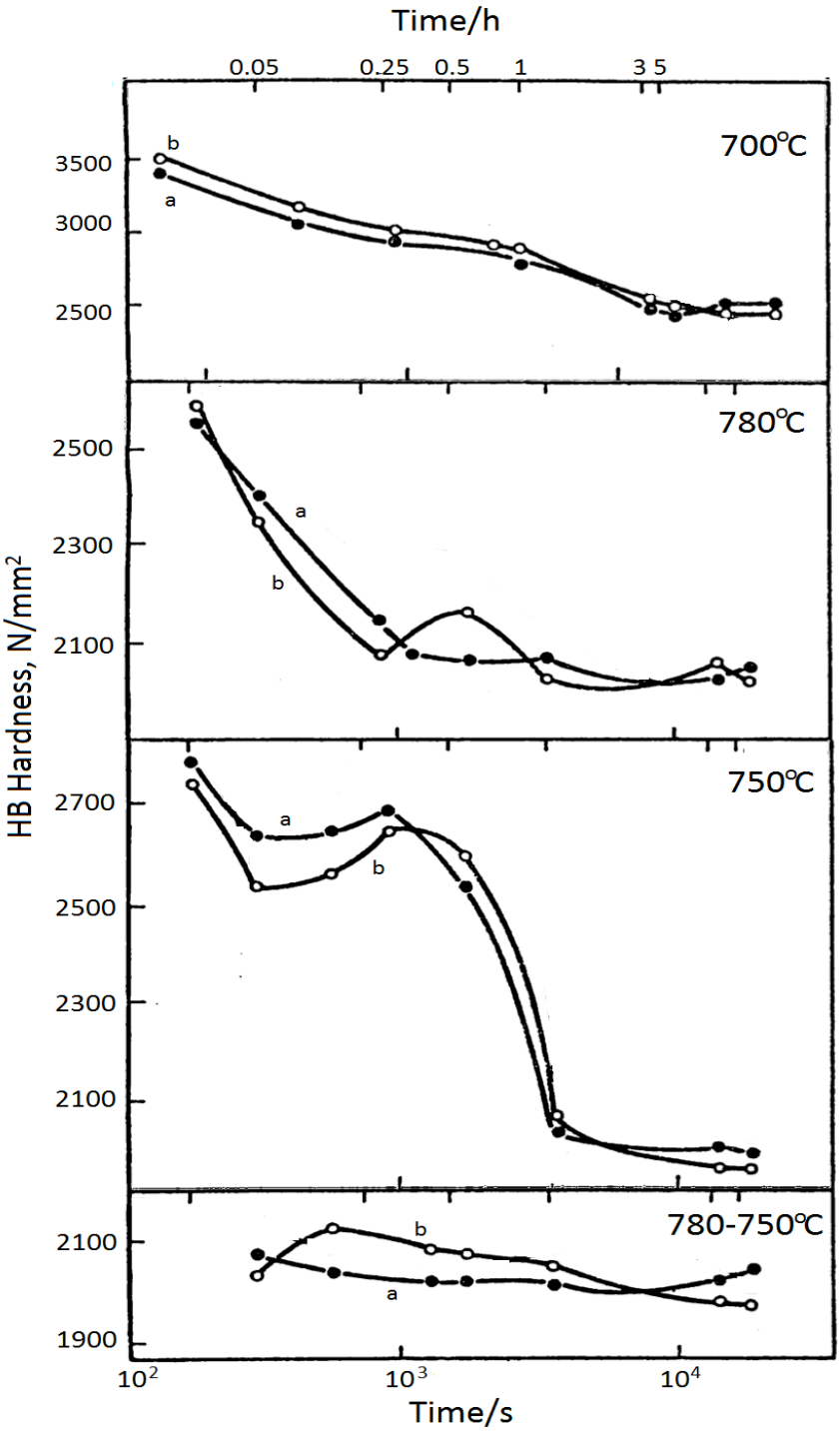

Figure 2.5: Influence of isothermal holding time at 700 °C, 780 °C, 750 °C, and 780 °C to 750 °C on hardness of 52100 type steel having structure of (a) lamellar pearlite, and (b) fine lamellar pearlite before heat treatment [4]. For isothermal annealing at 700 ˚C, owing to the relatively low diffusion mobility of carbon and chromium at this relatively low temperature, the spheroidisation and softening took place slowly. Further holding at this temperature had little effect on reduction of hardness. However, at 750 to 780 ˚C, significant reduction was achieved. The anomalous increase in hardness resulted from the appearance of areas of lamellar pearlite in steel [4].

Spheroidising annealing time is reduced to 3 min and rapid annealing of 52100 steel, with induction heating, results in highly dispersed structure of divorced pearlite. Dolzhenikov showed that austenitisation at 850 ˚C for 30 s followed by the isothermal transformation at 650 ˚C for 17 min could result in the same machinability properties as those from conventional spheroidising annealing for 10 h; a hardness of 235 HV can be achieved in this condition [15].

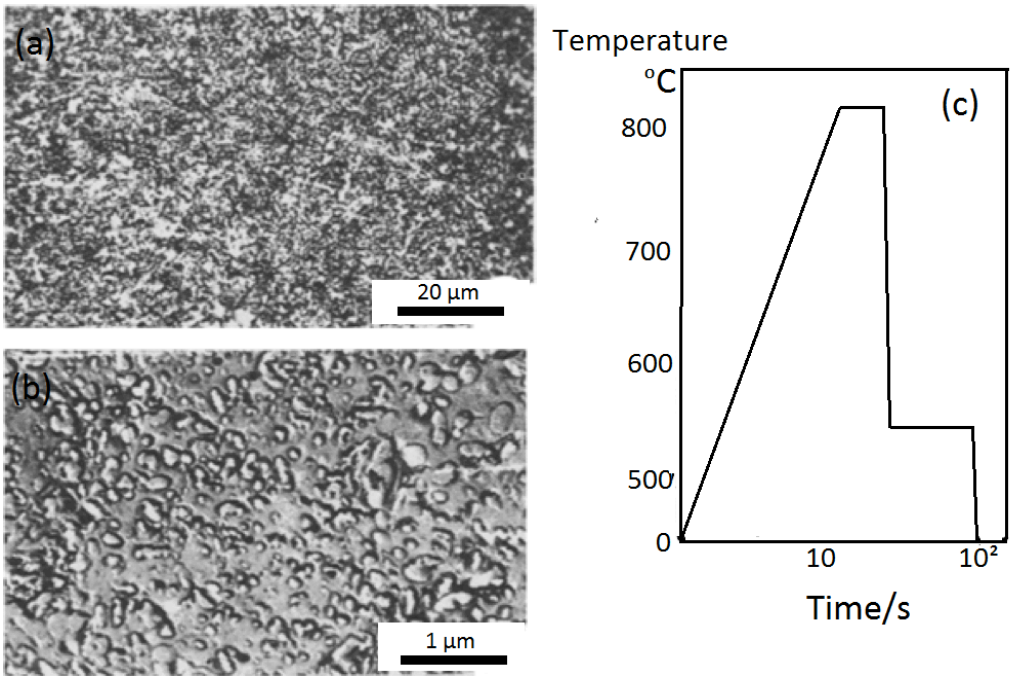

Figure 2.6: (a), (b) Microstructure after isothermal annealing at 550 ˚C for 2 min; (c) temperature graph for annealing the steel with chemical composition of Fe-1.0C-0.26Mn-0.3Si-1.37Cr-0.012S-0.019P (wt%) [15].

The spheroidisation can be accomplished using two heat treatments, namely, subcritical and intercritical. The former comprises heating in the region below the eutectoid temperature and holding for a prolonged duration in order to spheroidise the pearlitic structure. It is applied mainly for hypoeutectoid steels. Intercritical annealing involves heating steels in the region with partial austenite and cementite ($\gamma + \theta$) followed by slow cooling and is more suited to hypereutectoid steels because it reduces the proeutectoid cementite layers at the prior austenite grain boundaries into spheres. The latter is often used in the bearing industry [16]. Finer microstructures in general tend to spheroidise more rapidly during subcritical annealing [4].

O'Brien and Hosford presented spheroidisation experiments on a medium-carbon steel using both methods [13]. The results reveal that the subcritical spheroidisation occurs faster than the

intercritical treatment. It results in shorter times for good formability in medium–carbon AISI 4037 steel with chemical composition of Fe-0.37C-0.80Mn-0.22Si-0.25Mo (wt%). A higher hardness could be achieved by subcritical annealing due to finer dispersion of carbides. They also suggested that it should be used instead of the inctercritical process (Fig. 2.9 and Fig. 2.10).

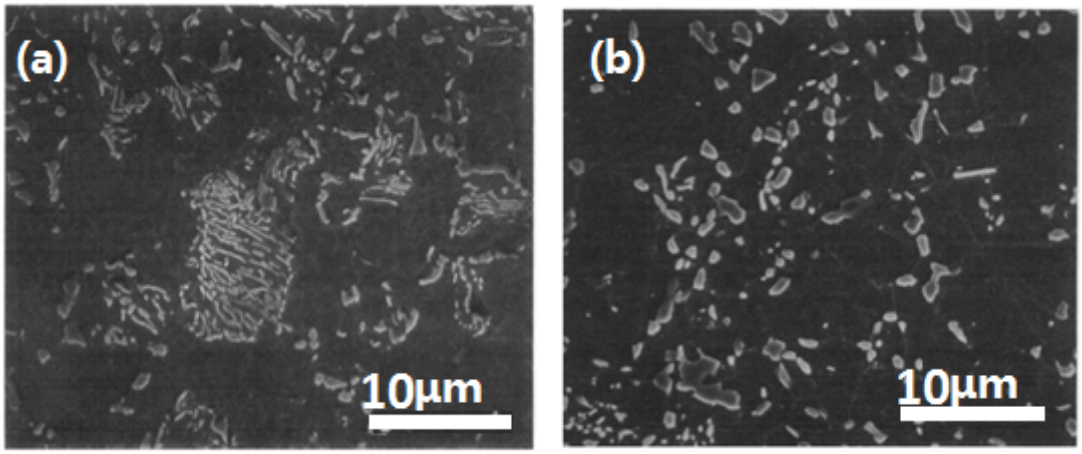

Figure 2.9: Microstructures attained for intercritical annealing [13]. (a) 4h - unspheroidised coarse particles; (b) 12 h - nearly complete spheroidisation.

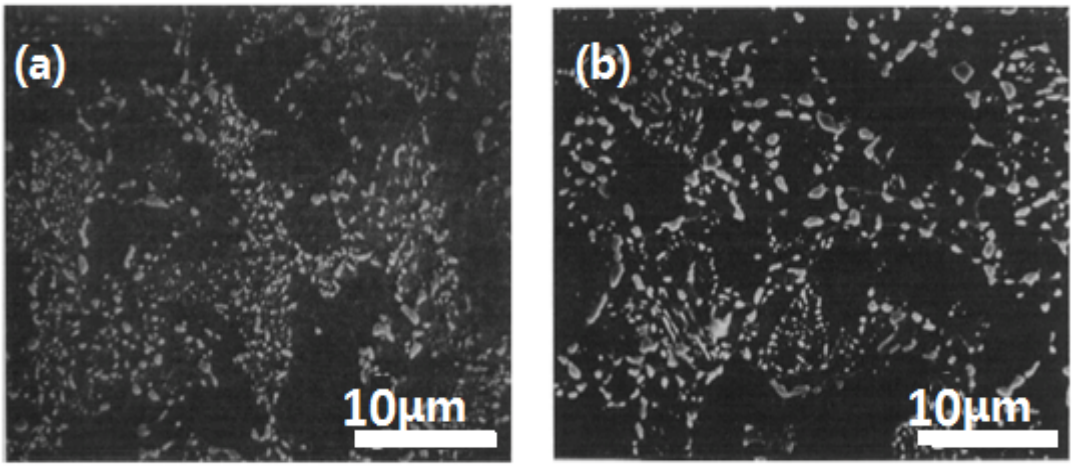

Figure 2.10: Microstructures attained for subcritical annealing [13]. (a) 4h – the spheroidisation is nearly complete, though the carbide size is very small; (b) 12 h – the carbide size has increased but is still much finer than in Fig. 2.9b.

2.4 Factors influencing spheroidising

The refinement of lamellar pearlite accelerates speroidisation by breaking-up the thin cementite lamellae [4]. The steel sometimes is first heat-treated to produce the finest possible pearlite so that faster dissolution of the carbides can be achieved during the spheroidisation process [5]. It has been

shown for 52100 steels that fine, lamellar pearlite dissolves more rapidly than spheroidised cementite [17].

The pearlite transformation in austenite proceeds by nucleation and growth. Hagel confirmed that a part of the free-energy change during pearlite formation is spent to provide energy during ferrite-cementite formation and the remaining on diffusion [18]. Cobalt increases the free-energy change, while it is reduced by manganese and molybdenum, for example, in eutectoid steels [18].

The initial structure influences the mechanism of the spheroidisation transformation. The carbon and chromium concentrations also have strong effects on the kinetics of spheroidisation. A relatively high carbon concentration can speed up the spheroidisation process by providing a greater density of nucleation sites on which the carbides form and grow. This is one of the reasons for the success in soft-annealing bearing steels with relative ease. Chromium, on the other hand, helps in reducing the interlamellar spacing of pearlite which is often the starting microstructure for a spheroidising anneal [19, 20]. Kim [21] concluded that in hypereutectoid high carbon chromium bearing steels, an increase of silicon content shrinks the austenite phase field, which leads to an increase in the volume fraction of cementite at the annealing temperature, resulting in incomplete spheroidisation. Brown and Krauss [22] studied the effect of phosphorus content on spheriodisation and characterised the carbide distribution in the 52100 bearing steel. Two 52100 steels with different phosphorus contents, 0.023 and 0.009 wt% respectively, were investigated. It was found that a large amount of phosphorous retards the spheroidisation but the mechanism has not been defined. Small concentrations (0.03 wt%) of hafnium are known to disrupt the lamellar pearlite and promote the formation of divorced pearlite [23].

Oyama confirmed early research that a divorced eutectoid transformation including a well-defined soaking time and temperature for austenitising followed by air-cooling could be utilised to obtain fully spheroidised structures in steels [24]. This treatment eliminates the need for isothermal processing to develop fully spheroidised structure. Both temperature and time of soaking dictate the kinetics of carbide dissolution. The influence of an increase in austenitisation temperature (Fig. 2.11) is similar to that of a protracted soaking time. If the time of austenitisation is too long, the likelihood of DET taking place is reduced. The microstructure just after the completion of austenitisation consists of austenite with a non-uniform carbon concentration and fine cementite particles is optimum for forming a DET structure [24].

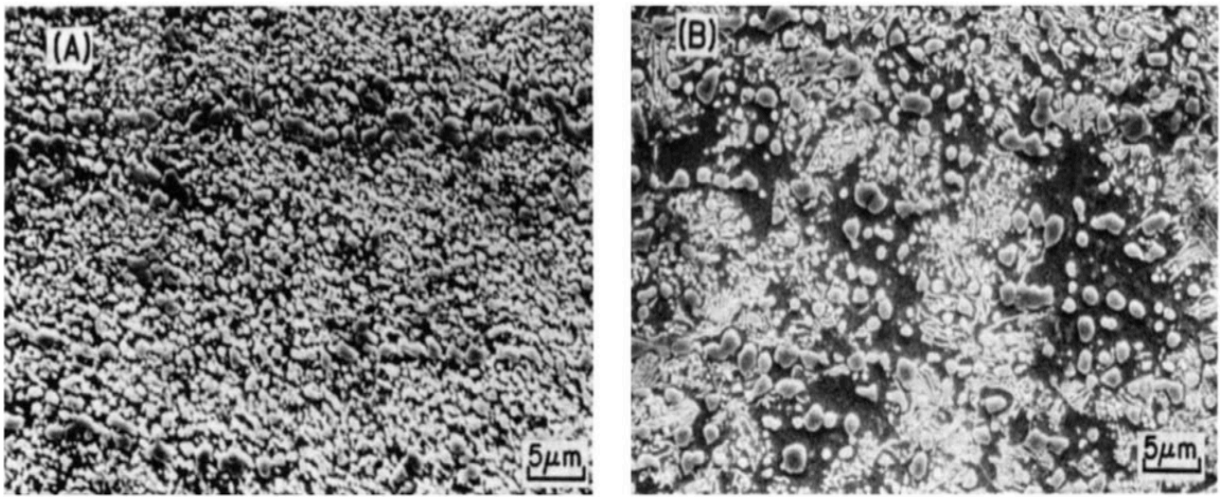

Figure 2.11: Scanning electron micrographs of 1.5 wt% C steels demonstrating the effects of soaking time on the DET [24]. (a) A spheroidised microstructure obtained after soaked at 800 °C for 1 h. (b) A mostly pearlitic microstructure obtained after soaking at 800 °C for 48 h. A uniform carbon concentration is achieved in the austenite with large cementite particles; pearlite formation is promoted in this condition due to the coarsening of the proeutectoid carbides with the accompanying loss of nucleation sites for carbide precipitation from austenite.

2.5 Details about Divorced Eutectoid

As stated previously, for hypereutectoid steel, the annealing time for softening the steel can be greatly shortened from 10-16 h to 18 min by exploiting the DET reaction. In this process, ferrite grows into the austenite matrix while the pre-existing small cementite particles present in the austenite absorb the partitioned carbon and become bigger. Therefore, the final DET product is a ferrite matrix filled with spheroidised cementite particles [6].

The concept of divorced pearlite has been discussed since 1920 [25], that the carbide particles existing in hypereutectoid steels give rise to the formation of globular particles of cementite during the transformation of austenite. Verhoeven and Gibson [26] proposed the detailed mechanism as illustrated schematically in Fig. 2.12. Lamellar pearlite can only form under conditions that permit the nucleation of cementite and the establishment of cooperative growth with ferrite during continuous cooling [1], so it forms at a slightly lower temperature than the divorced pearlite [27].

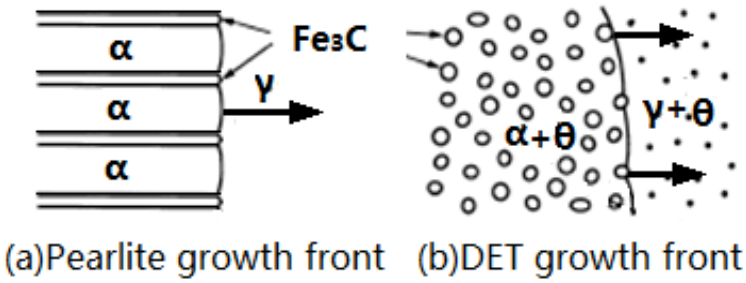

Figure 2.12: Two modes of eutectoid transfomation [26]. (a) For lamellar pearlite transformation, the product phases grow as coupled pairs at the growth front and produce the pearlite structure. (b) The divorced eutectoid transformation occurs if the austenite contains cementite particles with a space of a few micrometres or less. It produces a mixture of austenite and spheroidised cementite (γ+θ) at the ferrite/austenite (α/γ) boundary.

In the DET mode (Fig. 2.13), the eutectoid transformation product appears as the dark phase (ferrite) filled with some white small dots (cementite particles), embedded in the martensite matrix. The product is formed at the cusped shaped austenite/ferrite growth front that proceeds into the austenite. Thus the spheroidised carbides grow onto the pre-existing cementite particles (arrowed in Fig. 2.13b) and form from the austenite matrix at the growth front directly.

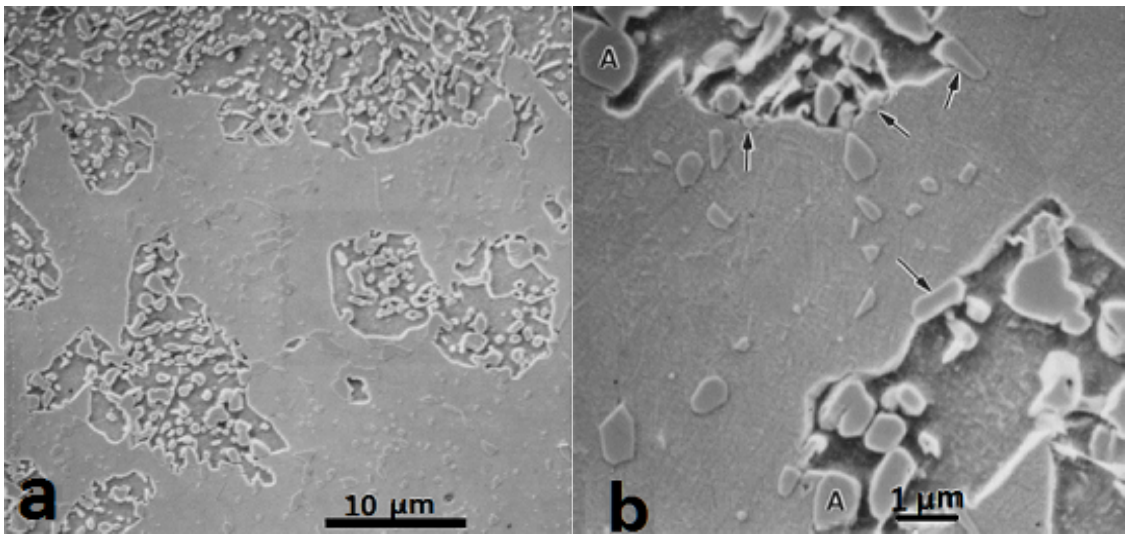

Figure 2.13: Scanning electron micrographs showing the reaction front of the DET in the sample with a starting microstructure of fine array of cementite particles homogeneously distributed in the austenite [26]. (a) The growth front for the DET in type 1 sample. (b) A higher magnification micrograph of Fig. 2.13a. The large particles labelled A could sometimes affect the boundary shape.

Verhoeven [26] also stated that the velocity of the divorced eutectoid transformation is faster because of the small diffusion distance of a few micrometers and the growth of particles occurs along

the austenite/ ferrite transformation front. By setting up a simple model during the transformation when a mixture of austenite and cementite is cooled below the eutectoid temperature, they predicted a plot that compares the velocity of DET against the experimental data for the velocity of lamellar pearlite [28], which is illustrated on Fig. 2.14.

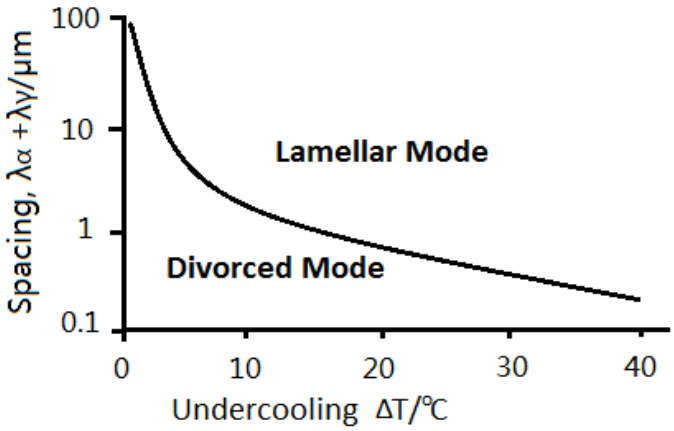

Figure 2.14: Effects of undercooling temperature ΔT and spacing between cemnetite bands on eutectoid transformation product [26]. Finer spacing between undissovled cementite particles and lower austenitisation temperatures favour the formation of divorced pearlite [6].

2.6 Bainitic microstructure

Bainite is a nonlamellar aggregate of plate-shaped ferrite with intervening carbides formed by the decomposition of austenite at a temperature in between that of martensite and fine pearlite temperature [29]. This is displayed clearly in the time-temperature-transformation (TTT) diagram in Fig. 2.15. Each ferrite plate is roughly 10 μm long and 0.2 μm thick. As shown in the figure, there are two kinds of bainite, which can be distinguished as upper bainite and lower bainite. Lower bainite forms at a lower temperature usually less than 350 °C [30], with carbon diffusing into both austenite and ferrite (Fig. 2.16), while upper bainitic-ferrite is free of precipitation and the carbides grow from the carbon-enriched residual austenite to decorate the boundaries of ferrite plates.

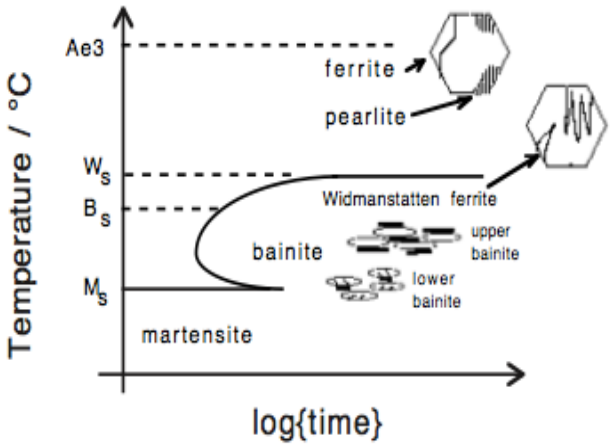

Figure 2.15: TTT diagram showing the different domains of transformation with schematic illustration of the microstructure of each phase [31].

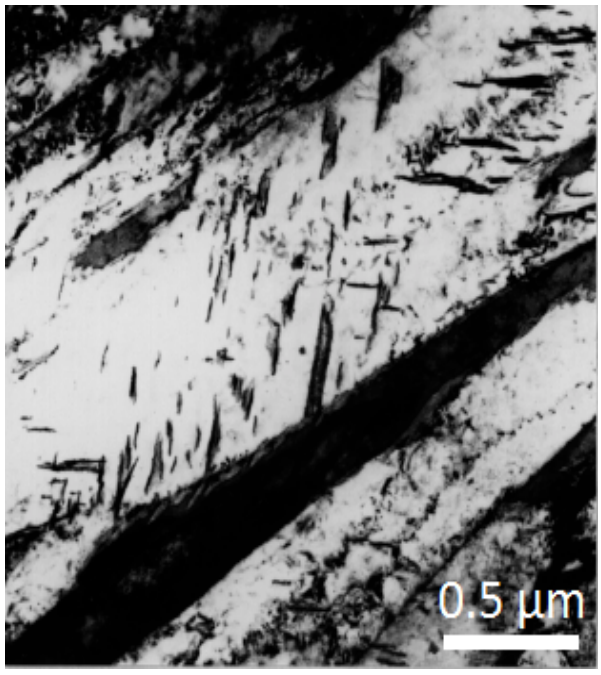

Figure 2.16: Transmission electron micrograph of lower bainite consisting of ferrite plates containing an array of fine carbide particles [31].

An extraordinary combination of toughness, ductility and strength can be obtained without the use of expensive alloying elements. This is one of the reasons why the bainitic microstructure is popular in recent industrial applications. Bainite and martensite are two well-known strong phases in steels which can greatly increase the strength. However, to ensure satisfactory values of both strength and toughness, martensite normally requires tempering after quenching, whereas bainite does not

[32]. Nevertheless, it is still time-consuming to produce steels with the bainitic structure [29].

Bhadeshia and Edmonds [33] found that bainite formation involves the repeated propagation of displacive sub-units that are supersaturated; the collection of parallel platelets is known as a ‘‘sheaf’’. The sheaf has a morphology that is platelike (Fig 2.17). The thickness of the subunit depends on transformation temperature, with a typical value of about 0.05 μm at 250 °C [31]. These subunits are found to be separated from each other by carbon-enriched retained austenite films [34].

It has been claimed [35] that the bainite transformation is similar with martensite, that involves a displacive transformation mechanism, rather than reconstructive, and is accompanied by a shape deformation. In this mechanism, although bainite growth is diffusionless, carbon must partition into the residual austenite shortly after growth is stopped. The rate of the bainite reaction needs to be considered in terms of distinct steps [35]. Carbide precipitation, for example, influences the kinetics mainly by removing carbon either from the supersaturated ferrite or from the residual austenite [35]. Some alloying elements such as Si and Al can suppress or delay carbide precipitation during the bainite reaction [31]. Bainitic reaction stifles after the austenite carbon reaches a certain value. A limited amount of bainitc ferrite therefore can form during isothermal transformation [13].

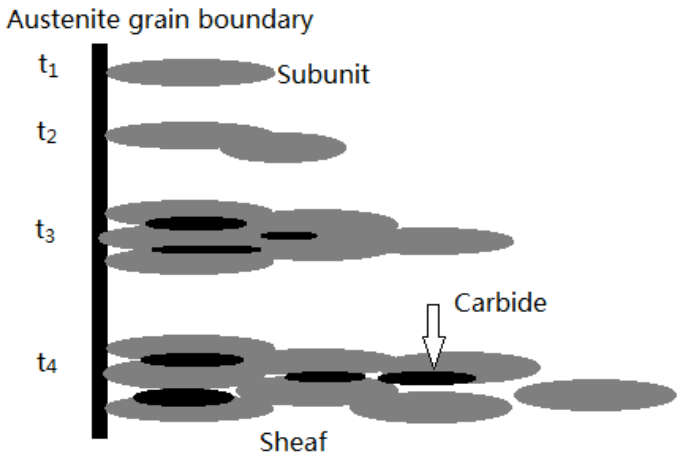

Figure 2.17: Schematic illustration of the evolution of a bainite sheaf as a function of time [35]. A sub-unit nucleates at an austenite grain boundary and grows at a certain rate. The new sub-units then nucleate at its tip and the sheaf structure is developed in this process [35].

2.7 Superbainite

Through isothermal heat treatment at low temperatures, normally ranging from 125 °C to 300 °C, a structure consisting of a mixture of extremely thin bainitic plates (20-40 nm) and a certain amount of stable carbon-enriched retained austenite (Fig. 2.18) has been obtained in relatively high-carbon steel containing Cr and Mo, known as superbainite [32, 36]. This kind of steel is exceedingly strong and easy to manufacture with affordable cost, and can be made in large chunks [37]. The bainite is the hardest ever achieved, approaching 700 HV [38].

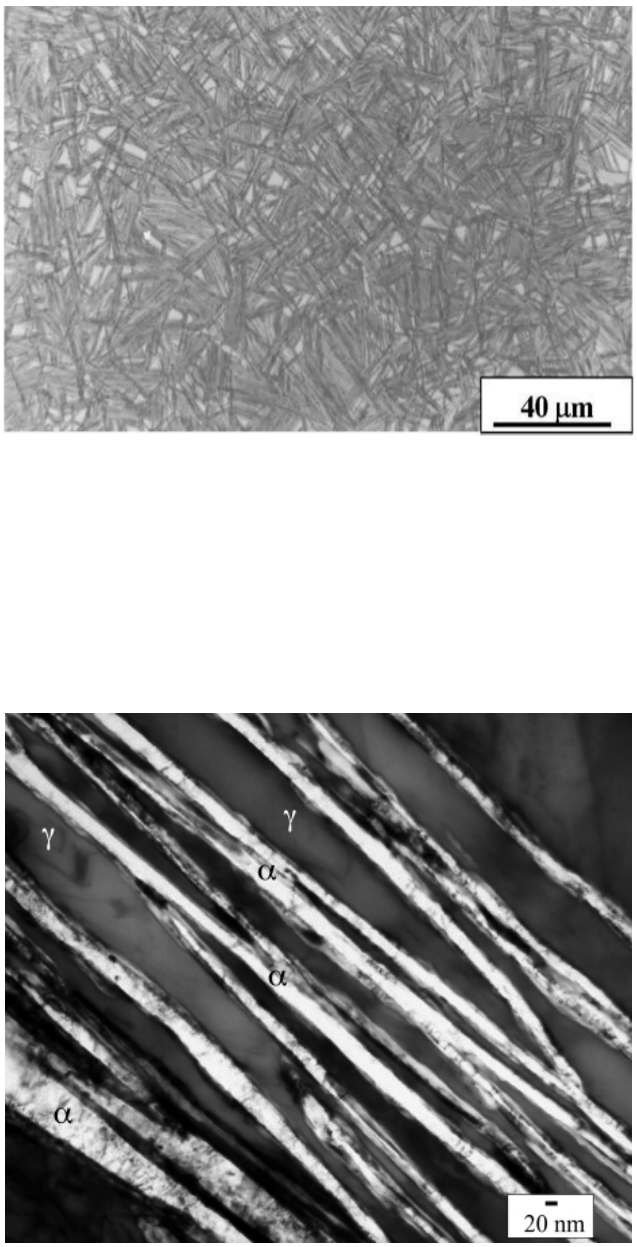

Figure 2.18: Optical and transmission electron micrograph of Fe-0.98C-1.46Si-1.89Mn-0.26Cr-0.09V wt% transformed at 200 °C for 5 days [38].

A prolonged holding time increases the total volume fraction of bainite and the yield strength values [39], while a decreased transformation temperature leads to thinner bainite plates [37]. Although the bainite transformation times can be reduced sharply by increasing the isothermal transformation temperature, the degree of hardening then decreases due to a coarsening of the structure. The highest level of hardness can be achieved by isothermally heat treatment of the superbainitic steel at 200 °C, while 250 °C facilitates faster transformation and greater ductility with a small reduction in strength [40].

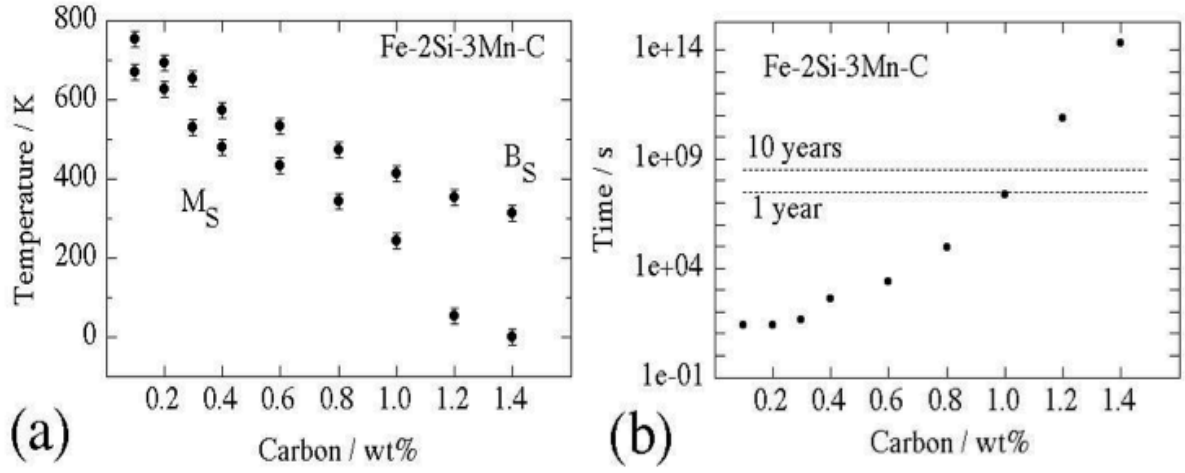

Figure 2.19: (a) The calculated transformation start temperatures in Fe-2Si-3Mn (wt%) steel as a function of carbon concentration. There is no lower limit to the bainite start temperature (B_s) in principle. (b) Time required to initiatie bainite at the bainite start temperature [37].

The alloy composition can also have a remarkable effect on the transformation. Carbon concentration tends to lower the temperature at which bainite can be induced to grow (Fig. 2.19) [37]. The superbainitic steel shown in Table 2.2 contains manganese, vanadium and chromium for hardenability. The large amount of silicon (up to 1.5 wt%) is to eliminate the precipitation of cementite from austenite during banite formation since silicon is insoluble in cementite [31]. Molybdenum is to prevent temper embrittlement due to phosphorus [36]. Aluminium and cobalt could increase the strength level but lower the strain hardening rates at the same time. Furthermore, the additions of aluminium and cobalt accelerate the transformation of austenite to ferrite resulting in a finer scale and higher phase fraction of bainitic ferrite [38]

Table 2.2

Chemical compositions of common superbainitic steel and SAE 52100 steel [6]

	C	Si	Mn	Mo	Cr	Cu	Al	Co	Nb	V wt%
Superbainite	0.83	1.9	2.28	0.24	1.44	0.12	0.044	1.55	0.023	0.11
SAE 52100	1.03	0.23	0.30	<0.01	1.28	0.10	-	-	-	-

2.8 Summary

The cold formability and machinability of steels are improved by an annealing treatment known as spheroidisation. The structure of coarse carbides in ferrite is developed by spheroidising, which can in principle be achieved by inducing a divorced eutectoid transformation, rather than the cooperative growth of ferrite and cementite in lamellar form from austensite. The divorced eutectoid can be regarded as an economical way of reaching the spherodised state. However, this requires the presence of an optimised distribution of proeutectoid cementite particles in the austenite, so that superbainite in its present form poses difficulties since it is fully austenite prior to transformation.

Chapter 3
Experimental Method

3.1 Material selection

Spheroidisation via the divorced eutectoid reaction has never before been investigated for a superbainitic alloy since it is normally almost fully austenitic at the usual austenitisation temperature. Furthermore, the applications that it is currently used for does not require a fully softened condition.

Previous work [41] has shown that because the superbainite has a much lower austenitisation temperature than conventional bearing steels, it necessitates 42 days of tempering at 708 °C to achieve a hardness of about 250 HV and cannot be softened below this value without extreme measures. Under equilibrium conditions, 52100 steels become fully austenitic at temperatures greater than 900 °C, but in practice, austenitisation at 1040 °C for 20 min will dissolve all the cementite [42], whereas superbainite is generally fully austenitic at 880 °C according to the phase diagram calculation presented in Fig. 3. Furthermore, spheroidisation treatments must begin with a martensitic or bainitic structure and then very long heat treatments are required to get to the hardness quoted above [1].

Mass/kg	Phase	Mass fraction of component within phase		
		Fe	C	Si
9.9362E+01	FCC_A1	0.9171500	0.0077496	0.0191219
2.0582E-01	FCC_A1	0.0042761	0.1504457	0.0000000
4.3172E-01	CEMENTITE	0.7686577	0.0672022	0.0000000

		Mn	Mo	Cr
9.9362E+01	FCC_A1	0.0227922	0.0018857	0.0139593
2.0582E-01	FCC_A1	0.0014235	0.2362395	0.0406111
4.3172E-01	CEMENTITE	0.0347803	0.0092920	0.1033418

		Cu	Al	Co
9.9362E+01	FCC_A1	0.0012077	0.0004428	0.0155597
2.0582E-01	FCC_A1	0.0000001	0.0000000	0.0001167
4.3172E-01	CEMENTITE	0.0000000	0.0000000	0.0090906

		Nb	V
9.9362E+01	FCC_A1	0.0000003	0.0001308
2.0582E-01	FCC_A1	0.1116019	0.4552854
4.3172E-01	CEMENTITE	0.0000039	0.0076315

(a)

Mass/kg	Phase	Mass fraction of component within phase		
		Fe	C	Si
9.9801E+01	FCC_A1	0.9164438	0.0080143	0.0190379
1.9899E-01	FCC_A1	0.0049425	0.1516134	0.0000000

		Mn	Mo	Cr
9.9801E+01	FCC_A1	0.0228426	0.0019734	0.0143427
1.9899E-01	FCC_A1	0.0014110	0.2163476	0.0431534

		Cu	Al	Co
9.9801E+01	FCC_A1	0.0012024	0.0004409	0.0155307
1.9899E-01	FCC_A1	0.0000001	0.0000000	0.0001257

		Nb	V
9.9801E+01	FCC_A1	0.0000004	0.0001710
1.9899E-01	FCC_A1	0.1153882	0.4670180

(b)

Figure 3: The calculated equilibrium compositions of austenite and cementite for the mean values in the steel described as ordinary superbainite (Table 2.2) at (a) 860 °C; (b) 880 °C. The cementite particles are all dissolved at 880 °C.

A divorced eutectoid route would in principle be faster, but it would be necessary to increase the carbon concentration of the superbainite to allow sufficient proeutectoid cementite to exist at the austenitisation temperature. It is this cementite that provides the sink for carbon when ferrite forms, and hence prevents the onset of lamellar pearlite. Samples of the original superbainite were remelted to add further carbon. They were then sent to TWI Ltd for chemical analysis (Table 3.1). The final carbon concentrations were aimed to be 0.9 wt% and 1 wt% as calculated using MTDATA below, but only 0.85 wt% C and 0.94 wt% C were obtained in practice.

Table 3.1
Chemical compositions of new steels (wt%)

	C	Si	Mn	P	S	Cr	Mo	Ni	Co	V
A	0.85	1.75	2.15	<0.01	0.003	1.39	0.24	0.03	1.42	0.1
B	0.94	1.78	2.20	<0.01	0.003	1.42	0.24	0.03	1.45	0.1

3.2 Experimental procedures

3.2.1 Simulations

Most experiments reported in this thesis were carried out using the Thermecmaster thermomechanical simulator; this is an instrument that can simultaneously record the temperature, time, load and radial strain. To monitor the specimen temperature, the sample should be centrally attached with a thermocouple by spot welding on its surface. The sample was induction heated in a high vacuum and cooled to the isothermal transformation temperature range using helium gas quenching. As specified by the system, the sample is machined into a cylinder with 8 mm in diameter and 12 mm in height along the rolling direction. The heating rate was 10 °C s^{-1} for all experiments.

Austenitisation temperature tests

The Thermec experiments were done by heating 0.85 wt% C steel to 840 °C and 900 °C and holding at each temperature for 20 min, followed by quenching to room temperature; for the 0.94 wt% C steel the corresponding temperatures were 840 °C, 870 °C and 970 °C. The exact amount of cementite that failed to dissolve during austenistisation depends also on the austenitisation time and

the starting microstructure [1]; 20 min is chosen here as an approximation to equilibrium since cementite kinetics can be quite rapid [1].

10 h spheroidisation anneal

The samples were heated to 840 °C and held for 1 h, cooled to 750 °C at 25 °C h^{-1}, and then further cooled to 690 °C at 10 °C h^{-1} followed by air-cooling from 680 °C. This standard heat treatment was introduced in Hewitt's work [5], as discussed in the section 2.2.

Direct quenching tests

For further observation on the time-evolution of microstructures during spheroidisation, samples from alloys A and B were quenched from 815 °C, 750 °C and 740 °C, respectively, during the 10 h spheroidisation annealing that mentioned above.

200 °C 10 days isothermal transformation process

In order to look at the consequence of the higher carbon concentrations on the superbainite itself, the new samples of 0.85 wt% C and 0.94 wt% C were first held at 840 °C for an hour in a tube furnace, then quickly transferred into an oven at 200 °C and held for 10 days followed by air-cooling. It is important to ensure that the cooling rate from 840 °C to 200 °C is fast enough to avoid the pearlite transformation. It is also essential to prevent the martensite formation, so when cooling from the tube furnace, the samples were kept enclosed in a quartz tube to keep the temperature. A thermocouple was attached on each sample to record the cooling rate.

10 h isothermal transformation process

To observe the isothermal transformation process in detail with some accurate recorded data, six more Thermec experiments were done. Both samples were austenitised at 840 °C for 1 h and then isothermally heat treated at 200 °C, 250 °C and 300 °C and held there for 10 h, followed by quenching to room temperature. The rate of cooling from 840 °C was 25 °C s^{-1}.

3.2.2 Microscopy

Optical, scanning and transmission electron microscopy were used to characterise microstructures. The specimens for optical and scanning electron microscopy were mounted and their cross sections were investigated. The surfaces were ground starting with 240-grit silicon carbide grinding paper and finishing with 2500-grit, then polished using diamond paste of 6 μm and

1 μm grade and etched in 3 vol. % nital solution or ferric chloride solution. The analysis was carried out on a JEOL 5800LV and a Camscan MX2600 scanning electron microscope. Transmission electron microscopy was done by using a JEOL 2000FX microscope operated at 200 kV. Samples were sliced into thin pieces and machined into 3 mm diameter discs. These were then ground down to 100 μm thickness using 1200 grit silicon paper, for electropolishing at 50 V using a twin-jet unit. The electropolishing solution contained 15% perchloric acid and 85% ethanol.

3.2.3 Hardness

To know how the heat treatments process affects the hardness of the steel, Vickers hardness measurements were taken with a microhardness tester with a diamond pyramidal indenter at a load of 10 kg. Hardness values were obtained as the mean of six readings.

Chapter 4
Results and Discussion

4.1 Phase diagram calculation

The main process of DET is to grow the spherical particles of proeutectoid cementite that exist in the austenite, by the absorption of carbon that is partitioned into the austenite as ferrite grows, rather than inducing a cooperative growth of cementite and ferrite at a common front to form lamellar pearlite [6]. So the key to achieve DET is to maintain an adequate quantity of dispersed and undissolved cementite particles within the austenite prior to its transformation. Hence, during the heating process, it is better to retain about 3-4 wt% of fine cementite within the austenite matrix at the austenitisation temperature [1].

MTDATA is a software that is based upon critically assessed thermodynamic data for simpler sub-systems, and use a very robust algorithm to access the equilibrium state. It predicts the phases forming at equilibrium in systems containing many components and phases [43]. In this work, MTDATA was used to determine the amount of carbon that should be added into the ordinary superbainite. The equilibrium calculation was performed for the steel in Fig. 4.1a, which is summarised in Table 4.1. The phases allowed to exist in the equilibrium calculation are ferrite, austenite and cementite. As can be seen, for 0.83 wt% C steel at a typical austenitisation temperature (840 °C), there three phases are stable: the first FCC_A1 is austenite since the main component is Fe, whereas the second FCC_A1 phase is actually NaCl-type carbide due to the small fractions of carbide forming elements Nb, V and Mo. In addition, as there is only a small amount of cementite (1.3 wt%) revealed at the temperature, whereas about 4 wt% is common for DET, an extra amount of carbon is required in the range of 0.07 wt% - 0.17 wt%. This is predicted in Fig. 4.1b where there is 3.9 wt% of cementite for 1 wt% C steel. Therefore, it was decided to make 0.95 and 1 wt% C alloys. The change of cementite with increasing carbon can be more clearly observed in Fig. 4.2 where the temperature is set to 840 °C.

Mass/kg	Phase	Mass fraction of component within phase			Mass/kg	Phase	Mass fraction of component within phase		
		Fe	C	Si			Fe	C	Si
9.8508E+01	FCC_A1	0.9184515	0.0072366	0.0192878	9.5941E+01	FCC_A1	0.9198396	0.0074349	0.0198039
2.0575E-01	FCC_A1	0.0035438	0.1491490	0.0000000	1.7449E-01	FCC_A1	0.0034314	0.1484471	0.0000000
1.2864E+00	CEMENTITE	0.7677173	0.0672015	0.0000000	3.8848E+00	CEMENTITE	0.7831374	0.0671303	0.0000000
		Mn	Mo	Cr			Mn	Mo	Cr
9.8508E+01	FCC_A1	0.0226793	0.0017851	0.0131794	9.5941E+01	FCC_A1	0.0223307	0.0016821	0.0113371
2.0575E-01	FCC_A1	0.0013993	0.2535127	0.0365837	1.7449E-01	FCC_A1	0.0014017	0.2486395	0.0322717
1.2864E+00	CEMENTITE	0.0354658	0.0093205	0.1043146	3.8848E+00	CEMENTITE	0.0353515	0.0090690	0.0892392
		Cu	Al	Co			Cu	Al	Co
9.8508E+01	FCC_A1	0.0012182	0.0004467	0.0156149	9.5941E+01	FCC_A1	0.0012508	0.0004586	0.0157683
2.0575E-01	FCC_A1	0.0000000	0.0000000	0.0001050	1.7449E-01	FCC_A1	0.0000000	0.0000000	0.0001114
1.2864E+00	CEMENTITE	0.0000000	0.0000000	0.0091660	3.8848E+00	CEMENTITE	0.0000000	0.0000000	0.0095647
		Nb	V				Nb	V	
9.8508E+01	FCC_A1	0.0000002	0.0001003	(a)	9.5941E+01	FCC_A1	0.0000002	0.0000937	(b)
2.0575E-01	FCC_A1	0.1116651	0.4440413		1.7449E-01	FCC_A1	0.1316086	0.4340884	
1.2864E+00	CEMENTITE	0.0000032	0.0068112		3.8848E+00	CEMENTITE	0.0000036	0.0065044	

Figure 4.1: The calculated equilibrium compositions of austenite and cementite at a typical austenitisation temperature of 840 °C. (a) For the mean values in the steel described as ordinary superbainite (Table 3.1). (b) For the same composition with (a) but higher carbon content (1 wt%).

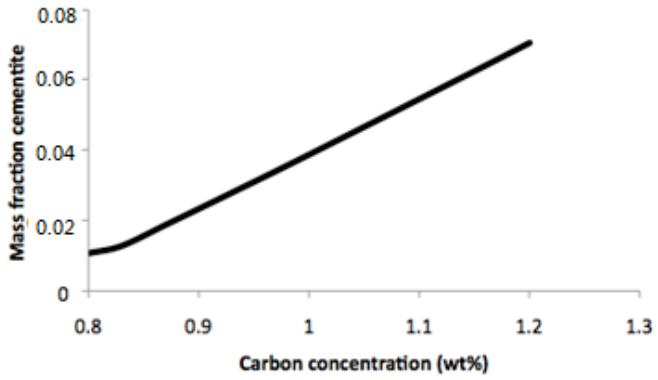

Figure 4.2: Phase fractions calculated using MTDATA for the mean values in the steel described as ordinary superbainite (Table 3.1), as a function of carbon concentration. The calculation permitted the existence of cementite and austenite only. The components included are Fe, C, Si, Mn, Mo, S, Ni, Cr, Cu, Al, Co, Nb and V.

Table 4.1

The calculated equilibrium compositions of austenite and cementite at a typical austenitisation temperature of 840 °C

	C	Si	Mn	Mo	Cr	Cu	Al	Co	Nb	V
Mean composition (wt%)	0.83	1.9	2.28	0.24	1.44	0.12	0.044	1.55	0.023	0.11
Austenite	0.75	1.93	2.26	0.23	1.32	0.12	0.045	1.56	0.023	0.10
Cementite	6.72	-	3.55	0.93	10.4	-	-	0.92	0.0003	0.68

To prove there is a right proportion of cementite particle; five thermomechanical stimulations were done using different austenitisation temperatures, which were selected using MTDATA software. The equipment used was the Thermecmastor Z simulator.

4. 2 Austenitisation temperature experiments

4.2.1 Relationship between austenitisation temperature and dilatometric strain

There is a change in density when martensite forms in steels, which can be measured using dilatometry. From the graph of the change in length as a function of temperature, some parameters such as martensite start temperature (M_s), upper critical temperature at which austenite begins to form on heating (Ac_1) and the temperature at which transformation of ferrite into austenite is completed upon heating in hypoeutectoid steel (Ac_3) can be extracted. In the plot, a deviation of the length due to thermal contraction is taken to imply the transformation. There are always uncertainties existed when detecting the expansion and so on as the dilatometer output contains noise. The offset method was therefore proposed to reduce the uncertainty to about ±12 °C, which is superior to the reported values of noise in published data. It also enables independent investigators to reach the same conclusions given identical data [44]. In this work, the technique is utilised for the dilatometric determination of Ac_1 and Ac_3 temperatures, with emphasis on noise in the experimental data.

Fig. 4.3 shows how the dilatational strain changes with increasing temperature for those two alloys with different austenitisation temperatures. According to the heating curves, Ac_1 and Ac_3 values were calculated using the offset method, given in the Table 4.2. This will be useful in determining heat treatments.

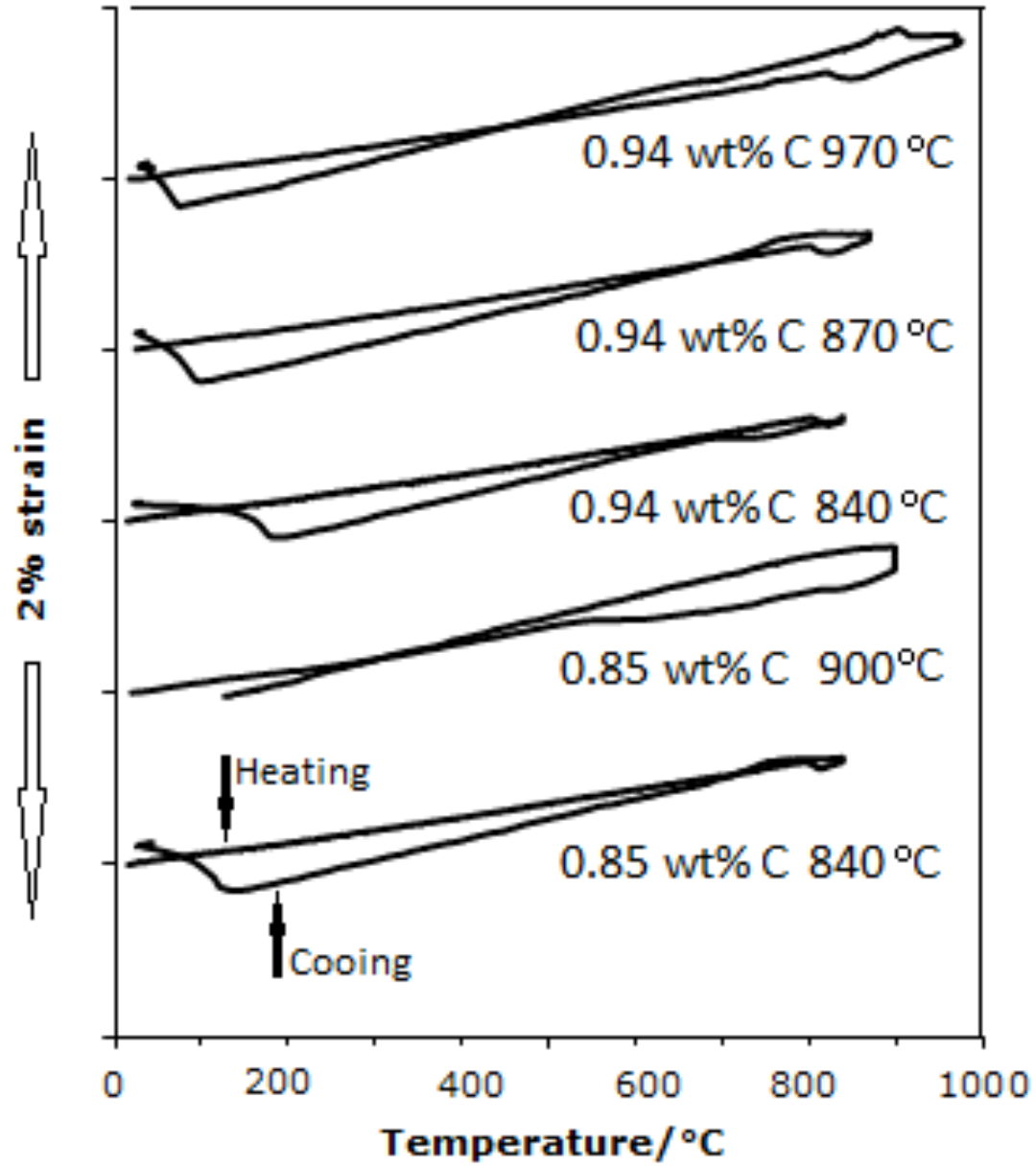

Figure 4.3: The relationship between temperature and strain. The heating cooling rate is 10 °C s^{-1} and the cooling rate is 25 °C s^{-1}.

Table 4.2

The Ac_1 and Ac_3 values calculated by using the offset method

Sample	Ac_1	Ac_3
0.85 wt% C	805°C	821°C
0.94 wt% C	817°C	840°C

4.2.2 Change of microstructure with austenitisation temperature and time

The austenitisation temperature and the time should affect the microstructures of the steel. The austenitising temperature also plays role in the divorced eutectoid transformation reaction [6] and when controlling the grain size, so that cracking can be avoided. Normally when austenite is cooled through the eutectoid temperature at a slow rate, it transforms into a lamellar pearlite [6], which is relatively hard to spheroidise. However, if the austenite contains a distribution of fine cementite particles, the transformation might occur by either the pearlite reaction or the DET reaction [25, 27, 45, 46]. The exact quantity of undissolved cementite is important at this stage, a value of around 4 wt% is known [1] desirable and an optimal combination of austenitisation temperature and time should be chosen to achieve this.

Figs. 4.4-4.9 indicate the microstructures of 0.83 wt% C, 0.85 wt% C and 0.94 wt% C steels after holding at different austenitisation temperatures for 20 min followed by quenching at a rate of 25 $^{\circ}C\ s^{-1}$. Fig. 4.4 shows the original steel without adding any carbon in (0.83 wt% C). It has been heated to 840 °C and held for 20 minutes, then quenched to room temperature. Apart from martensite and retained austenite, there is a number of undissolved cementite particles found, which is consistent with MTDATA result. The amount of cementite is slightly coarser than those obtained from 0.85 wt% C (Fig. 4.5) and 0.94 wt% C (Fig. 4.7) alloys. This is because there is a larger number of nucleation sites available for carbide precipitation from austenite in high carbon steels.

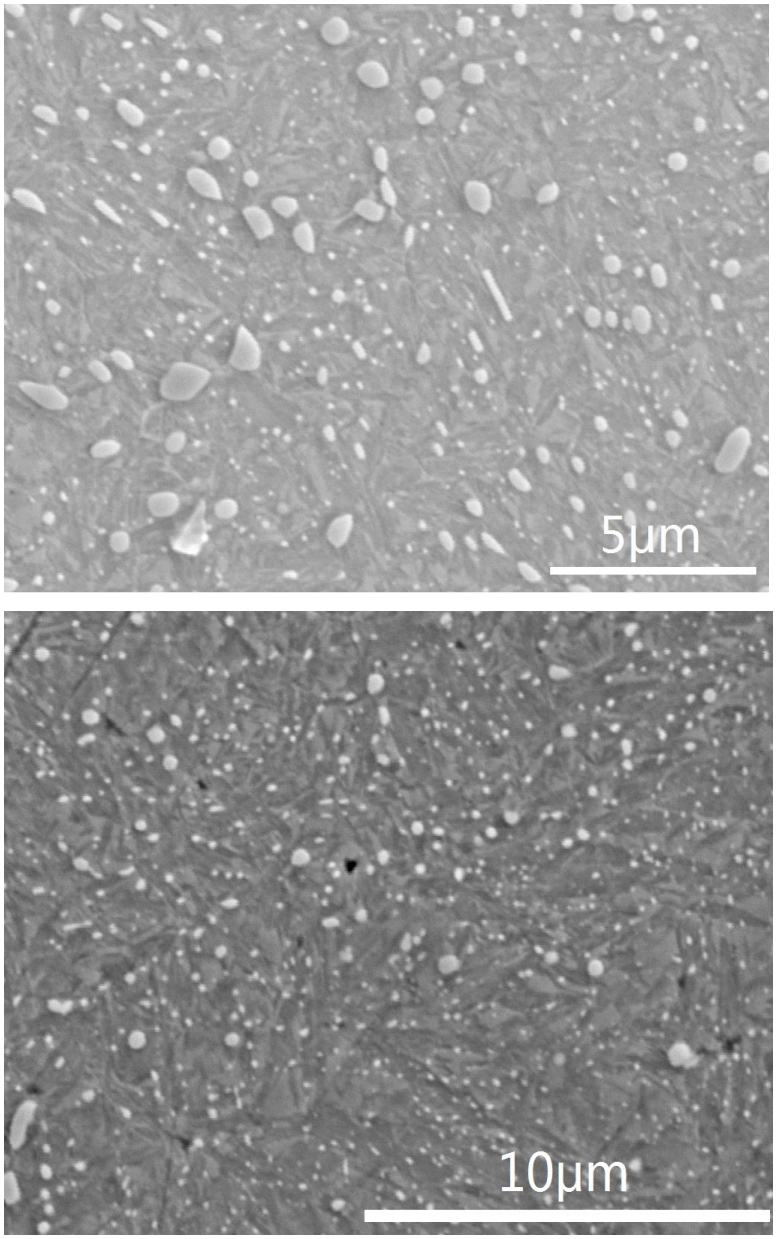

Figure 4.4: Scanning electron microstructure of 0.83 wt% C steel quenched from 840 °C.

Fig. 4.6 shows a typical martensitic structure with some of the untransformed austenite structure, plus a smaller quantity of cementite particles compare with those in Fig. 4.5. This is because the kinetic of cemnetite dissolution is faster at the greater austenitisation temperature, and the equilibrium fraction of cementite would be smaller. More carbon is dissolved in austenite at this temperature, making the austenite more stable. The thermodynamic stability of the cementite is enhanced by the enrichment of chromium so that the undissolved particles can be kept during the heat treatment [20, 47].

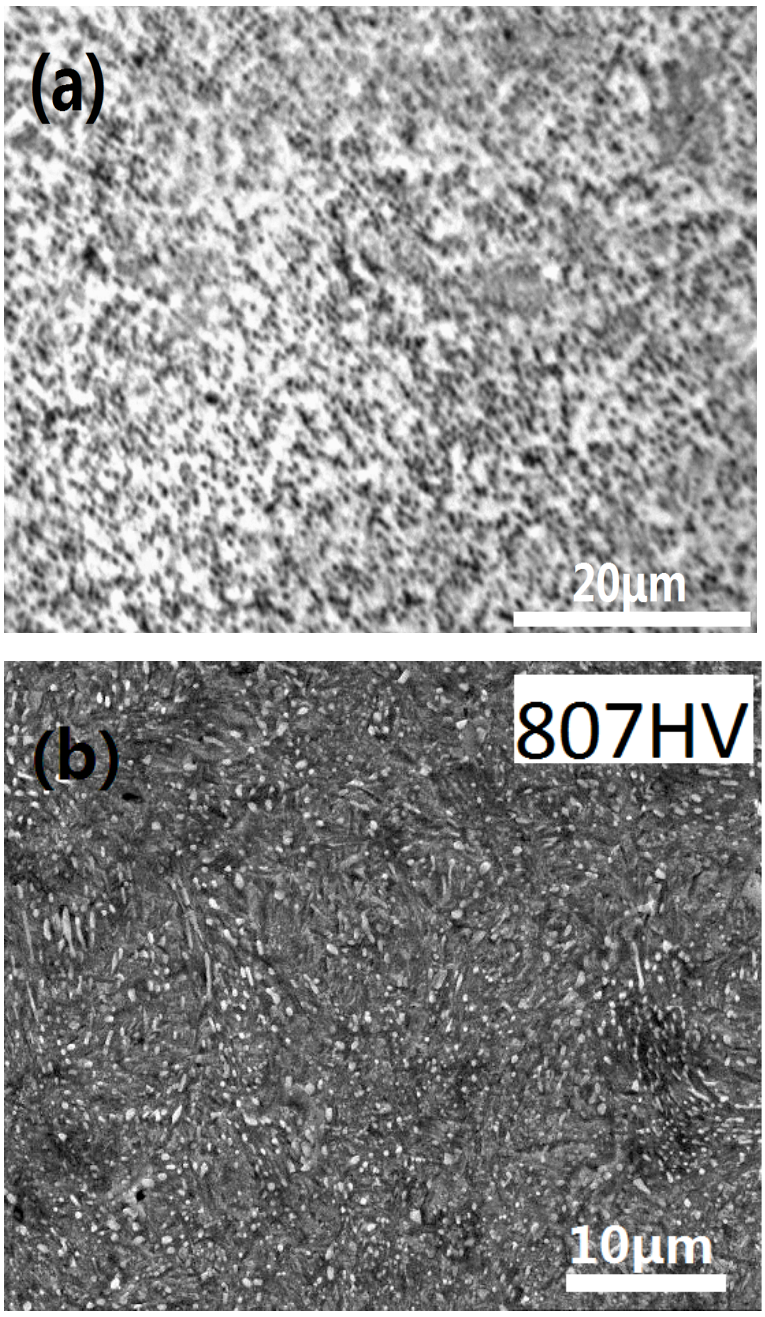

Figure 4.5: 0.85 wt% C steel quenched from 840 °C. (a) Optical microstructure, (b) scanning electron microstructure.

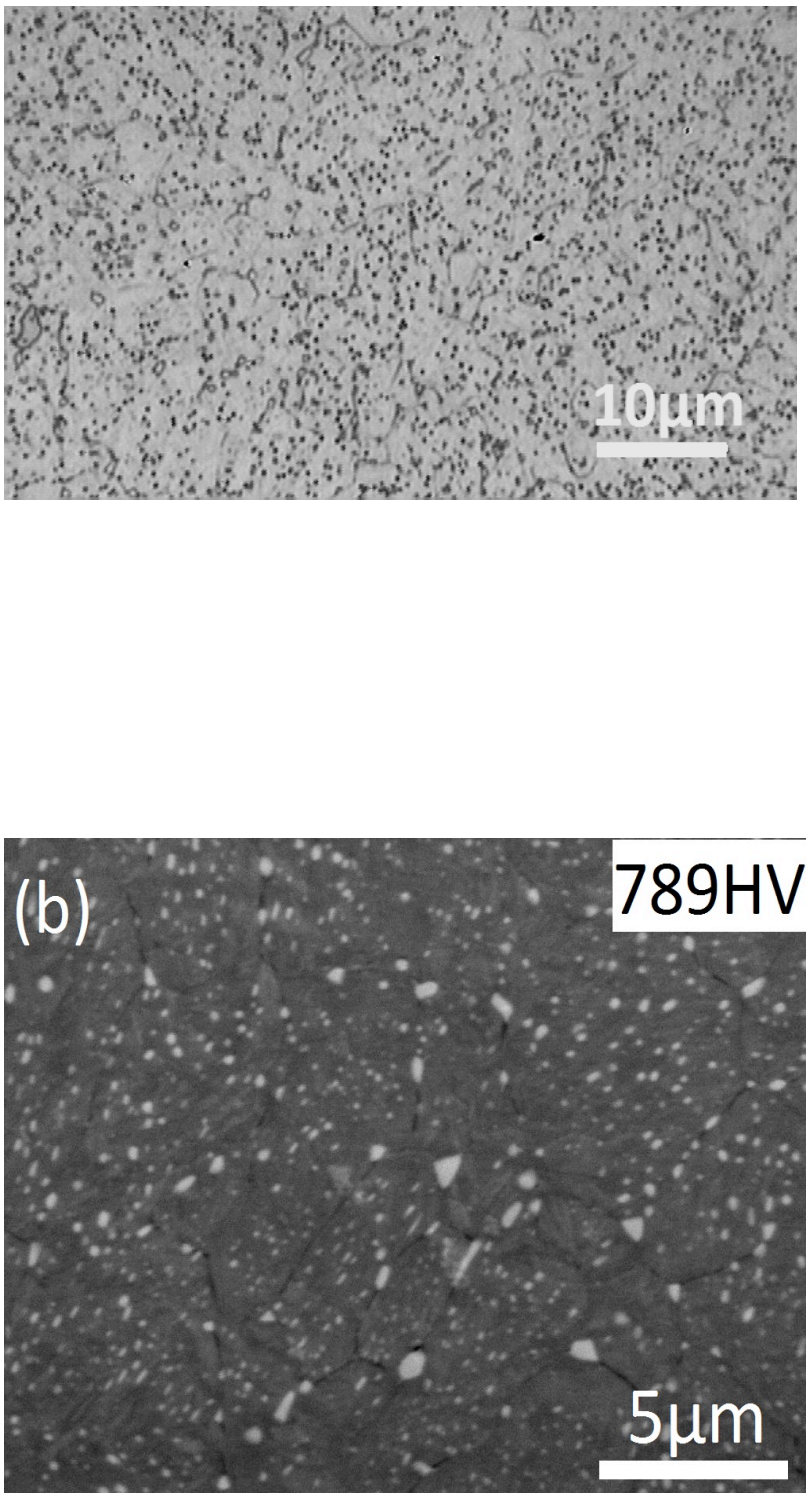

Figure 4.6: 0.85 wt% C steel quenched from 900 °C. (a) Optical microstructure, (b) scanning electron microstructure.

Figs. 4.7-4.9 show the 0.94 wt% C steel heating to 840 °C, 870 °C and 970 °C, respectively. The microstructure obtained from austenitising at 970 °C seems to show a notable change, where some abnormal growth of austenite can be observed. In addition to this, a few particles with significantly greater size are found. Both samples have numerous undissolved cementite particles when austenitised at 840 °C and 870 °C, in contrast to quenching from 900 °C and 970 °C where less and finer proeutectoid cementite is present due to the higher carbon concentration of the austenite.

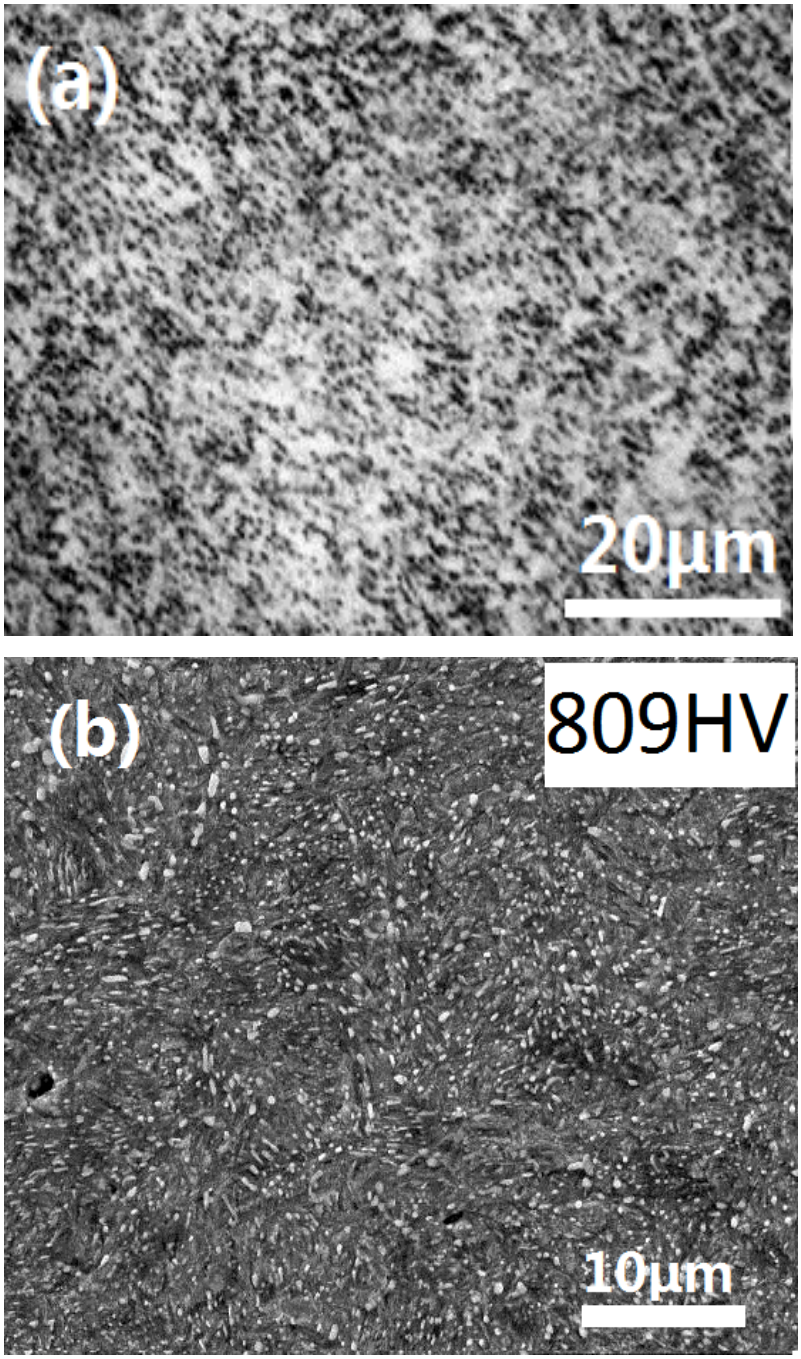

Figure 4.7: 0.94 wt% C steel quenched from 840 °C. (a) Optical microstructure, (b) scanning electron microstructure.

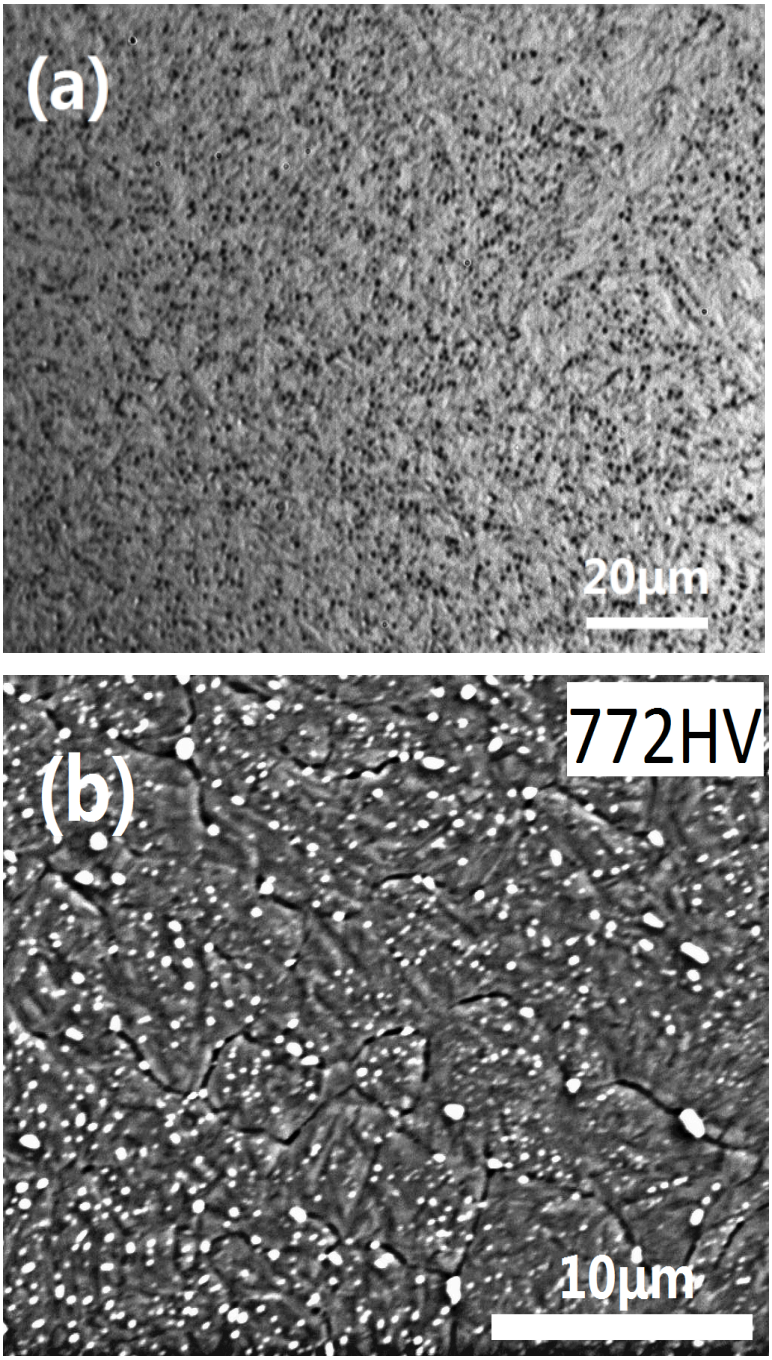

Figure 4.8: 0.94 wt% C steel quenched from 870 °C. (a) Optical microstructure, (b) scanning electron microstructure.

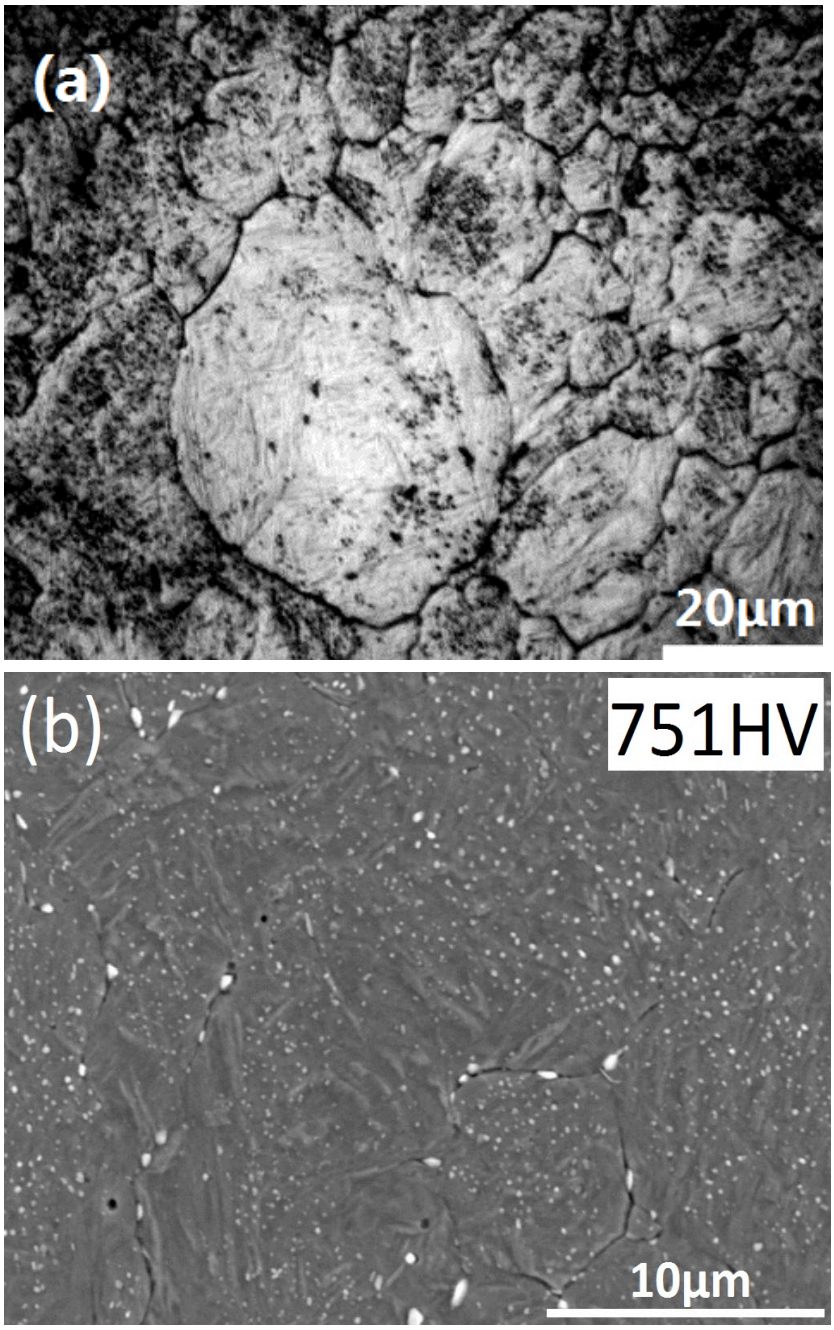

Figure 4.9: 0.94 wt% C steel quenched from 970 °C. (a) Optical microstructure, (b) scanning electron microstructure.

Figs. 4.10-4.11 illustrates the microstructures of 0.85 wt% C and 0.94 wt% C steels being austenitised at 840 ° C for 1 h followed by quenching to room temperature. The differences of size and amount of carbide between 0.85 wt% C and 0.94 wt% C samples are not obviously under this condition. However, the number of carbide particles is fewer for both steels compared to those with austenitisation time of 20 min.

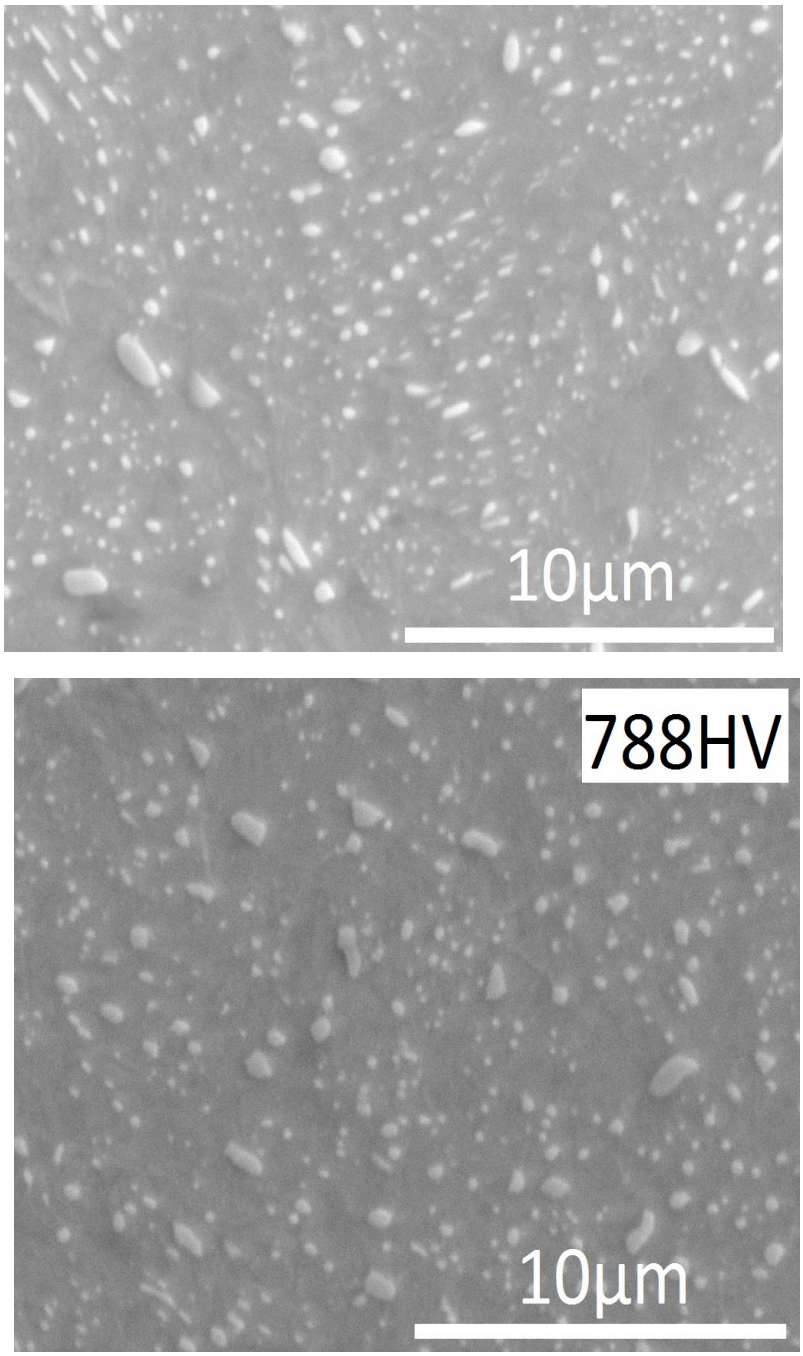

Figure 4.10: Scanning electron microstructure of 0.85 wt% C steel quenched from austenitisation at 840 °C for 1 h.

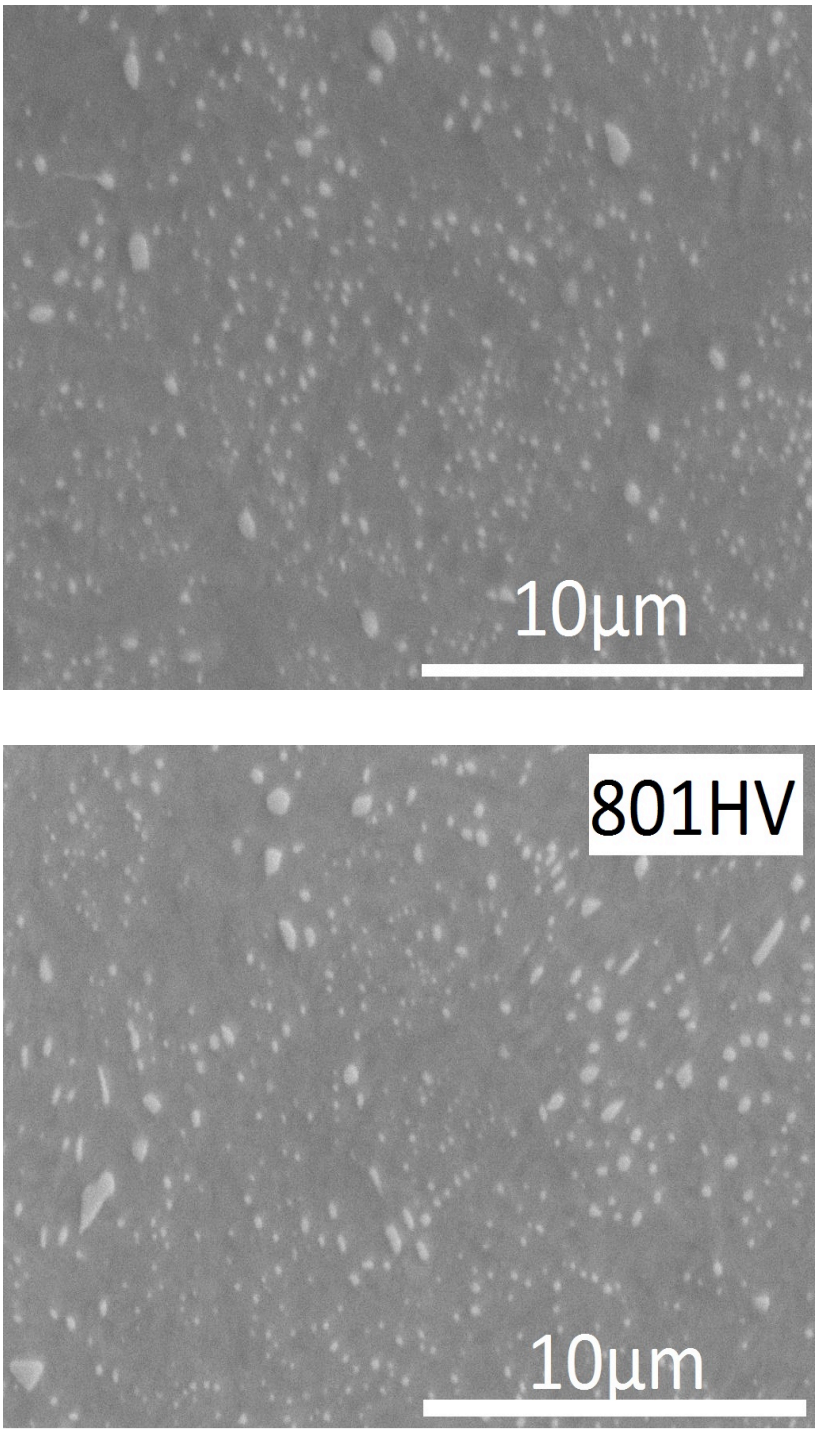

Figure 4.11: Scanning electron microstructure of 0.94 wt% C steel quenched from austenitisation at 840 °C for 1 h.

As expected, the combination of results agree reasonably well with previous studies [48] that excessively high austenitisation temperatures can cause a coarse austenite grain structure with fewer particles of the desired retained cementite; the following cooling process will then lack the required

number density of cementite particles, thereby form the lamellar carbide and promote the pearlite transformation. Also, a lower austenitisation temperature favours the divorced form of pearlite [6]. The results show that 840 °C is the appropriate austenitisation temperature given a greater amount of undissolved cementite, and because the austenite grain size remains fine, which is conducive to a divorced pearlite transformation.

4.2.2 Austenitisation temperature, time and hardness

Table 4.3 indicates the effect of austenitisation temperature and time on hardness of steels with different carbon concentration in the quenched condition. The equilibrium carbon contents of austenite at the temperatures concerned are also tabulated in this table, which were calculated using MTDATA. As is shown, increasing the austenitisation temperature when heat treating the samples does not increase the hardness of the quenched structure. The reason for this is because although the carbon concentration of the austenite (or of the martensite that forms on quenching) increases, so does the amount of relatively soft retained austenite [6]. Under the same austenitisation temperature (840 °C), the hardness results of 0.85 wt% C steel and 0.94 wt% C steel are very close, which could be due to the similar amount of carbon that dissolved into austenite during the process. Longer austenitisation time has comparable effect with higher austenising temperature on the hardness. Both these factors could stabilise the austenite phase, which leads to a higher volume fraction of retained austenite after quenching resulting in a decrease in hardness value.

Table 4.3

Variation of hardness after quenching from the austenitisation temperature

Carbon content (wt%)	Carbon content of austenite (wt%)	Heating temperature (°C)	Austenitisation time (min)	Hardness (HV)
0.85	0.726	840	60	788±17
0.85	0.726	840	20	807±29
0.85	0.823	900	20	789±21
0.94	0.737	840	60	801±14
0.94	0.737	840	20	809±43
0.94	0.815	870	20	772±13
0.94	0.921	970	20	751±38

4.3 Spheroidisation

4.3.1 Effect of spherodisation on the microstructure

To further investigate the performance of spheroidisation after different processes and examine its effect on the materials' properties and structures, several experiments were done which are demonstrated in Table 4.4. The spheroidisation process curves are shown in Fig. 4.12 and the resulting microstructures are shown in Figs. 4.13-4.16.

In Table 4.4, each sample was handled with two different heat treatments. Numbers 1 and 2 utilise the method that was suggested by Verhoeven [6], where numbers 3 and 4 are the continuous-cooling spheroidal anneal presented by Hewit [5] based on the work of Heron [9].

Table 4.4

Heating treatment procedures

Number	Heat treatment
1	0.85 wt% C, heat to 840 °C and hold for 1 h, cool to 722 °C (500 °C h^{-1}) and hold for 2 h, then cool to 690 °C and hold for 1h, air cool
2	0.94 wt% C, heat to 840 °C and hold for 1 h, cool to 722 °C (500 °C h^{-1}) and hold for 2 h, then cool to 690 °C and hold for 1h, air cool
3	0.85 wt% C, heat to 840 °C and hold for 1 h, cool to 750 °C (25 °C h^{-1}), further cool to 690 °C (10 °C h^{-1}), air cool from 680 °C
4	0.94 wt% C, heat to 840 °C and hold for an hour, cool to 750 °C (25 °C h^{-1}), further cool to 690°C (10 °C h^{-1}), air cool from 680 °C

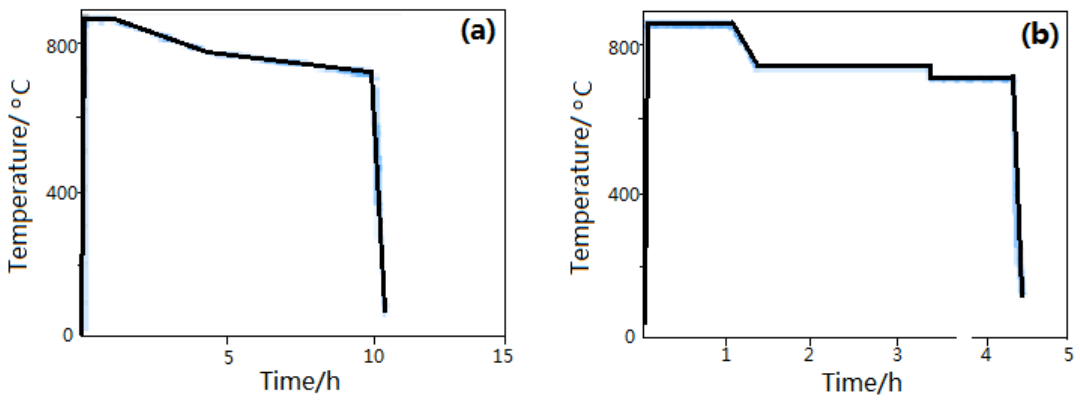

Figure 4.12: The routes adopted during spheroidisation heat treatment. (a) Process numbers 3 and 4; (b) process numbers 1 and 2.

The time required completing the process in Fig. 4.15b is about 6 h shorter than the typical continuous cooling process. From this point of view, Fig. 4.15b exhibits a much faster spheroidisation and hence recomme

Fig. 4.13 illustr not much of a difference observed

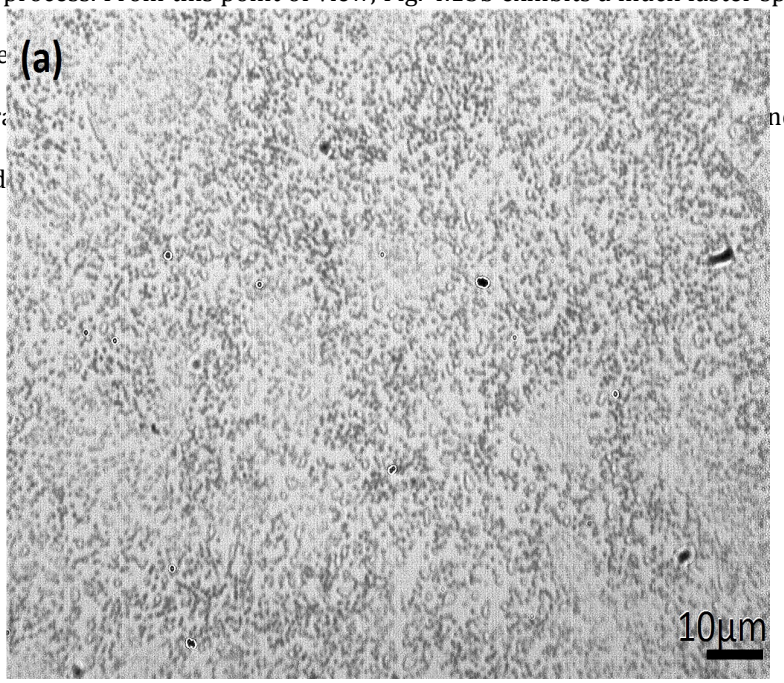

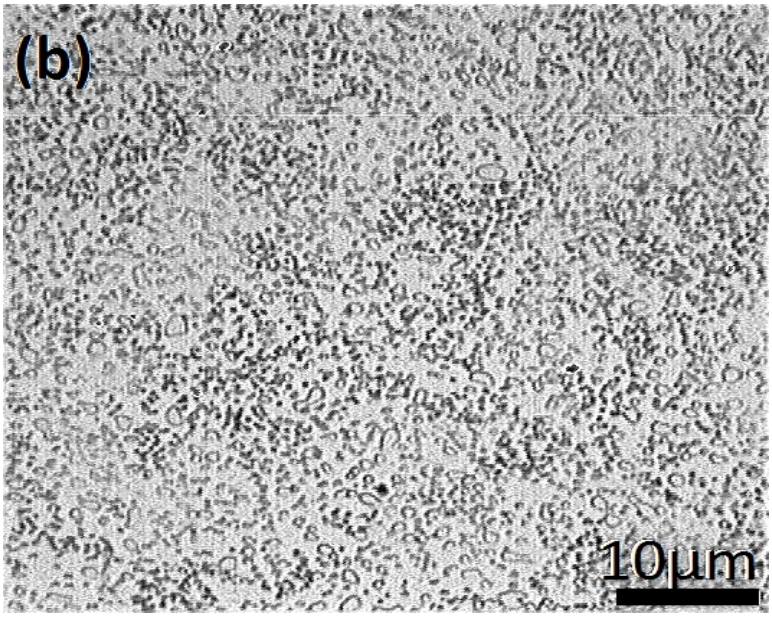

Figure 4.13: Optical microstructure of samples from (a) process number 1; (b) process number 3.

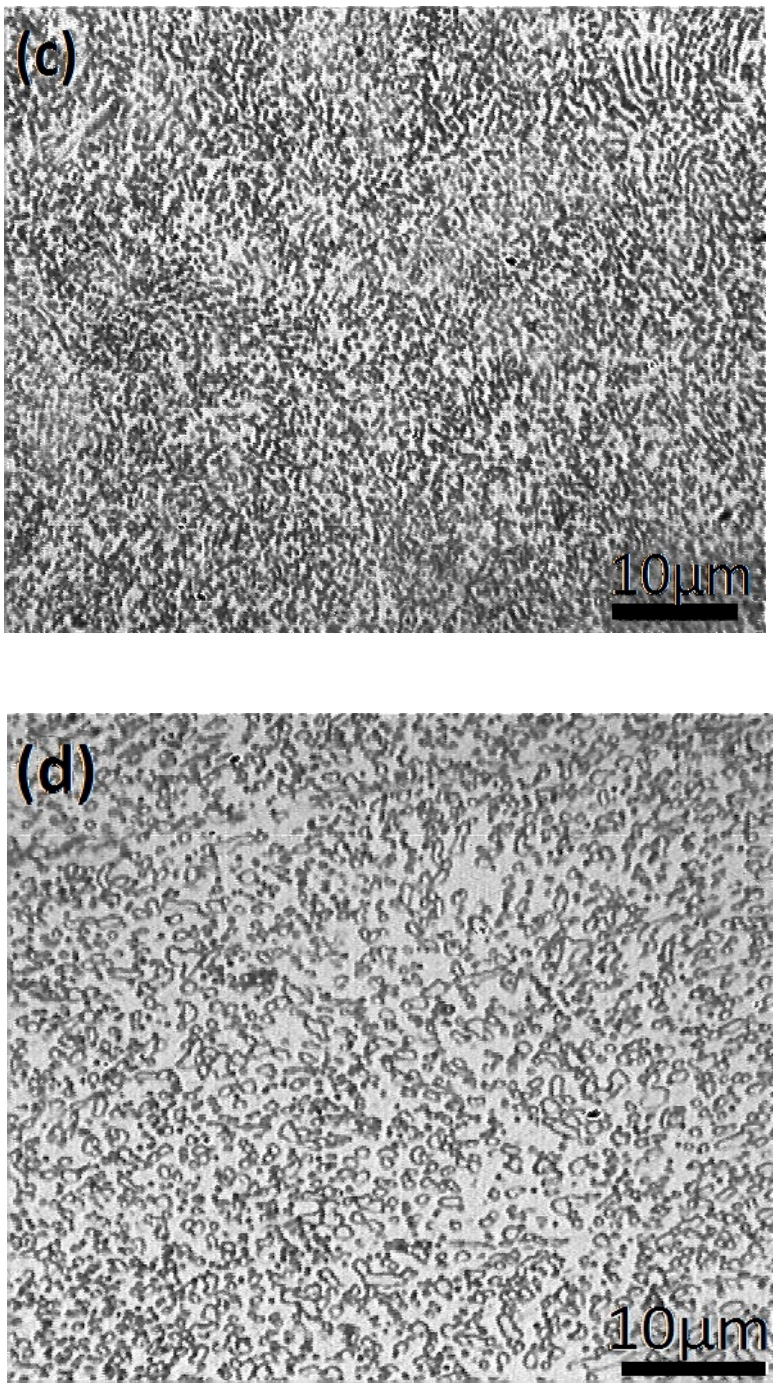

Figure 4.13: Optical microstructure of samples from (c) process number 2; (d) process number 4.

In Figs 4.14-4.15, the SEM results show that the 0.94 wt% C samples generally contain finer carbides than 0.85 wt% C samples. Most of the cementite particles are spheroidised as expected and no lamellar pearlite is found for all the samples. If we compare Fig. 4.14a with Fig. 4.15a and Fig. 4.14b with Fig. 4.15b, we can say that the two annealing processes do not have a great influence on the final microstructures as the carbide sizes and distribution are rather similar.

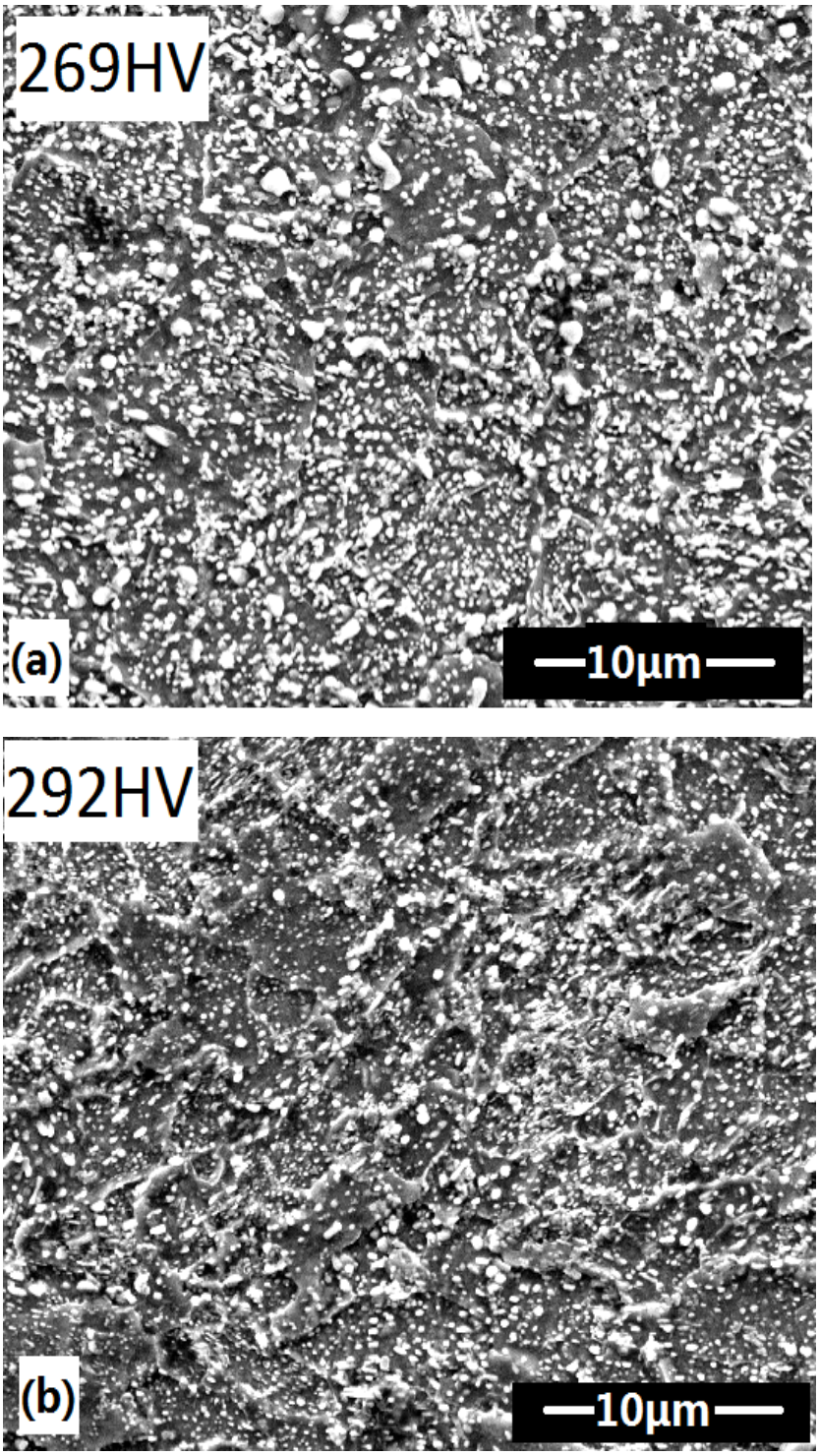

Figure 4.14: SEM results from the faster spheroidisation process. (a) 0.85 wt% C steel; (b) 0.94 wt% C steel.

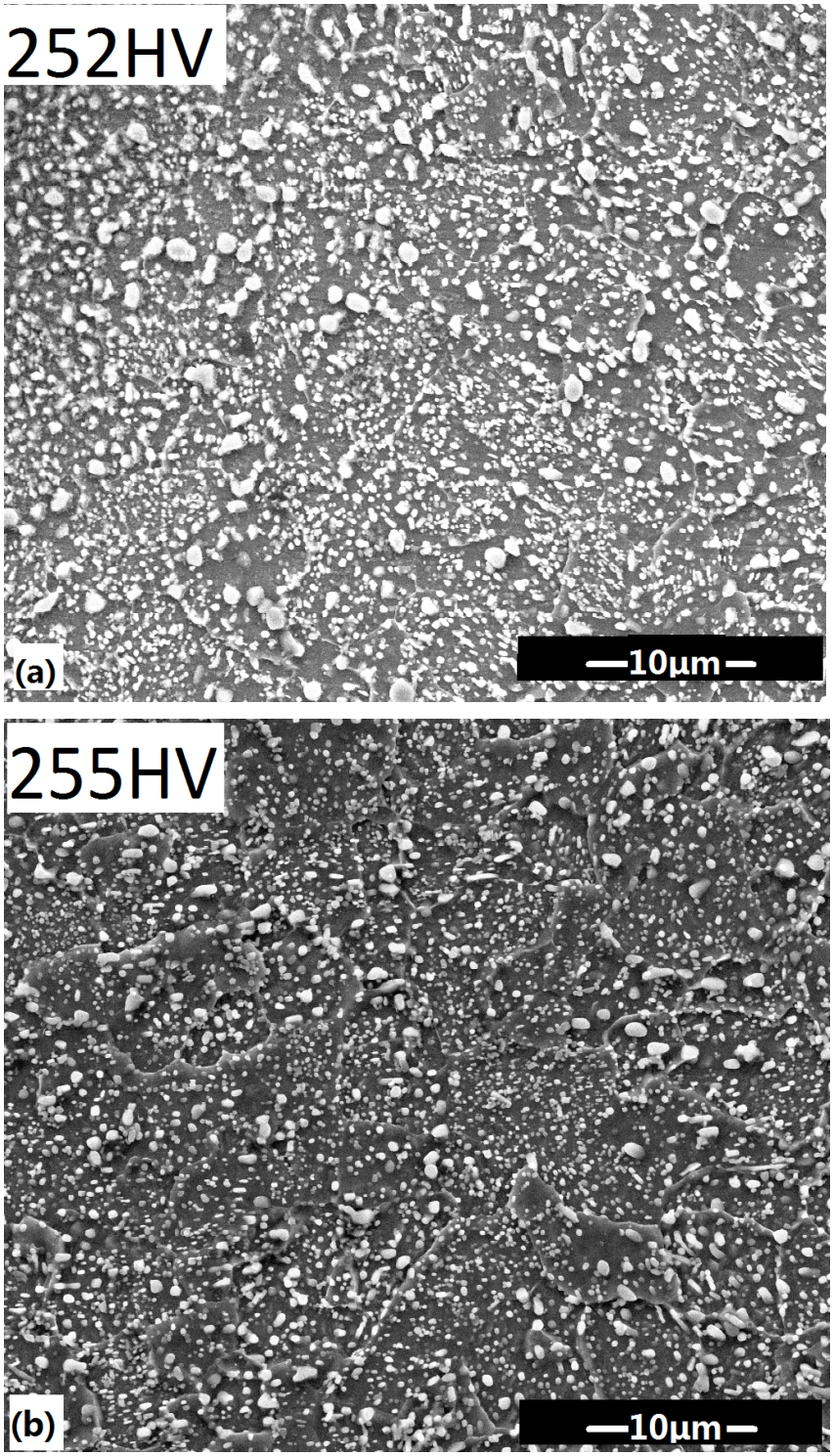

Figure 4.15: SEM results from slower spheroidisation process. (a) 0.85 wt% C steel; (b) 0.94 wt% C steel.

4.3.2 Effect on resulting carbide size and hardness

An imaging software program was employed, which measured an averaged diameter of each carbide particle. Analysis was done on digital images recorded directly from the SEM. The sizes of carbide particles and the relative hardness values are illustrated in Table 4.5. From the data, the average particle sizes for the four experiments are in the range of 1.2 μm to 1.4 μm. All the samples have achieved a hardness below 300 HV after annealing. Overall, the method introduced by Hewit (numbers 3 and 4) seems to perform a better degree of spheroidisation with coarser cementite particles and lower hardness. This result is consistent with the previous studies showing that the bigger size of particles, the softer of the material [1].

Table 4.5

Comparison of carbide size and hardness

Number	Carbide size (max. diameter μm)	Carbide size (min. diameter μm)	Mean size (diameter μm)	Hardness (HV)
1	2.43±0.11	0.31±0.12	1.37	269±4
2	1.56±0.09	0.42±0.10	1.22	292±9
3	2.55±0.13	0.27±0.06	1.42	252±5
4	2.49±0.05	0.30±0.04	1.40	255±4

4.4 Quenching during typical continuous cooling spheroidisation process

Quenching during the typical continuous cooling process (displayed as number 3 and 4 in Table 4.4) can reveal the microstructure at various stages above 740 °C of the treatment. During the 10 h spheroidisation annealing, experiments were carried out by quenching the samples at three different temperatures of 815 °C, 750 °C and 740 °C to the room temperature, for the 0.85 wt% C and 0.94 wt% C as illustrated in Fig. 4.16.

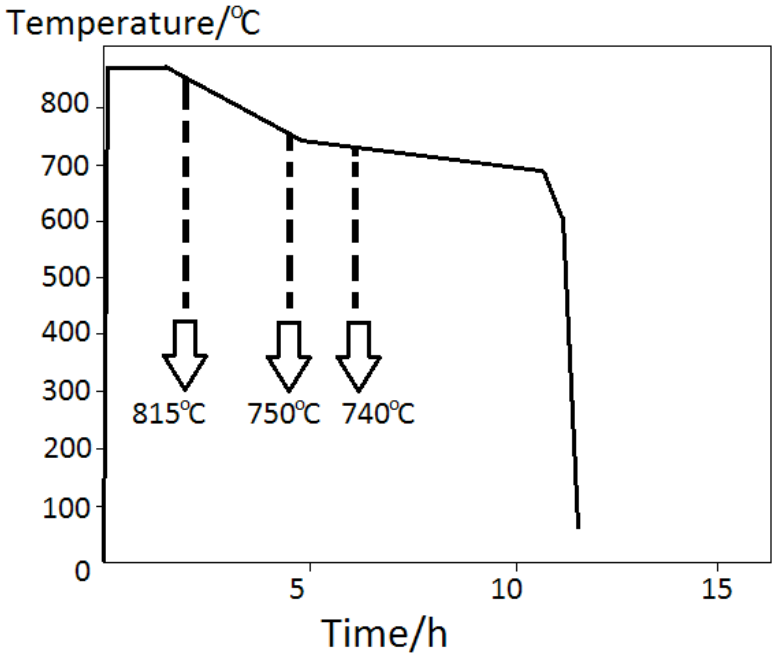

Figure 4.16: Temperature vs. time curve represents the process of different carbon-containing steel quenched at different stages of spheroidisation.

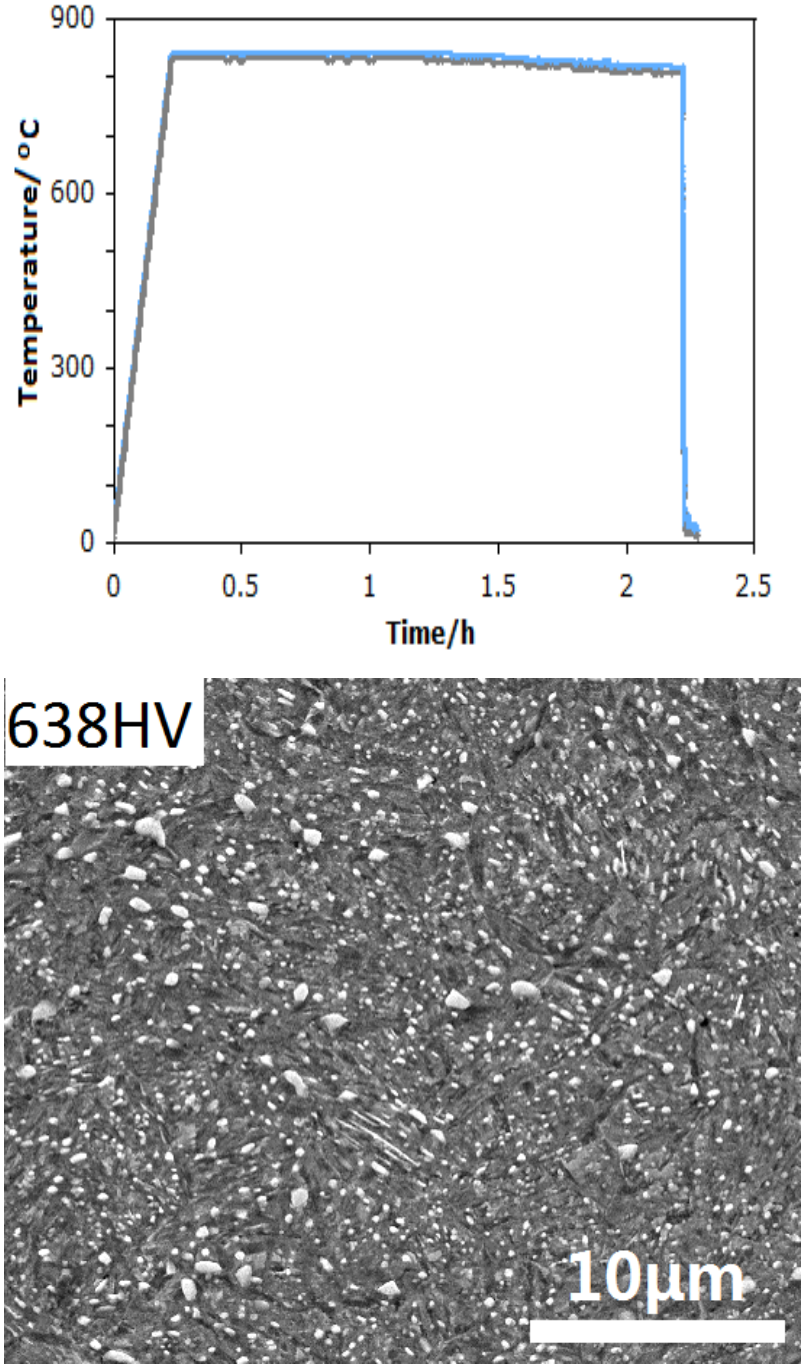

Figure 4.17: Process curve and SEM result of 0.85 wt% C steel quenched from 815 °C.

Figs. 4.17-4.19 indicate microstructures of 0.85 wt% C steel after quenching from 815 °C, 750 °C and 740 °C, respectively. As can be seen from Figure 4.17, carbides in both granular and angular shapes are obtained after quenching at 815 °C. Due to the cooling rate and temperature; there are still some carbides that do not fully spheroidise.

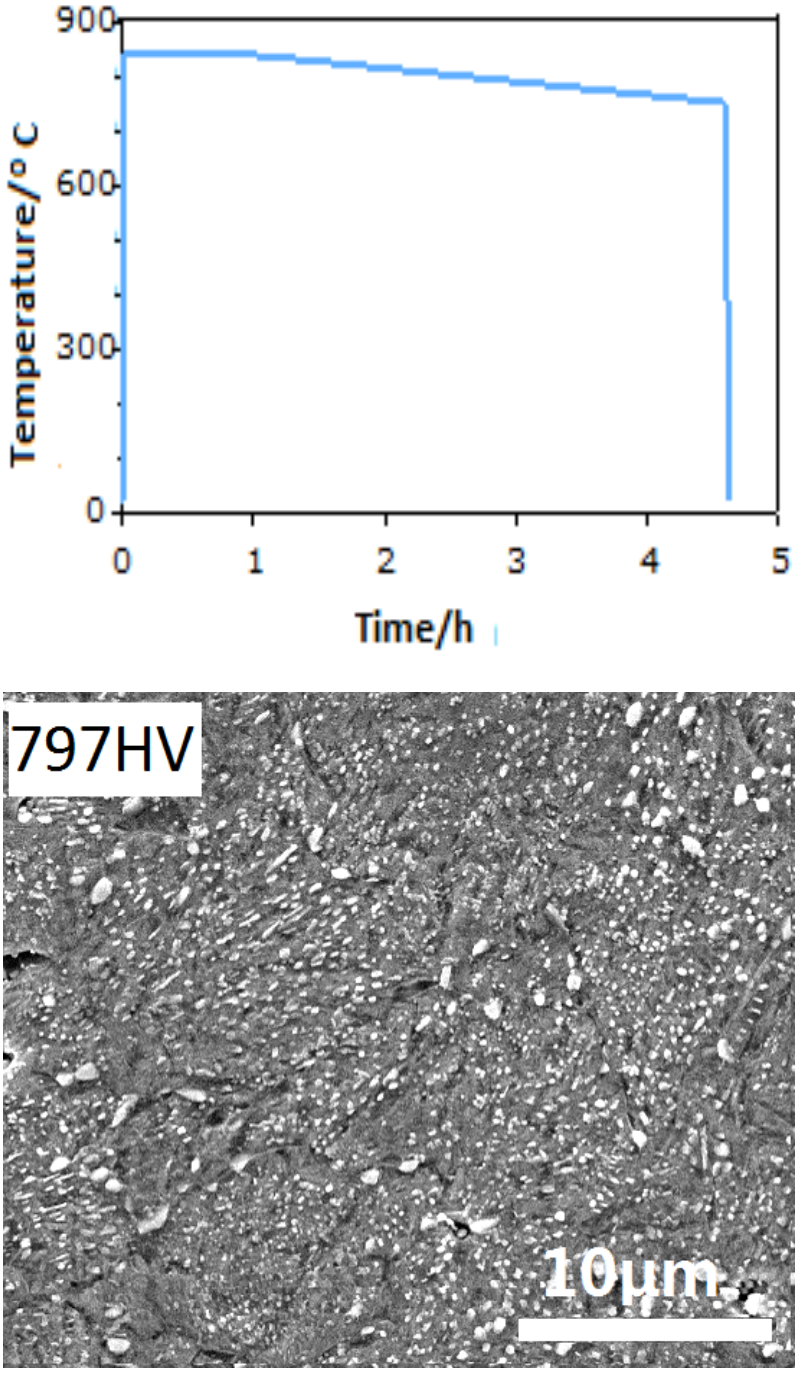

Figure 4.18: Process curve and SEM result of 0.85 wt% C steel quenched from 750 °C.

Fig. 4.18 shows the process curve microstructures of 0.85 wt% C steel quenching at 750 °C. As can be seen from the above figure, we can see that the degree of spheroidisation has increased. The microstructure contains more carbide particles. Similarly, because of the cooling rate or temperature, some large size carbides are found.

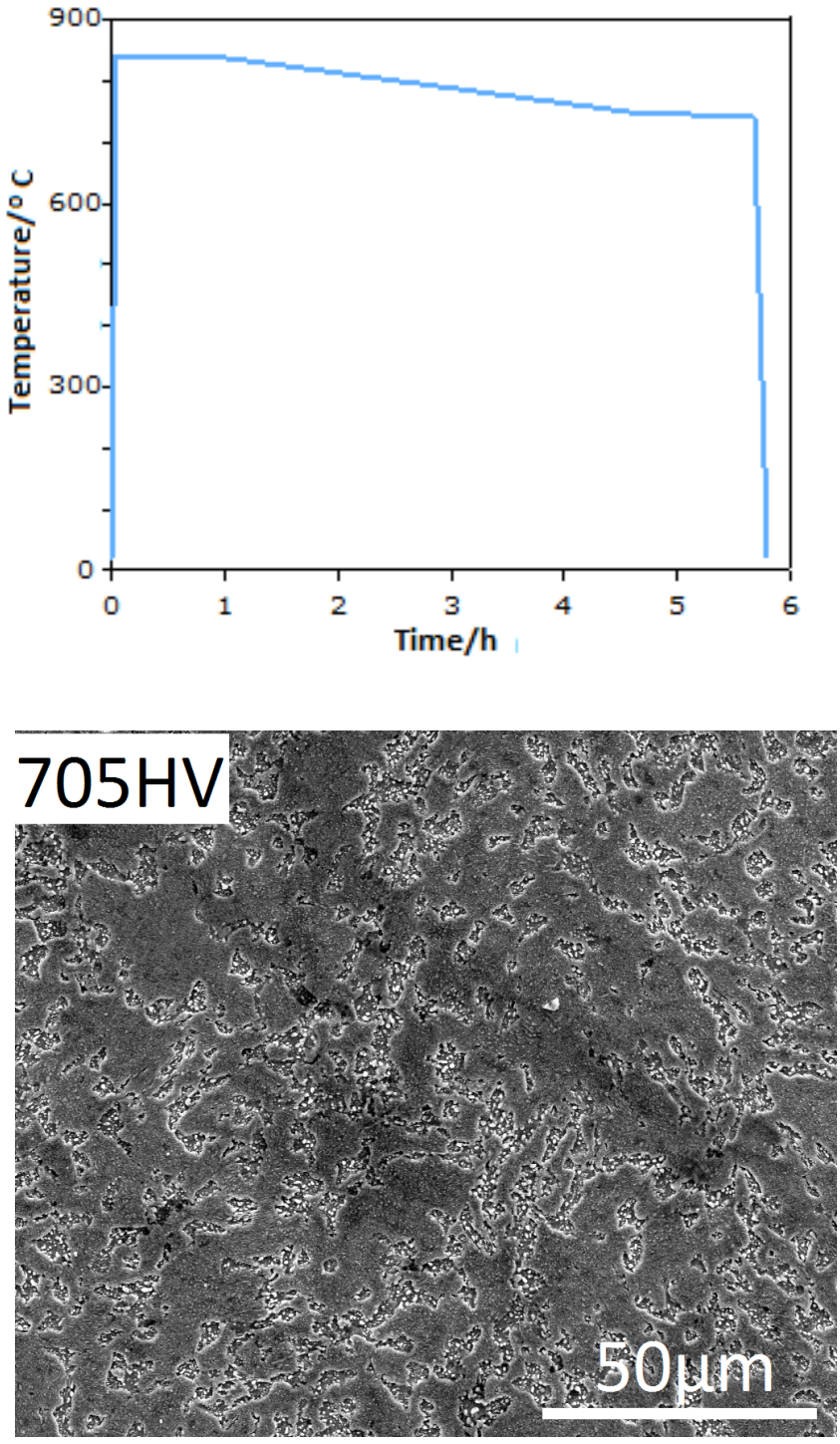

Figure 4.19: Process curve and SEM result of 0.85 wt% C steel quenched from 740 °C.

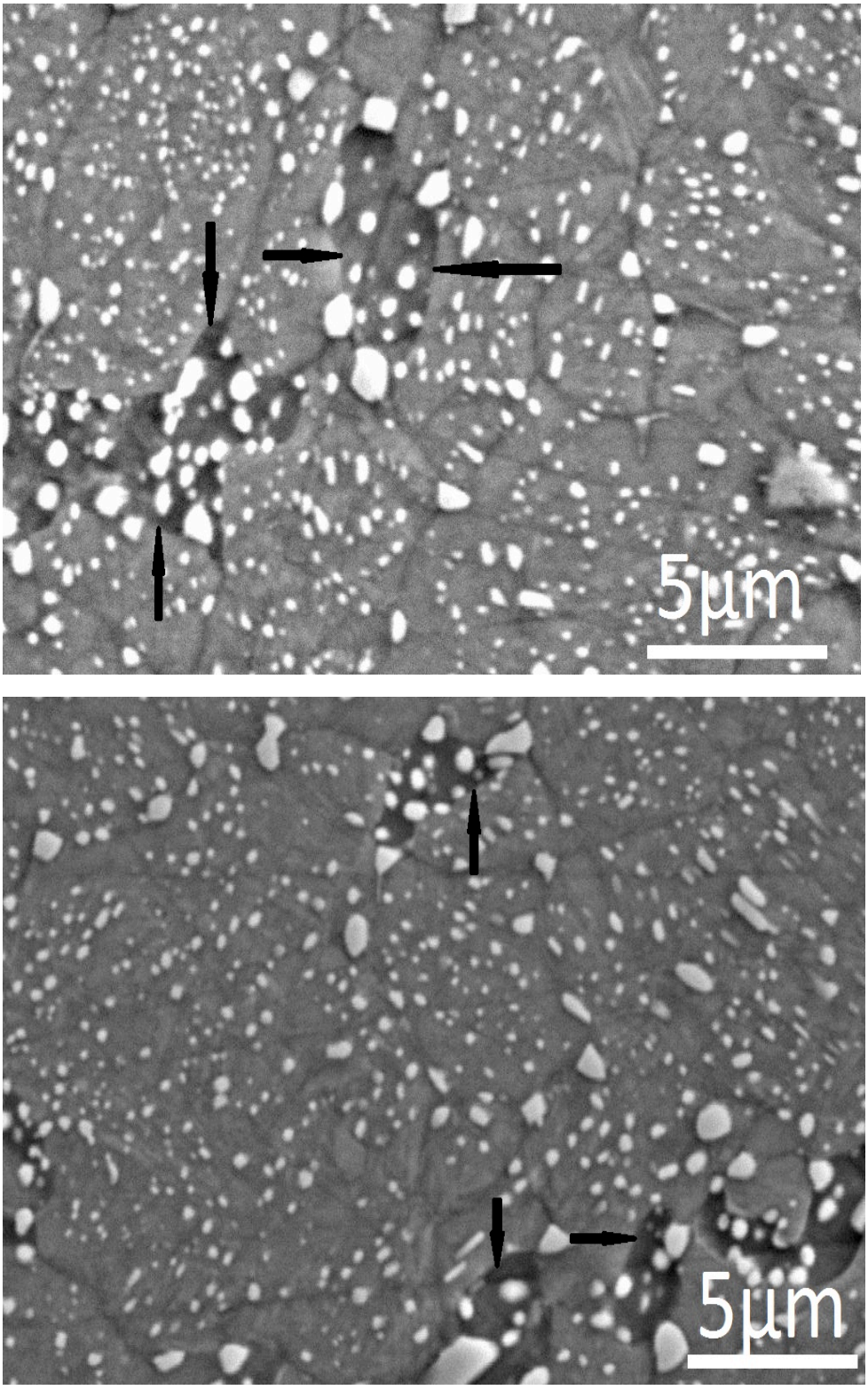

Figure 4.19: SEM result of 0.85 wt% C steel quenched from 740 °C.

Fig. 4.19 shows the microstructures of 0.85 wt% C steel after quenching from 740 °C. In this figure, the transformation front is a cellular-shaped austenite/ferrite phase boundary that moves into the austenite, as illustrated by the arrowed areas. Ferrite is presented as some dark blocks with

circular cementite particles on it, which indicates that there is a great increase in the extent of DET. There are more carbides particles exist at 740 °C, mainly spherical. Nevertheless, the sizes of the carbides are uneven. It can be also found that the cementite particles in the ferrite are generally bigger than those still in the martensite. This is because as DET occurs, an amount of carbon from austenite will diffuse into the existing cementite and make the particles larger.

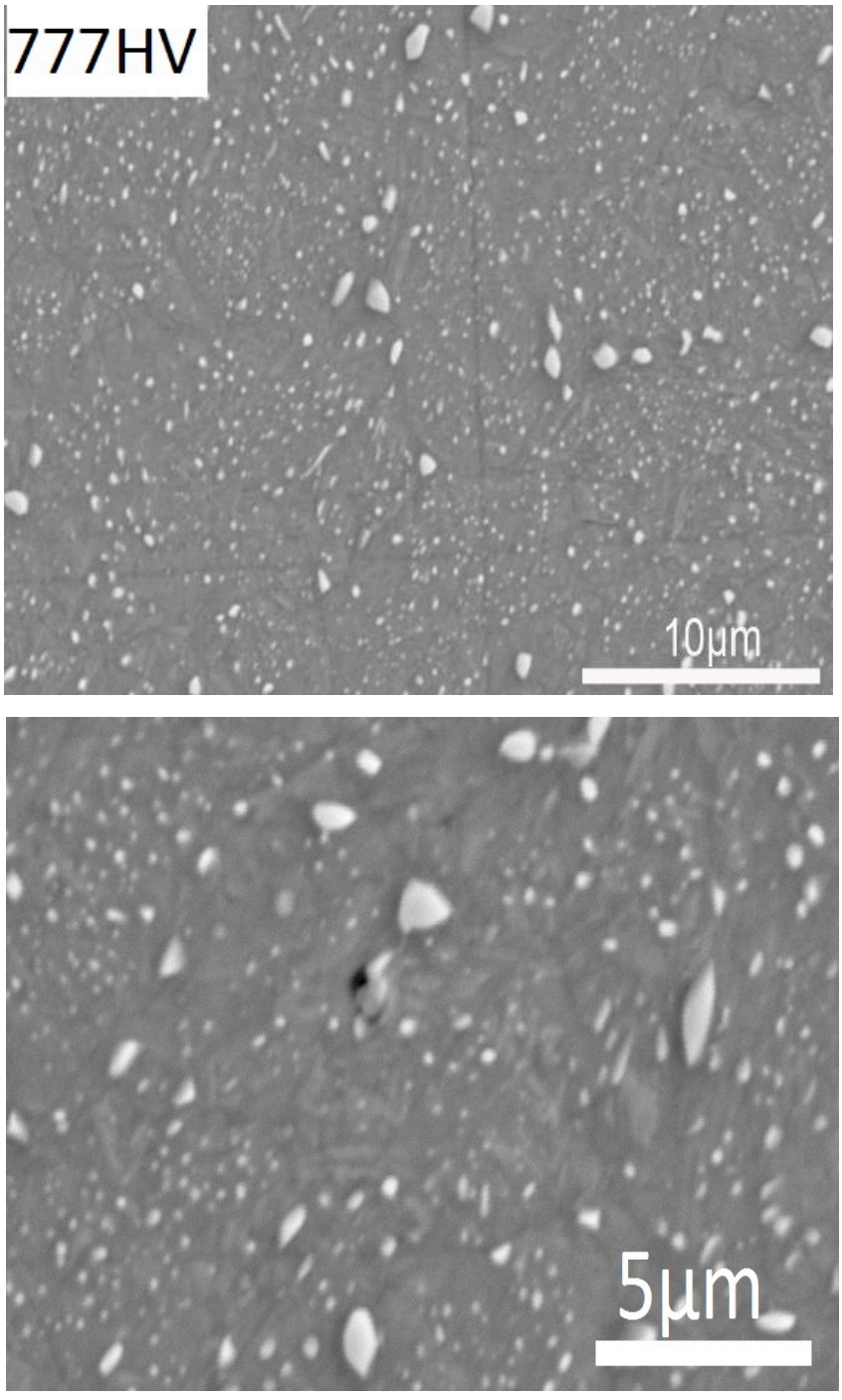

Figure 4.20: SEM results of 0.94 wt% C steel quenched from 815 °C.

As comparison, a different carbon-containing steel was prepared. Figs. 4.20-4.22 indicate the microstructure results of 0.94 wt% C steel after different quench temperatures. Fig. 4.20 shows the microstructure of 0.94 wt% C steel after 815 °C quenching. As can be seen, less carbide particles with uneven sizes in both granular and squared shapes are obtained. DET might not yet occurred at this temperature.

Fig. 4.21 shows the microstructure of 0.94 wt% C steel after 750 °C quenching. From the figure, it seems that some granular and angular shapes of carbides are found. The presence of ferrite shows that the DET has occurred.

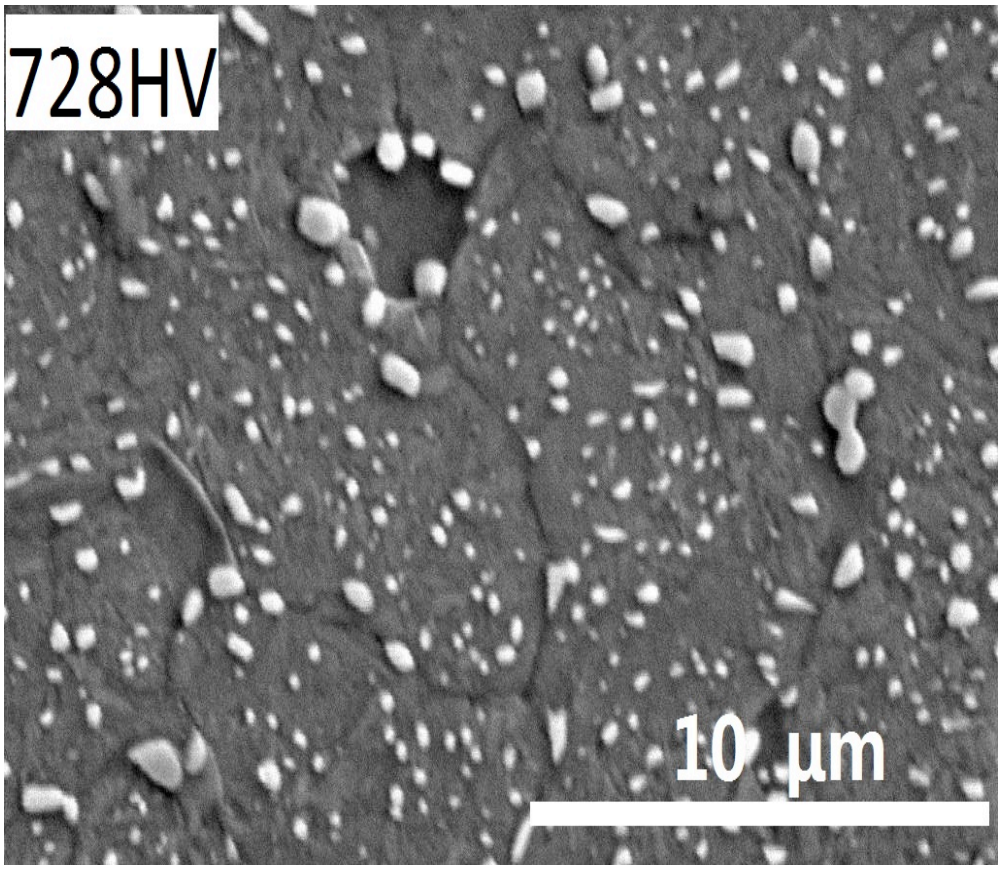

Figure 4.21: SEM results of 0.94 wt% C steel quenched from 750 °C.

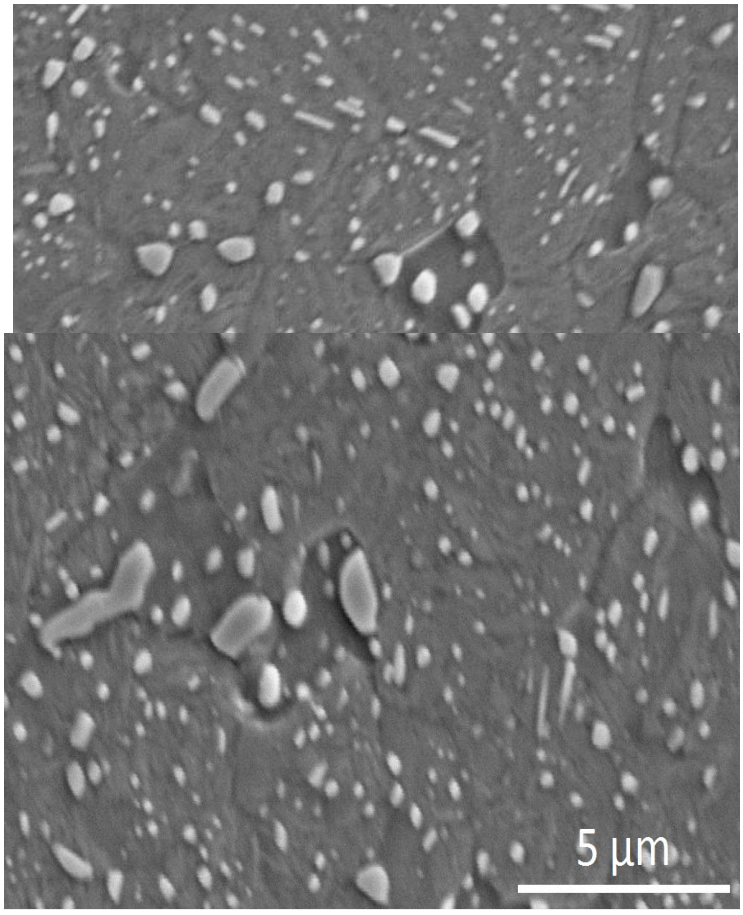

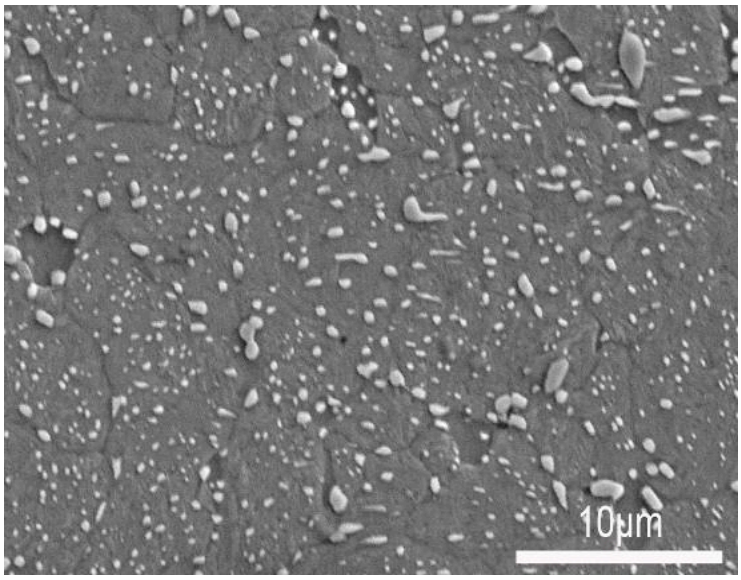

Figure 4.21: SEM results of 0.94 wt% C steel quenched from 750 °C.

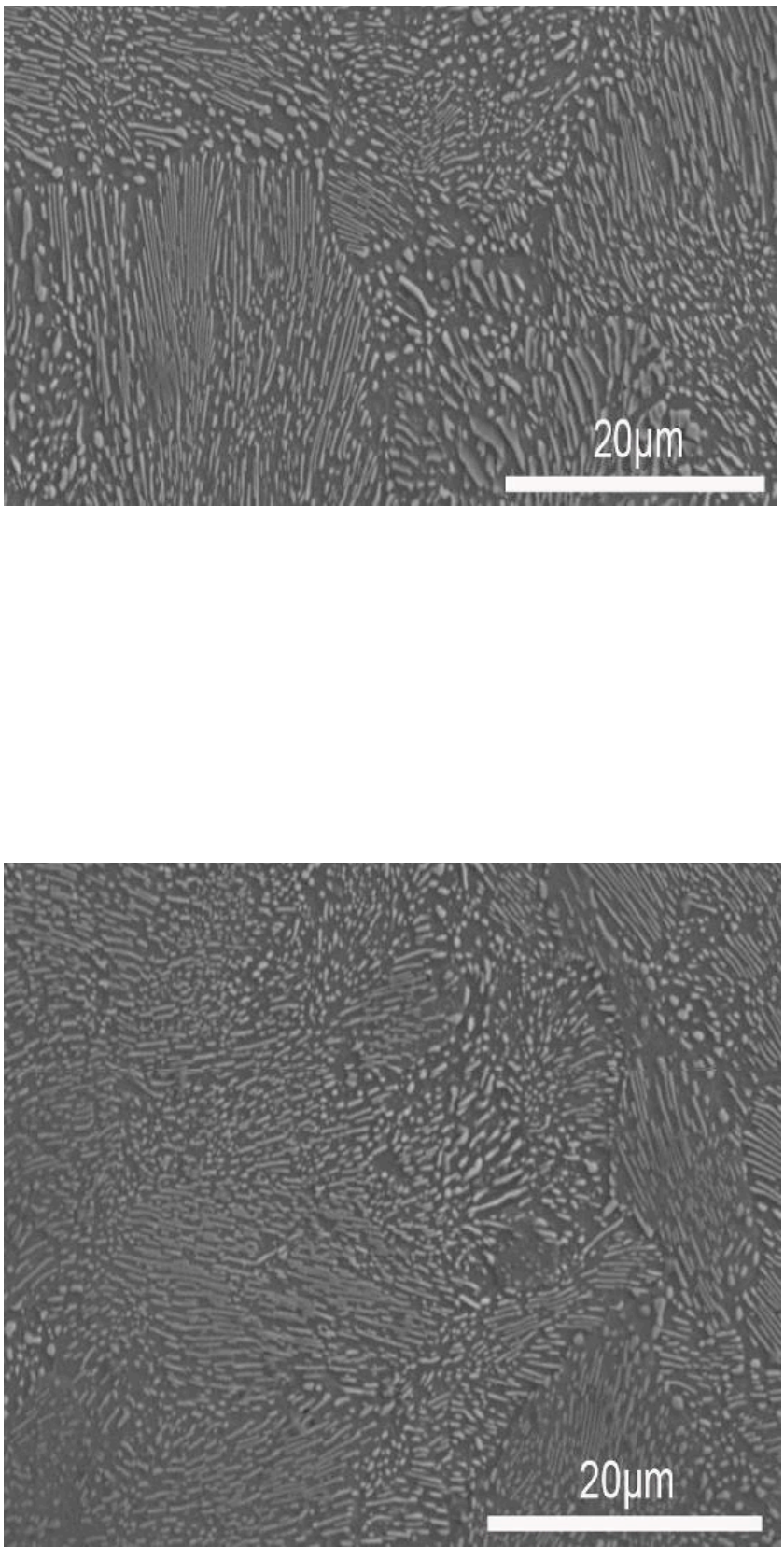

Figure 4.22: SEM results of 0.94 wt% C steel quenched from 740 °C.

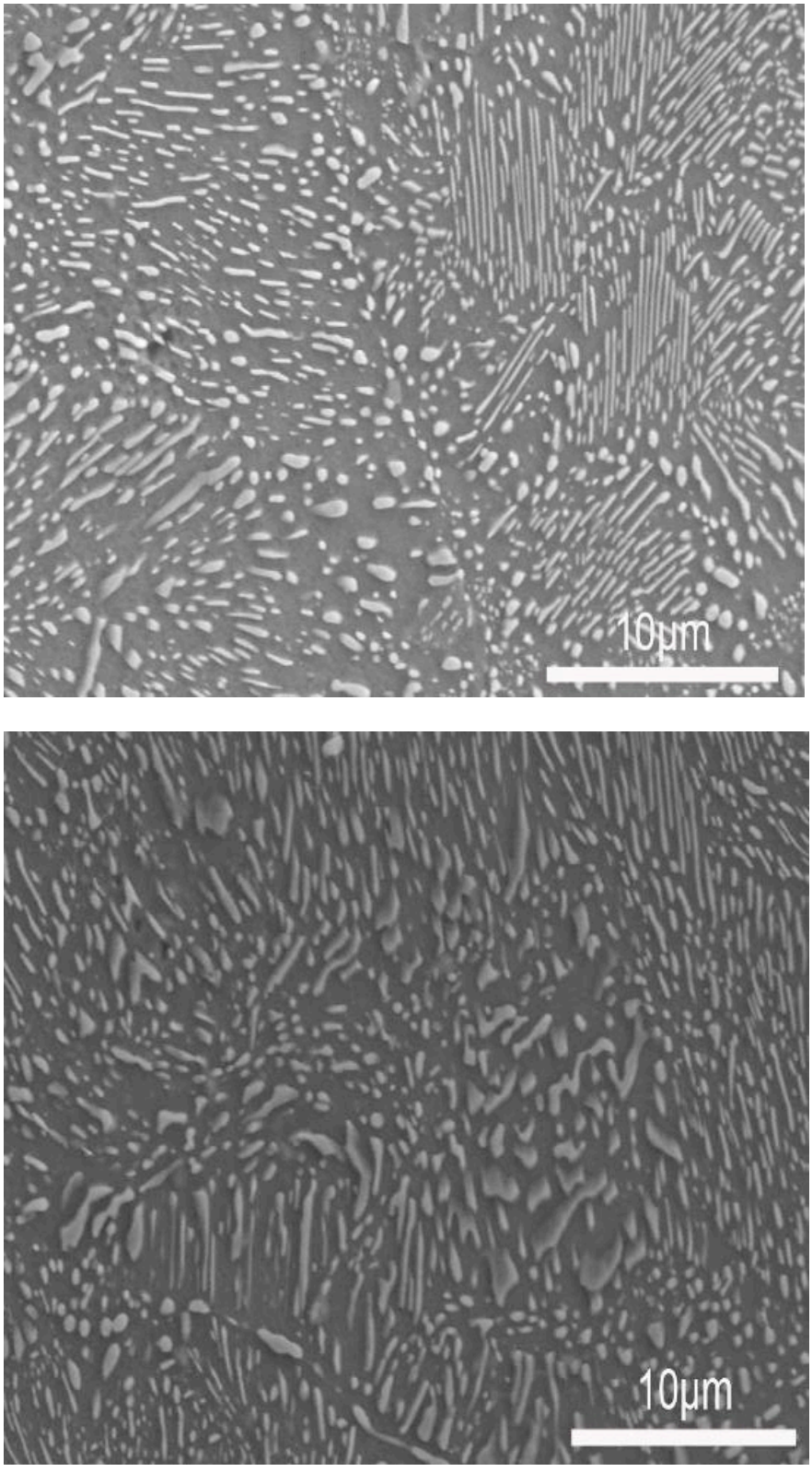

Figure 4.22: SEM results of 0.94 wt% C steel quenched from 740 °C.

Fig. 4.22 shows the microstructure of 0.94 wt% C steel after 740 °C quenching. In the figure, the pearlite transformation has completed at this temperature, some long and other spherical shapes of carbides are obtained after the process. However, due to the effect of cooling rate and temperature, there is still some cementite which has not fully spheroidised. In comparison with the 0.85 wt% C steel, DET occurs at a higher temperature in 0.94 wt% C steel. The hardness drop in Table 4.6 provides evidence that rapid spheroidisation is possible for superbainitic bearing steels.

Table 4.6
The hardness results

Carbon content	Hardness (HV)		
(wt%)	Quench from 815 °C	Quench from 750 °C	Quench from 740 °C
0.85	638±15	797±11	705±21
0.94	777±7	728±19	271±9

4.5 Isothermal transformation experiments

The extent of transformation was followed using micrographs, strain and hardness.

10 days isothermal transformation

Long isothermal transformation experiments were performed at 200 °C for 10 days. Figs. 4.23-4.24 show the microstructures of 0.85 wt% C and 0.94 wt % C steel, respectively. As can be seen from the figures, there is not much difference in the microstructure between two samples. Both alloys maintain a number of undissolved cementite particles embedded in the lower bainite matrix. But the sample with the higher carbon concentration tends to lead to slightly more and finer carbides.

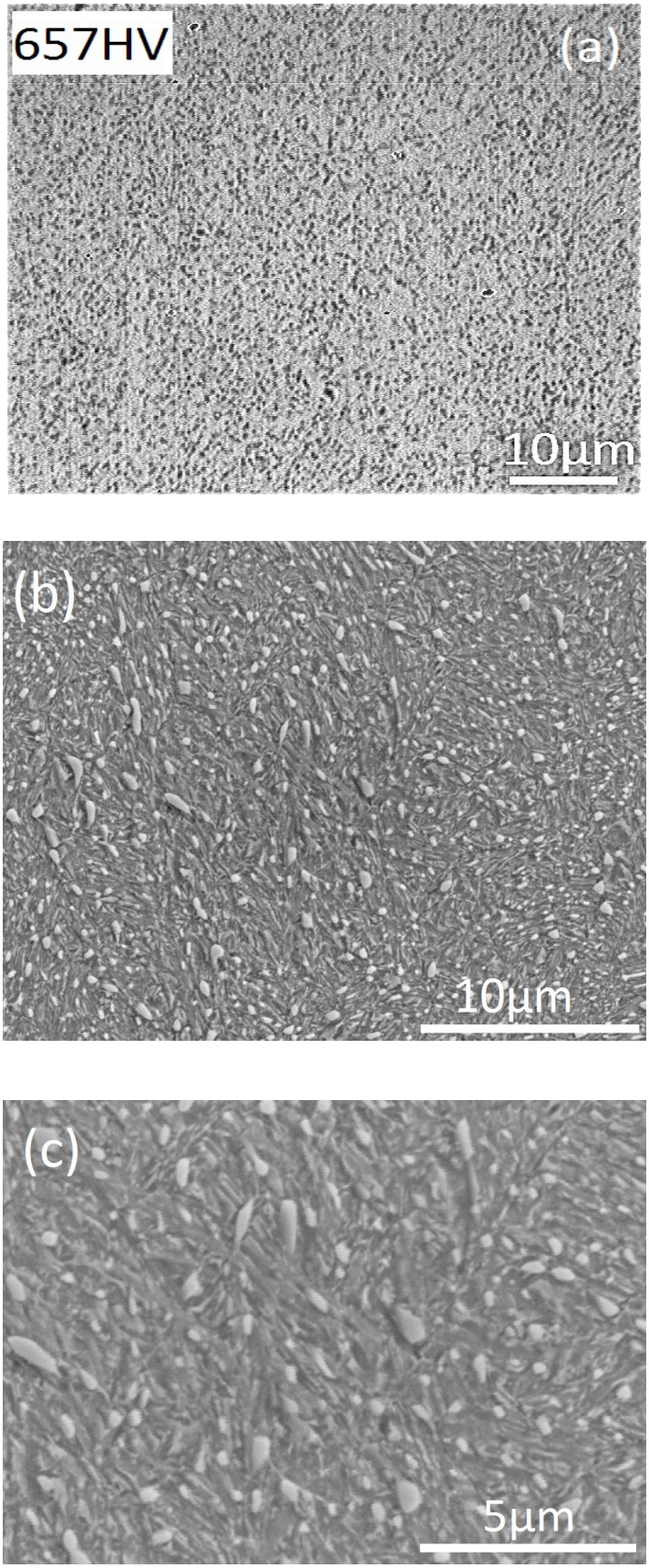

Figure 4.23: Microstructures of 0.85 wt% C steel held at 200 ° C for 10 days. (a) Optical microstructure; (b), (c) scanning electron microstructure.

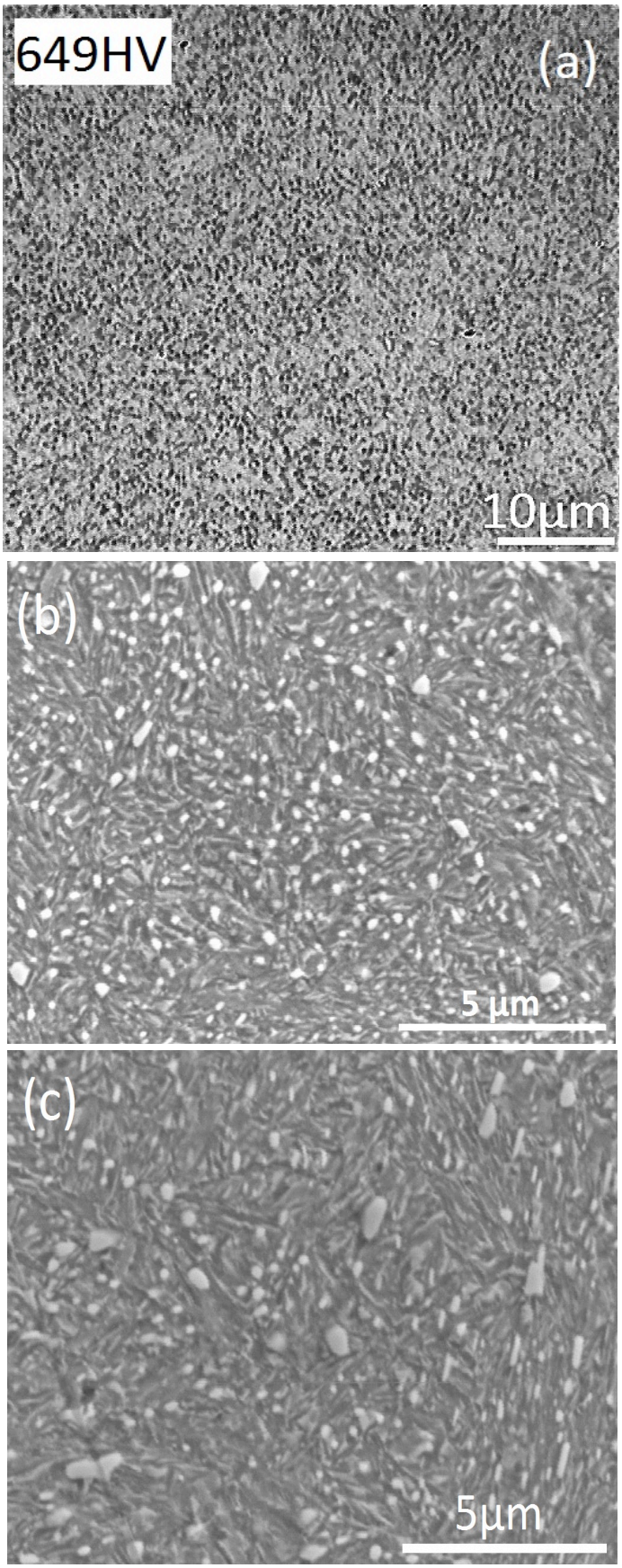

Figure 4.24: Microstructures of 0.94 wt% C steel held at 200 ° C for 10 days. (a) Optical microstructure; (b), (c) scanning electron microstructure.

Figs. 4.25-4.26 give the TEM micrographs of two samples, which provide further observations of the microstructures. From the figures, both alloys have transformed into the slender plates of bainite ferrite. There are fine carbides, possibly cementite particles, which precipitated from the plates. As calculated, bainite with similar sizes (100 nm) are obtained for both samples.

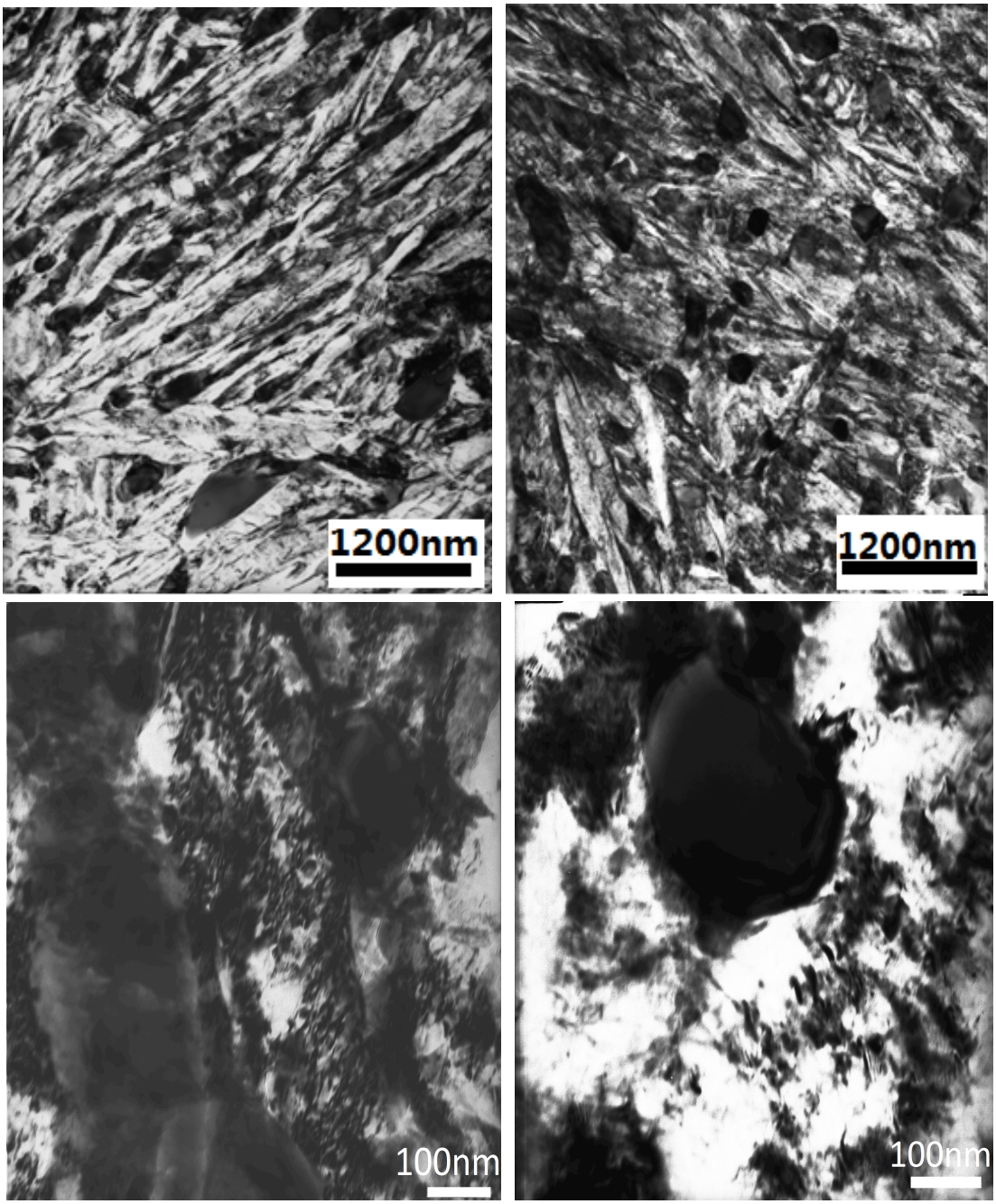

Figure4.25: TEM results of 0.85 wt% C steel held at 200 ° C for 10 days.

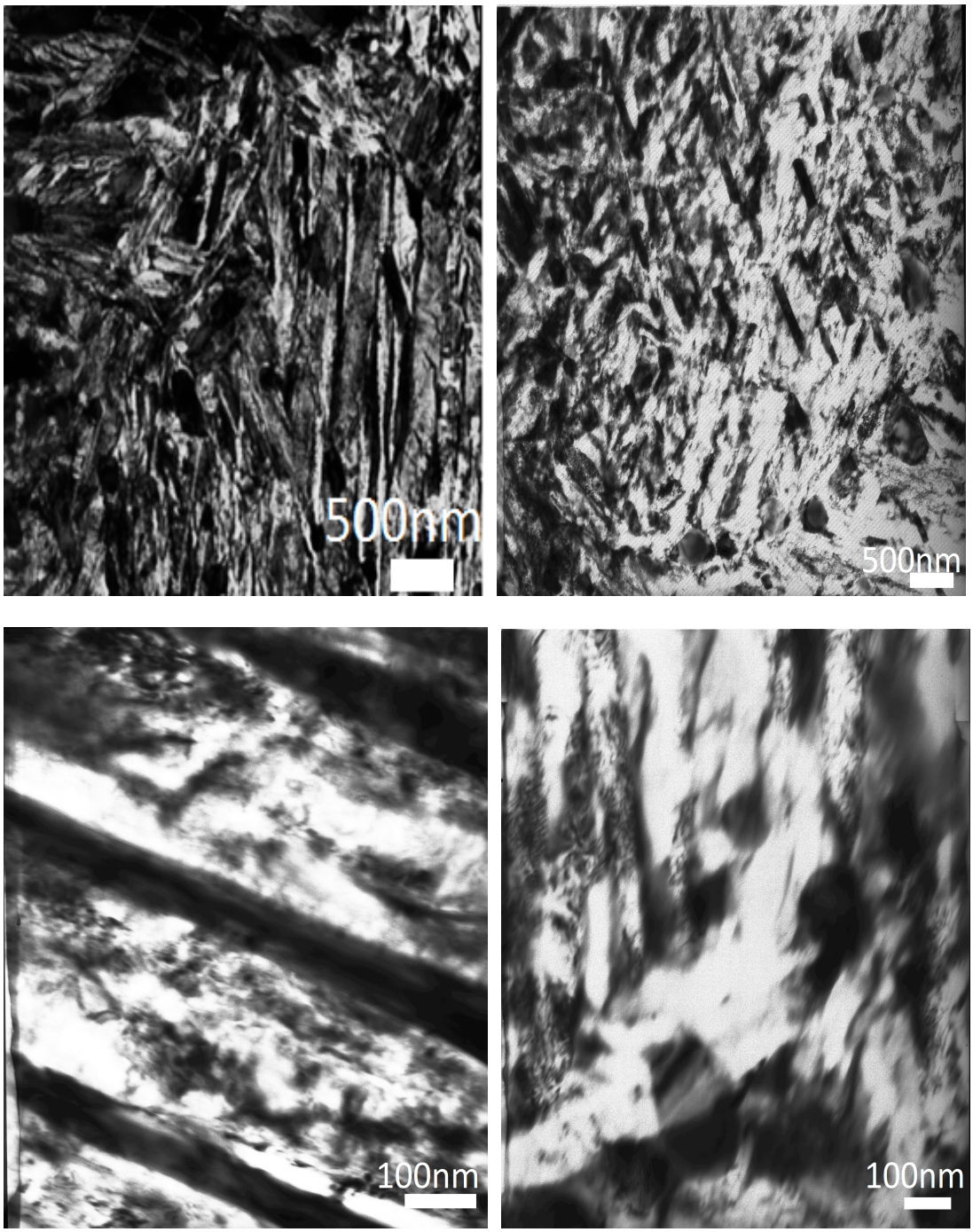

Figure 4.26: TEM results of 0.94 wt% C steel held at 200 ° C for 10 days.

10 h isothermal transformation

Holding the samples at different temperatures could offer more information during the transformation process.

4.5.1 Relationship between temperature, time and strain

Fig. 4.27 shows how strain changes with increasing temperatures for 0.85 wt% C and 0.94 wt% C alloys with different transformation temperatures. Dilatometry is often adopted to study phase transformations by monitoring volume/strain changes during transformation processes. As seen from the curves in Fig. 4.27, bainitic transformations take place in both alloys when holding them at 250 °C and 300 °C, whereas isothermal transformation at 200 °C does not induce obvious structure changes. However, although insignificant, 0.85 wt% C alloy shows slightly faster kinetics than that for 0.94 wt% C at 200 °C. This can be more clearly seen in Fig. 4.28, where the curves for 0.85 wt% C alloy at 200 °C give tails in the end comparing to flat curves for 0.94 wt% C alloy, indicating 0.94 wt% C alloy has not transformed at this temperature. In addition to this, martensite transformations are observed at the end of the curves for both samples quenched from 200 °C.

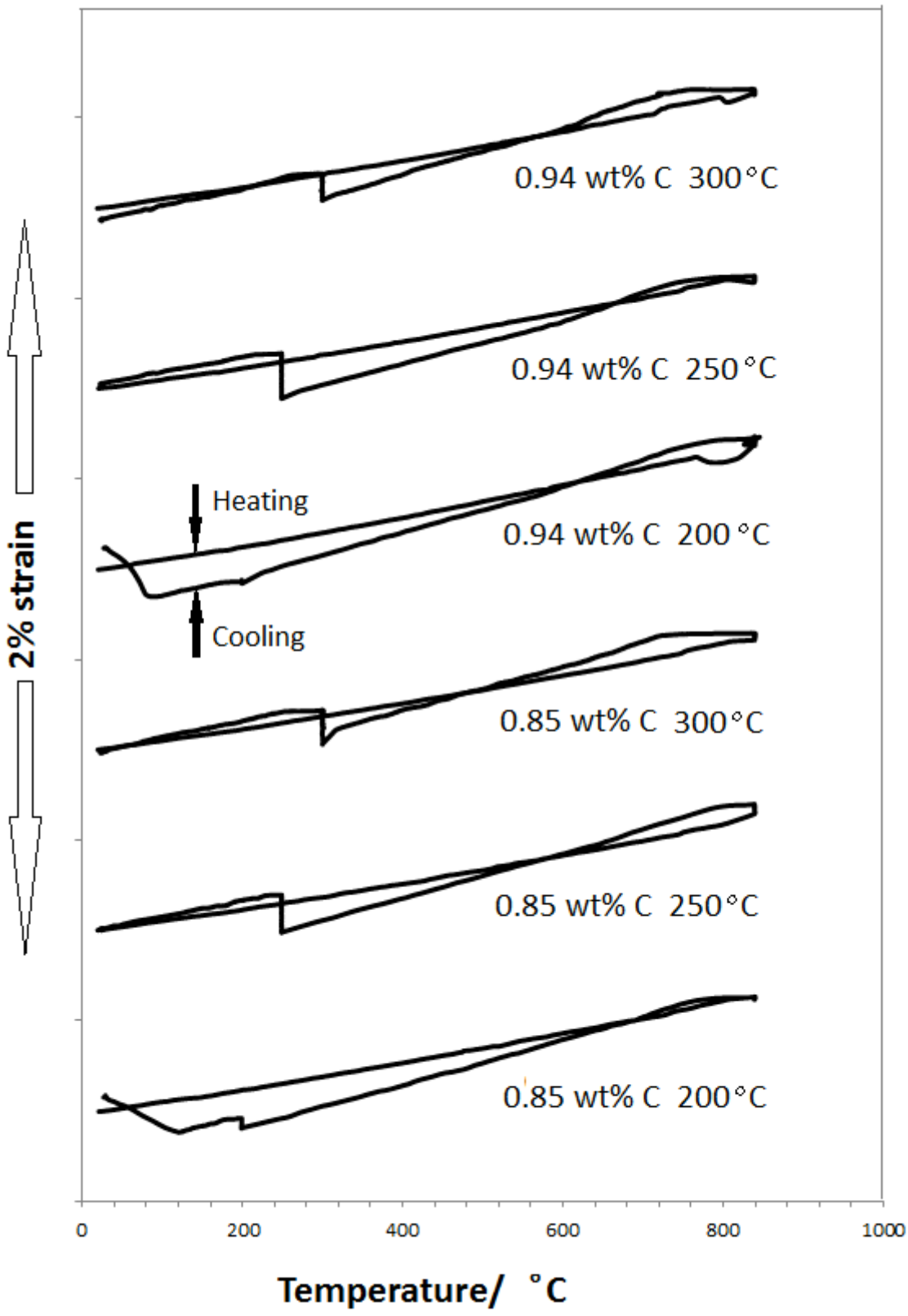

Figure 4.27: Heating and cooling dilatometric data for 0.85 wt% C and 0.94 wt% C alloys. The heating rate is 10 °C s^{-1} and the cooling rate is 25 °C s^{-1}.

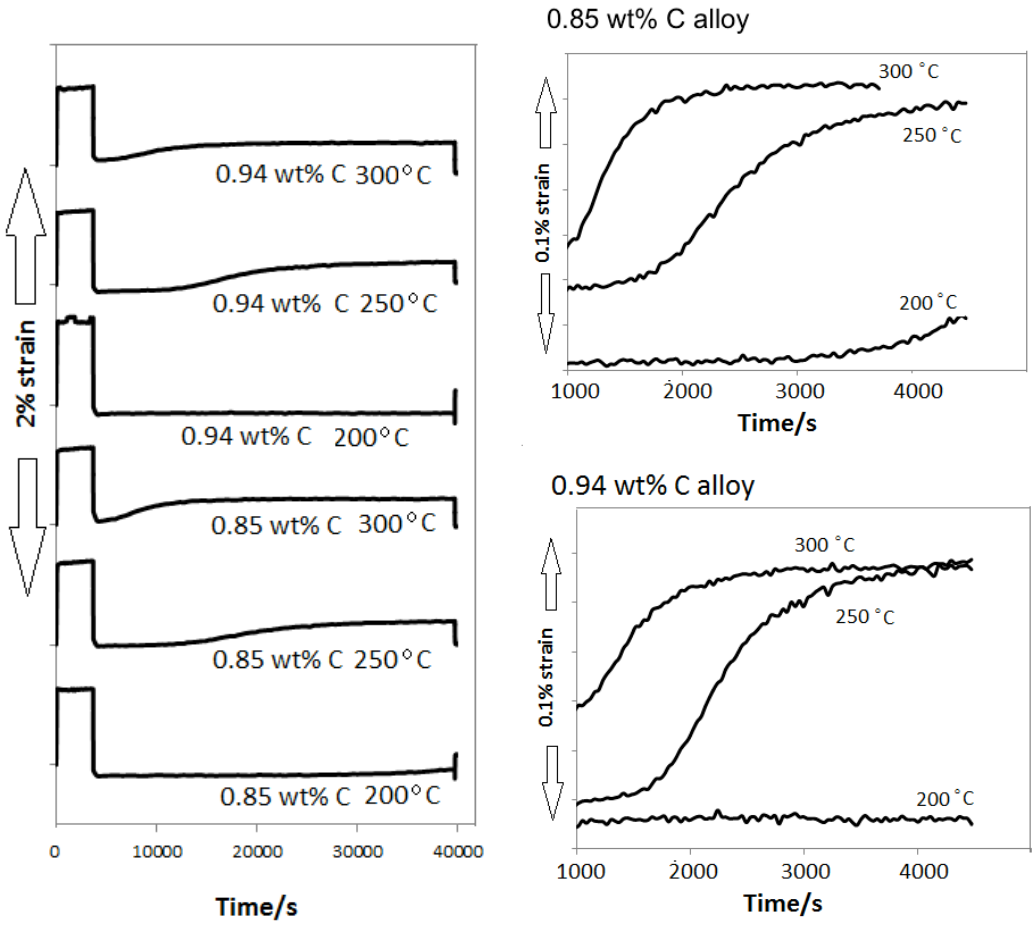

Figure 4.28: The relationship between time and strain of 0.85 wt% C and 0.94 wt% C alloys when holding at different temperatures.

Fig. 4.29 gives the detailed variation of strain and temperature when the samples are quenched from 200°C to room temperature. From the curves, it can be recognised that there is still martensite transformation, showing that 10 h holding time is insufficient to complete isothermal transformation for high carbon alloys at 200 °C. On the other hand, for samples quenching from 250 °C and 300 °C (Fig. 4.29), the bainitic transformation has finished since the transformation rate is faster a higher temperatures. Also, the completion of transformations is evident in Fig. 4.27 as there is no further transformation observed after the bainitic reaction.

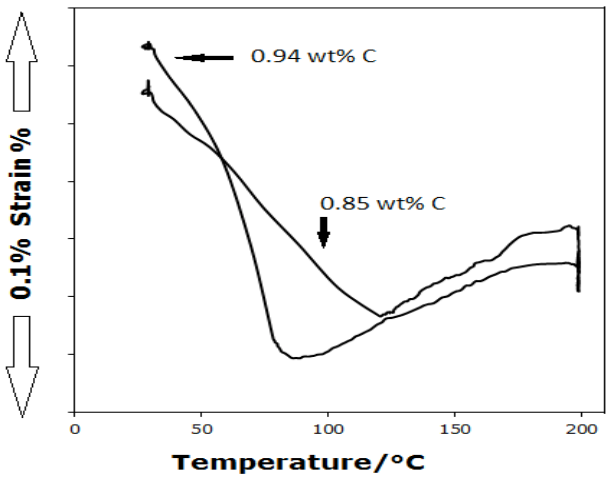

Figure 4.29: The variation of strain with temperature of 0.85 wt% C and 0.94 wt% C steels quenched from 200°C.

The change of strain associated with bainite transformation can be further investigated by comparing the above results to those of a normal superbainite alloy with composition of Fe -0.79C -1.56Si -1.98Mn -0.002P -1.01Al -0.24Mo -1.01Cr -1.51Co (wt%) [49]. Fig. 4.30a shows the radial strain recorded during the course of isothermal transformation to bainite under the influence of negligible stress (4MPa). In this figure, the strain is directly related to the volume fraction of bainite since there is no favoured variant and the transformation strain is isotropic [50, 51]. In the figure, the highest level of transformation increases with the undercooling below Bs. The detailed kinetics follows the typical "C" curve behaviour with the maximum rate being at an intermediate temperature. This is consistent with the results obtained in the present work. The maximum extent of strain rose occurred at 250 °C. Fig. 4.30b displays a comparison of the strain changed for the normal superbainite, 0.85 wt% C and 0.94 wt% C alloys during the isothermal transformation at 250 °C. The maximum degrees of transformation for the normal superbainite and 0.94 wt% C steel are similar, which is higher than the 0.85 wt% C steel. Also, the samples in this work show a slightly faster rate than the normal superbainite.

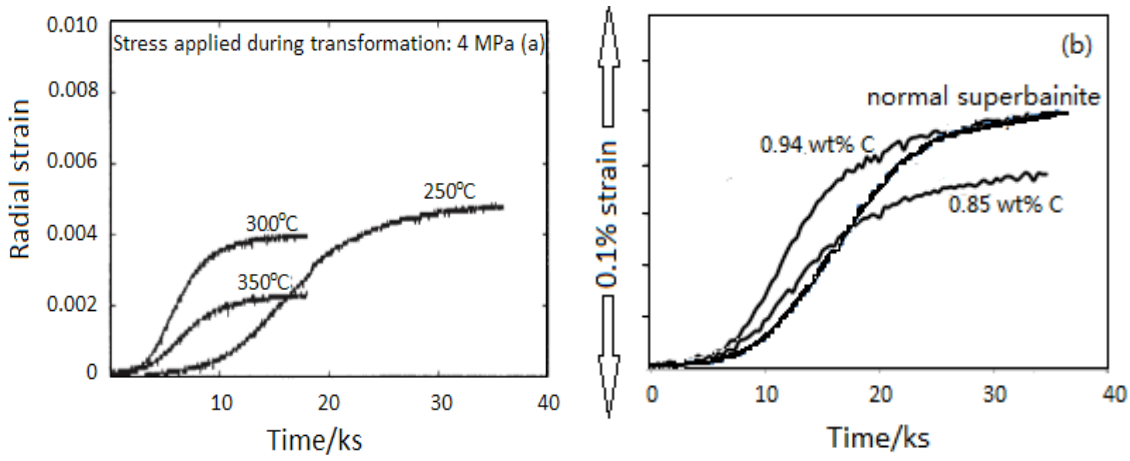

Figure 4.30: The change in radial strain during the transformation. (a) For a normal superbainite at various transformation temperatures [48]. (b) Comparison between different superbainite alloys at 250 °C.

4.5.2 Change of microstructures with transformation temperatures

Optical micrographs

Figs. 4.31-4.36 show a set of optical micrographs of 0.85 wt% C and 0.94 wt% C steels after isothermal transformation at 200 °C, 250 °C and 300 °C for 10 h. There are large amounts of carbide particles in both Fig. 4.31 and 4.32, but the bainitic structure is not clear. From Fig. 4.33, we can see the bainitic transformation has happened obviously at this temperature (250 °C), where Fig. 4.34 gives more carbide particles.

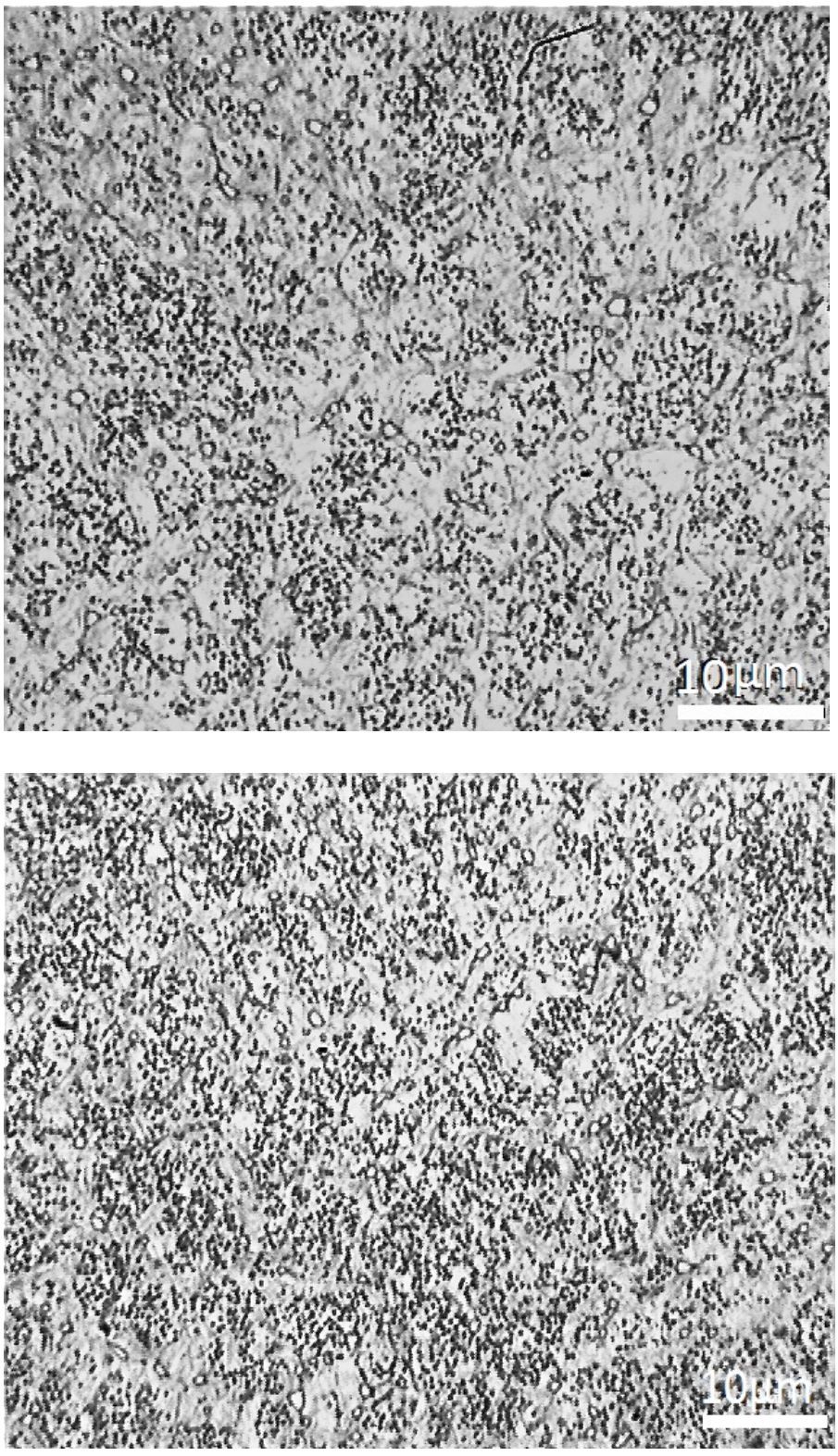

Figure 4.31: 0.85 wt% C, 200 °C, 10 h, quenched.

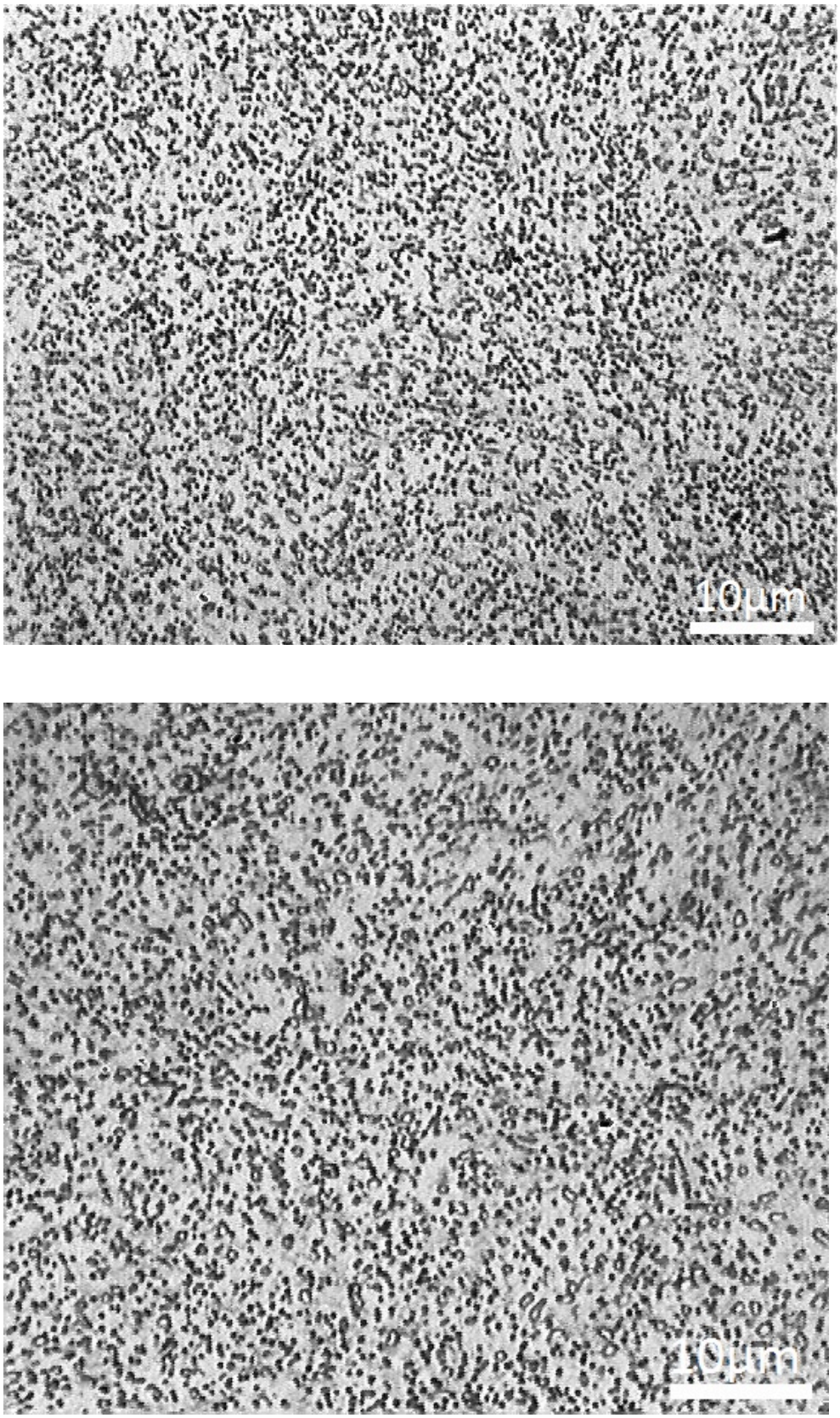

Figure 4.32: 0.94 wt% C, 200 °C, 10 h, quenched.

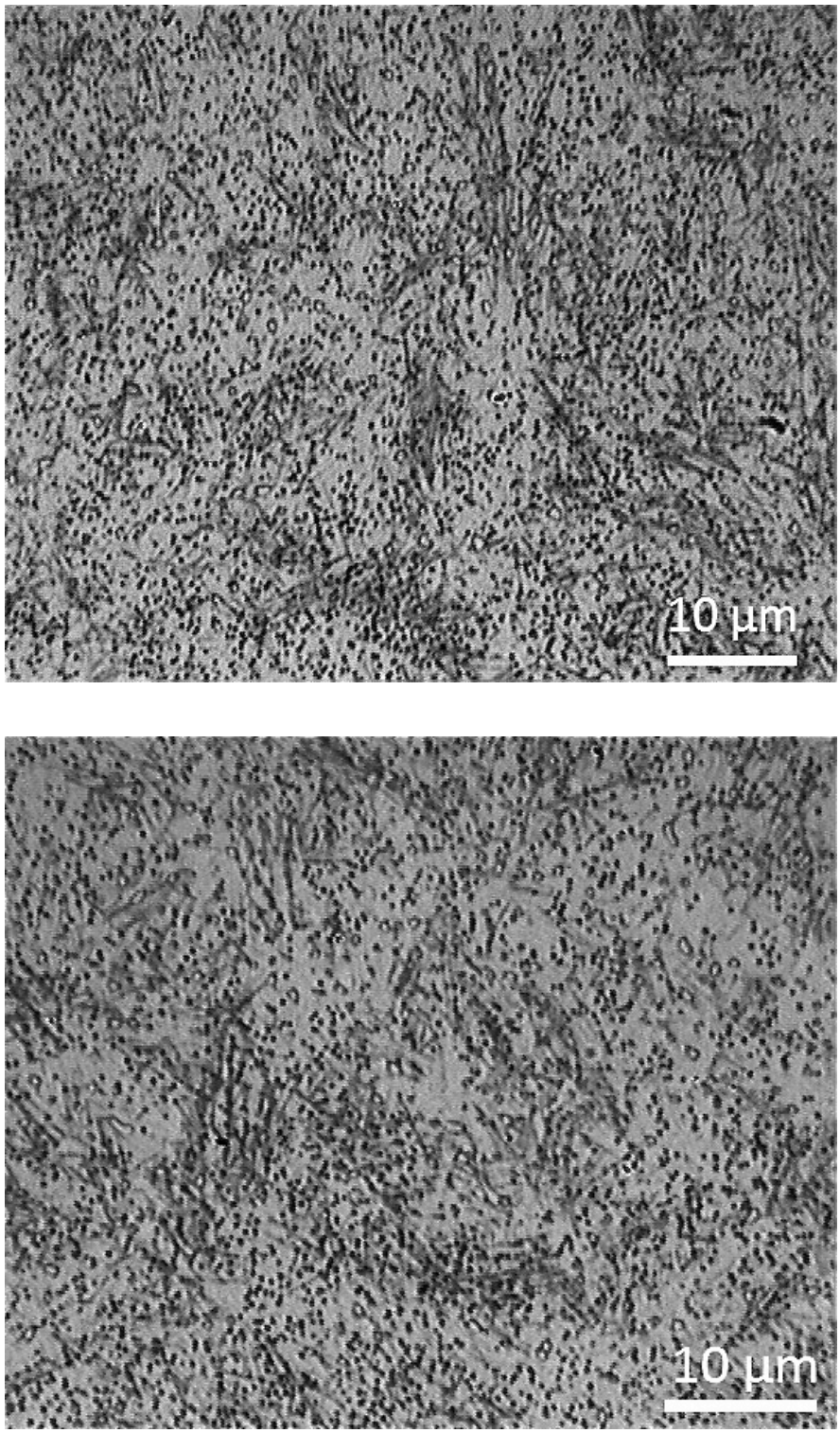

Figure 4.33: 0.85 wt% C, 250 °C, 10 h, quenched.

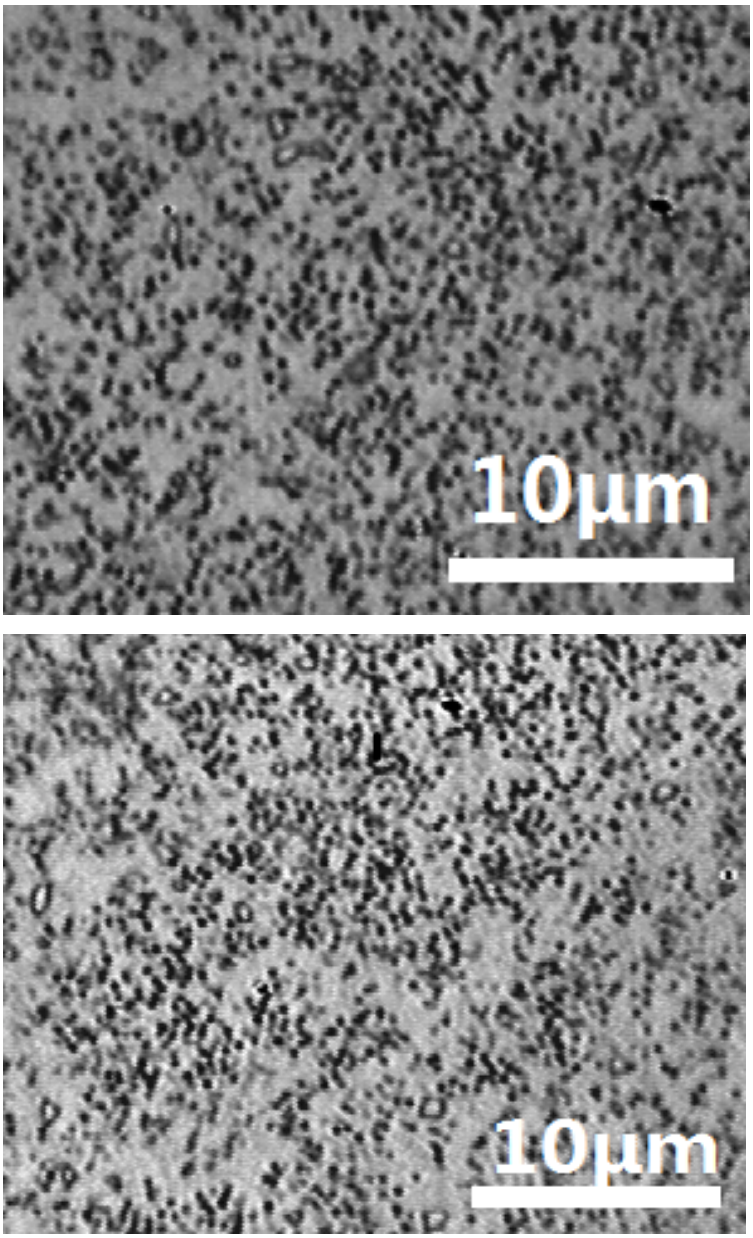

Figure 4.34: 0.94 wt% C, 250 °C, 10 h, quenched.

From Figs. 4.35-4.36, there are some carbide particles and bainite scattered in the matrix. The sizes of bainite produced for both samples after 10 h transformation at 300 °C are almost the same. The carbide particles of 0.94 wt% C steel are generally smaller than those of 0.85 wt% C steel.

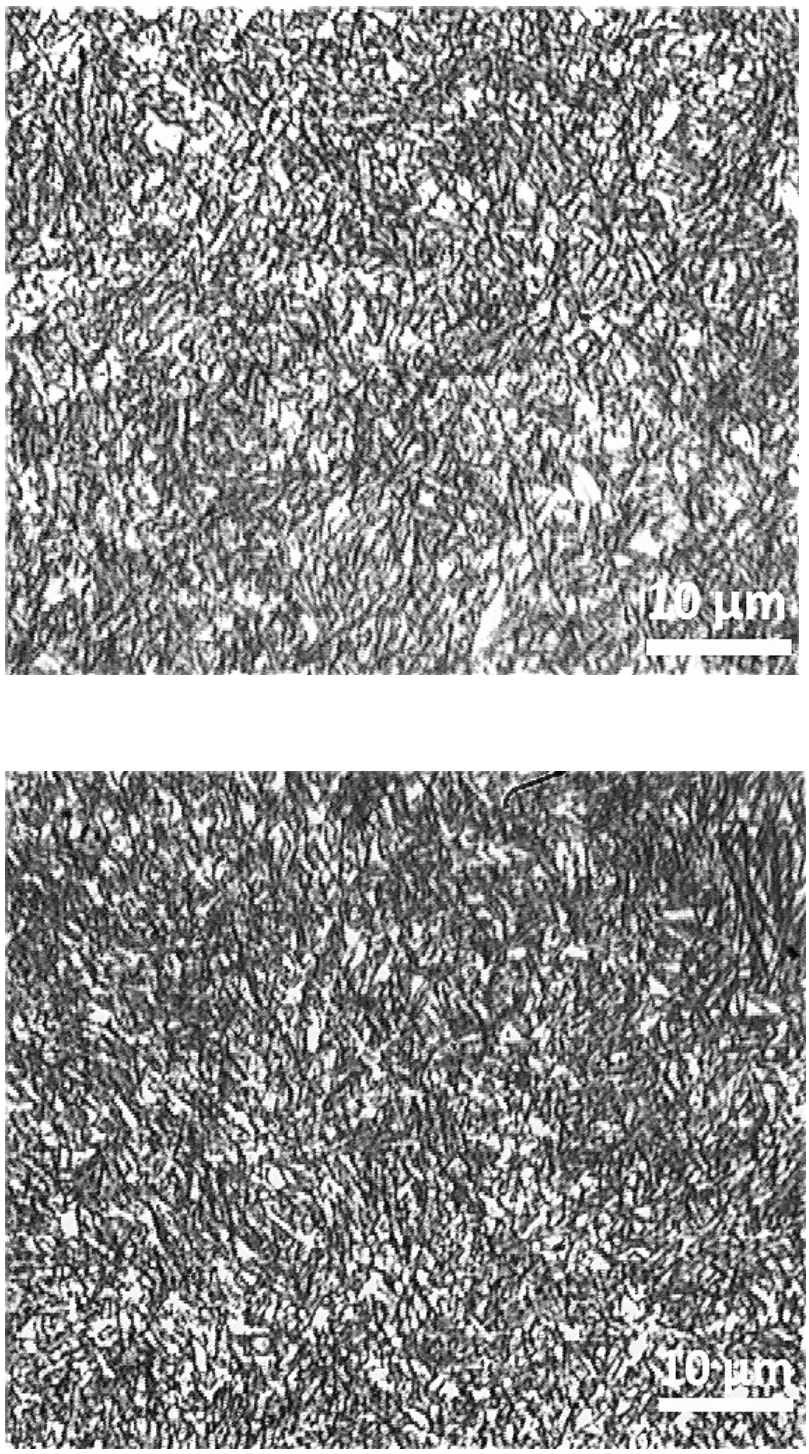

Figure 4.35: 0.85 wt% C, 300 °C, 10 h, quenched.

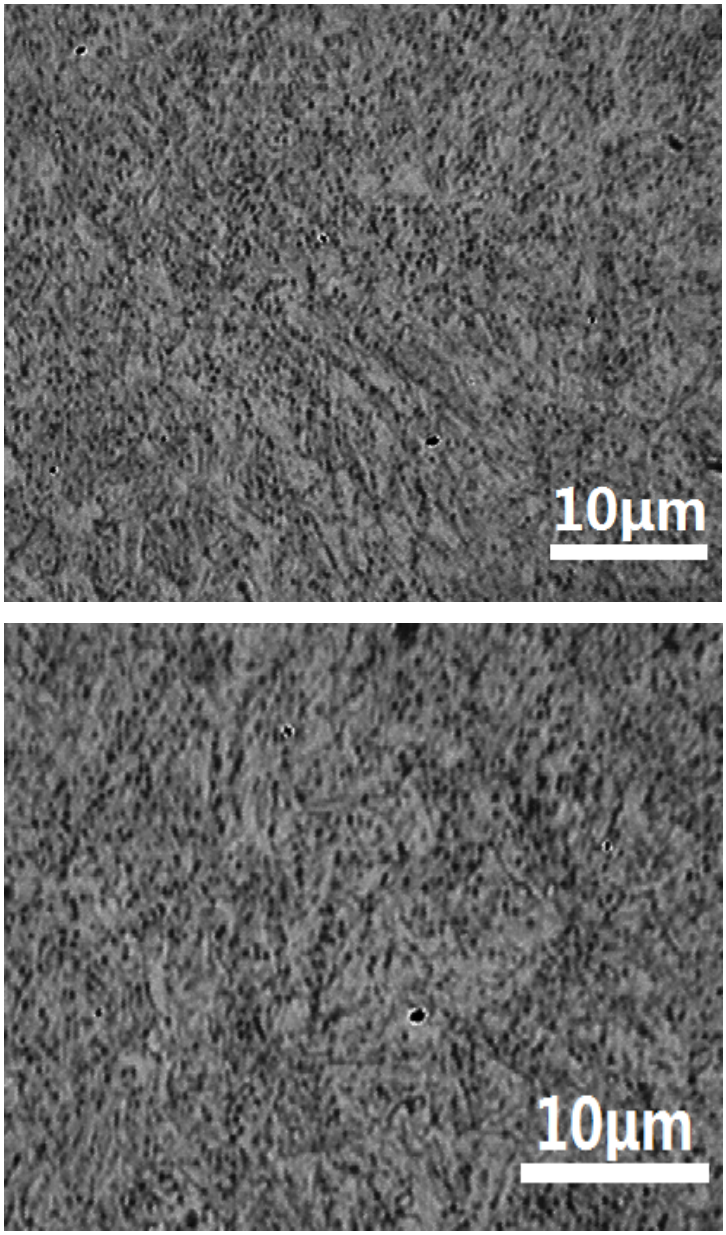

Figure 4.36: 0.94 wt% C, 300 °C, 10 h, quenched.

Scanning electron micrographs

In order to look at the microstructure more accurately, Figs. 4.37-4.42 give the SEM images of 0.85 wt% C and 0.94 wt% C steels after 10 h heat treatments at 200 °C, 250 °C and 300 °C.

Fig. 4.37 shows the spheroidised carbide particles with more uniform sizes, distributed in the matrix. Fig. 4.38 indicates the microstructure that is mainly consisting of spherical carbide particles with uneven sizes. Some long lamellae of carbides persist.

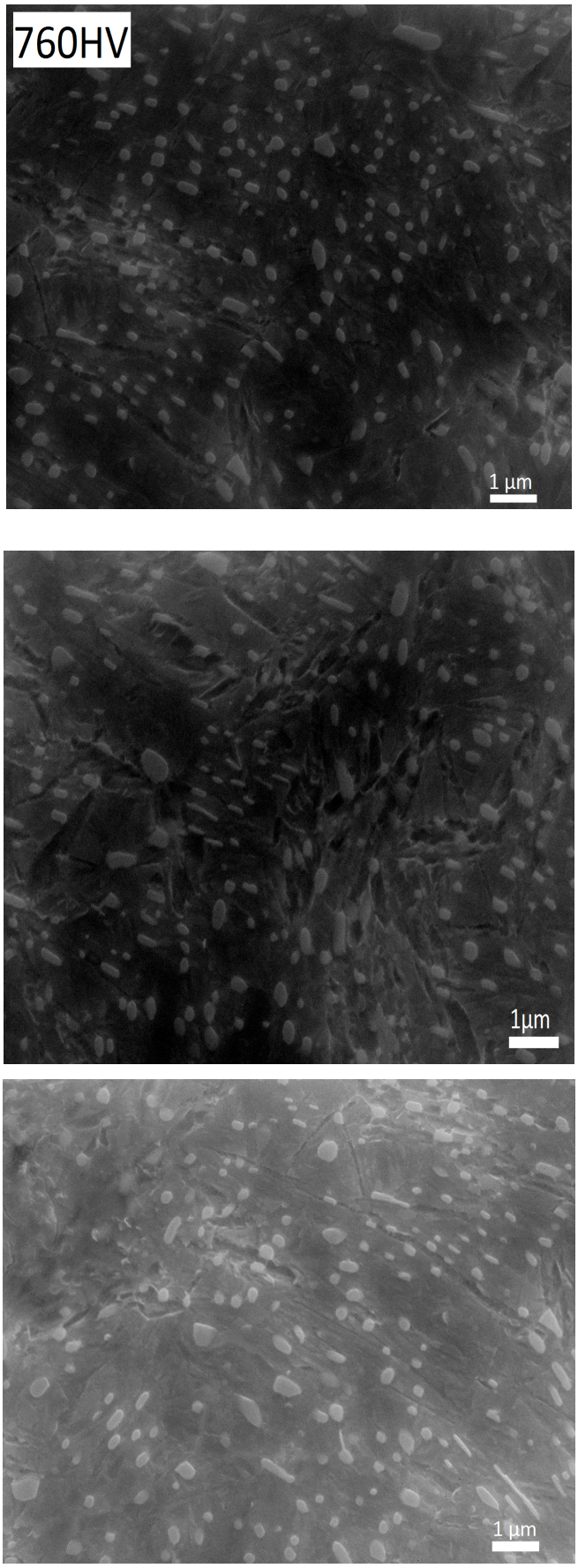

Figure 4.37: 0.85 wt% C, 200 °C, 10 h, quenched.

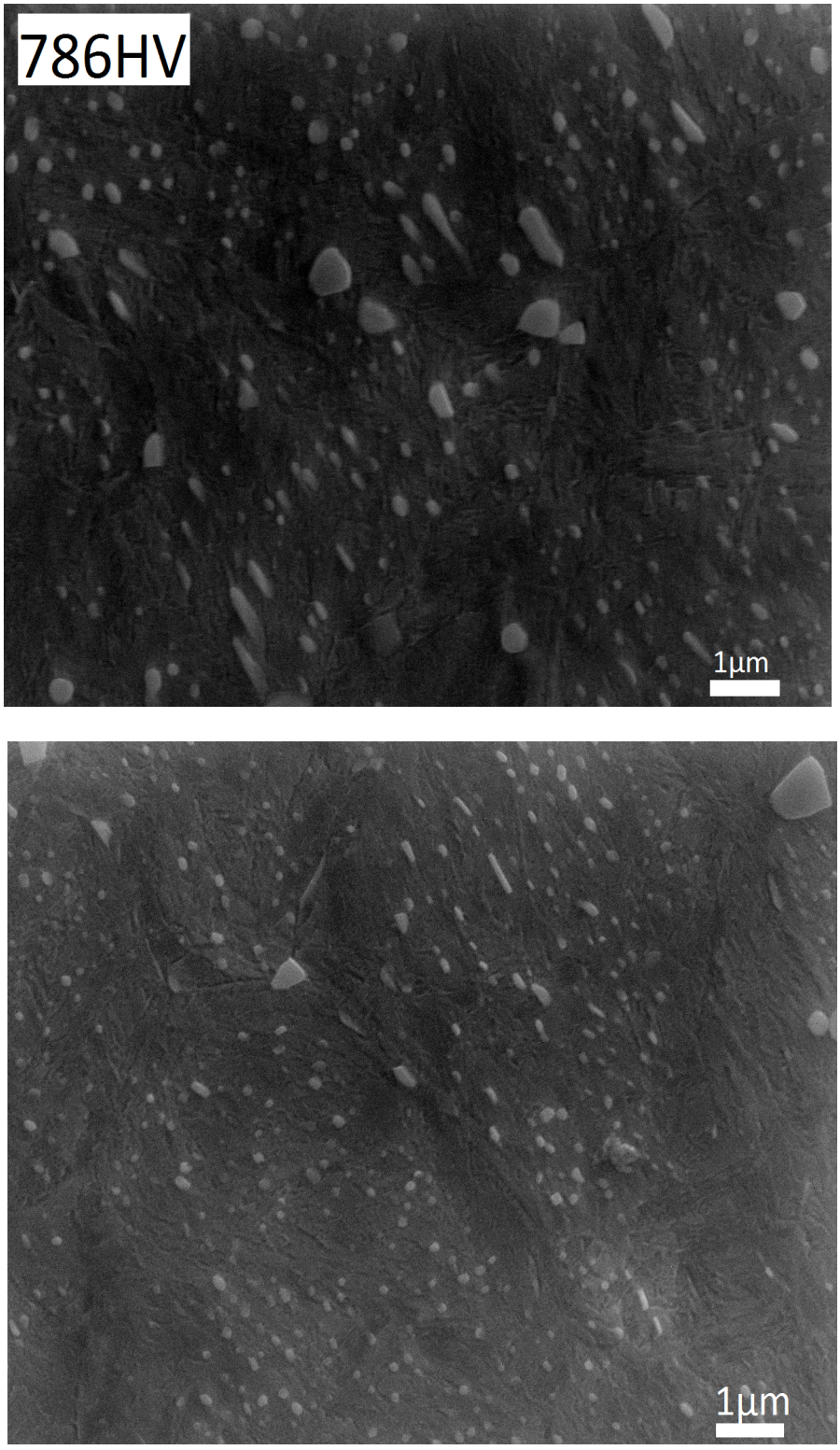

Figure 4.38: 0.94 wt% C, 200 °C, 10 h, quenched.

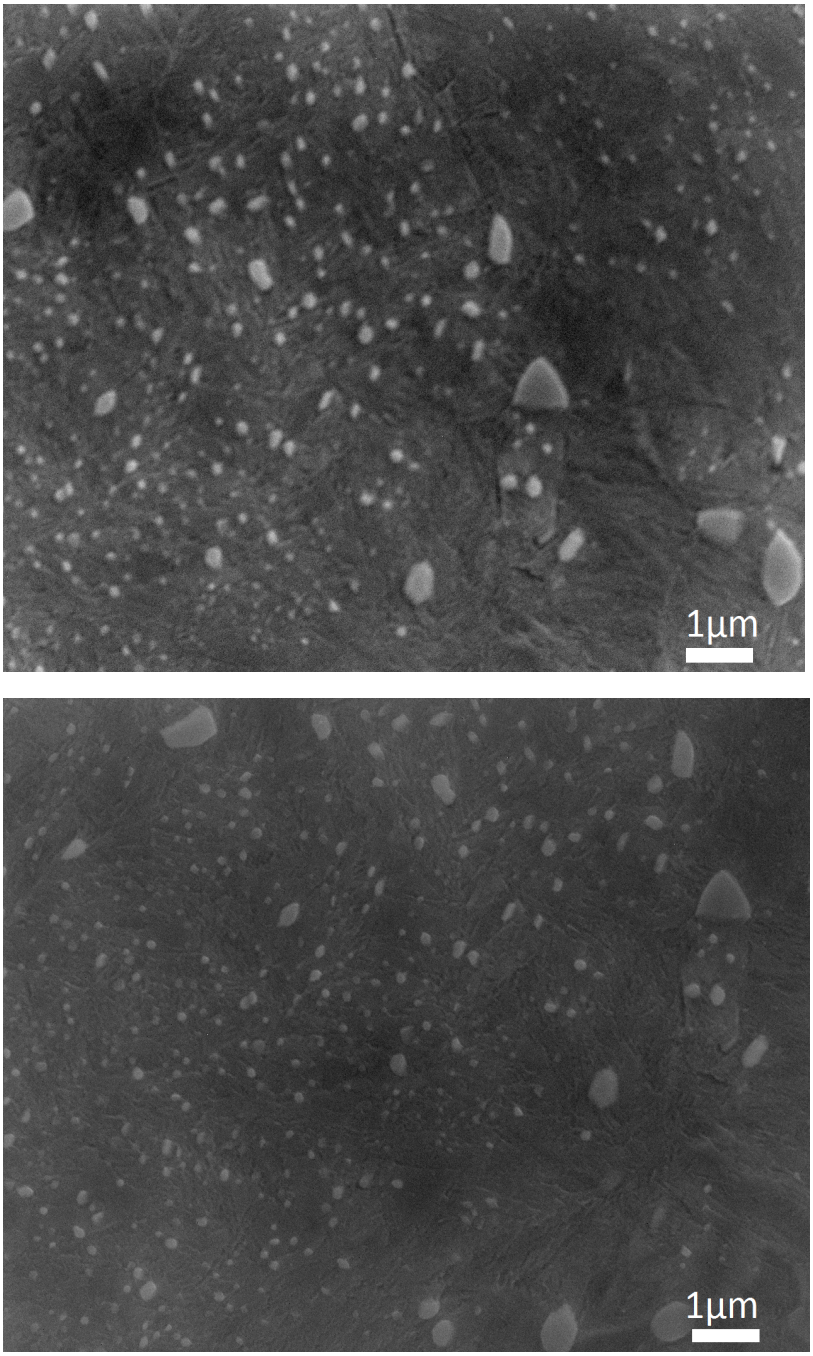

Figure 4.38: 0.94 wt% C, 200°C, 10 h, quenched.

Figs. 4.39-4.40 display the SEM results of samples quenching at 250 °C. It is clear that there are a large amount of proeutectoid cementite and some plate-like features in Fig. 4.39. In comparison with 0.85 wt% C steel, 0.94 wt% C steel with the same heat treatment (Fig. 4.40) also maintains a bainitic structure with similar sizes, but more undissolved carbides are found.

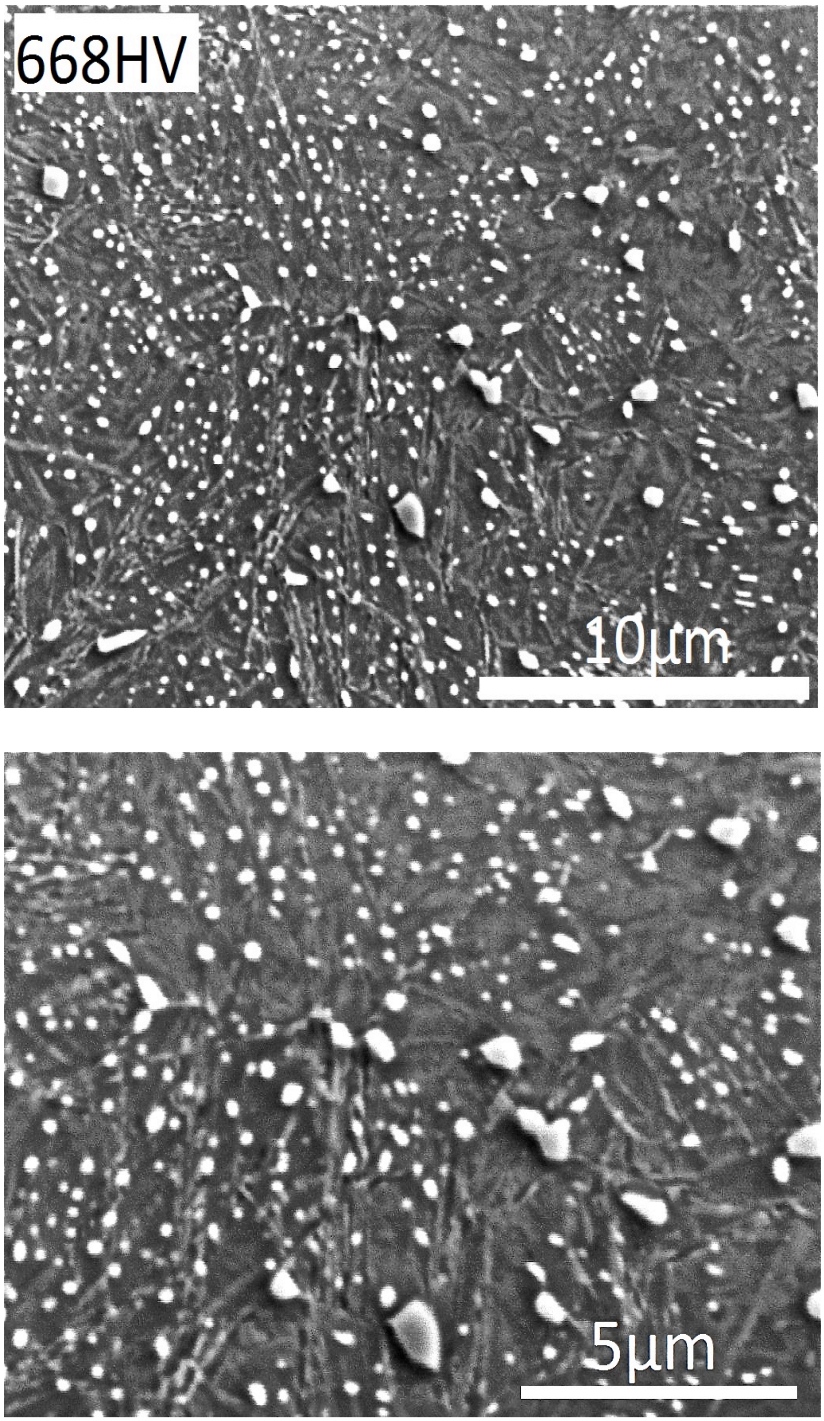

Figure 4.39: 0.85 wt% C, 250°C, 10 h, quenched.

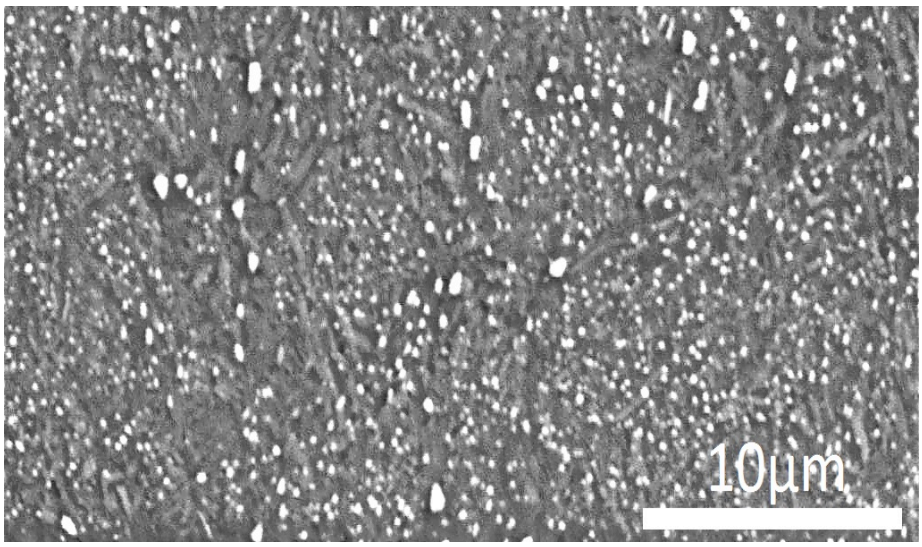

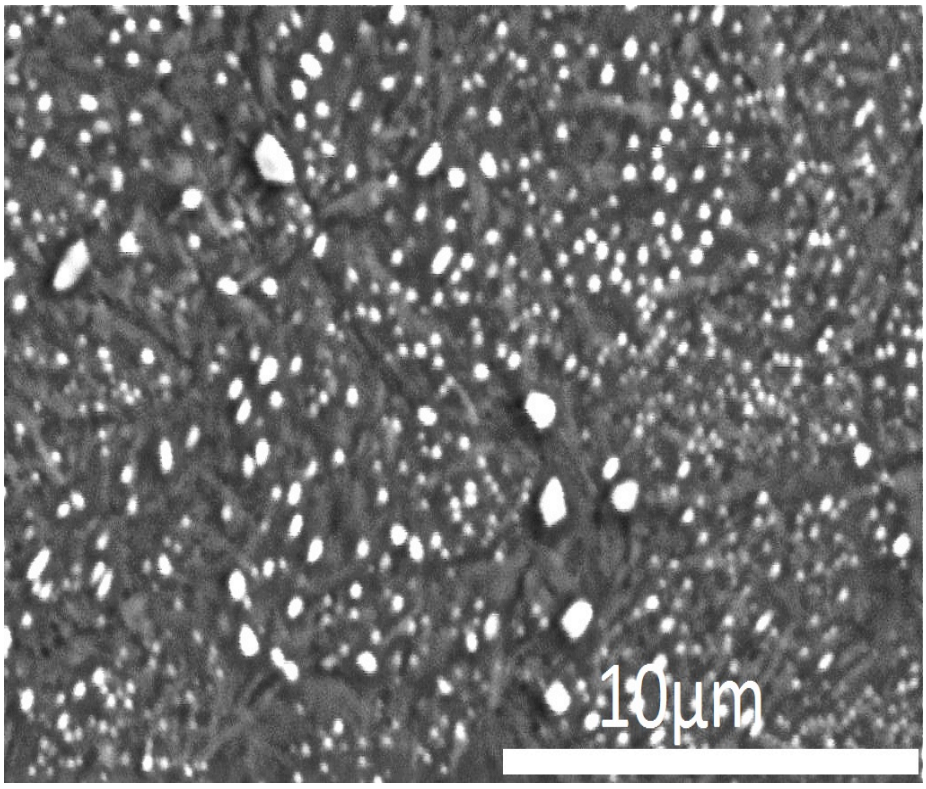

Figure 4.40: 0.94 wt% C, 250 °C, 10 h, quenched.

As can be seen from Figs. 4.41-4.42, when the isothermal transformation temperature increased to 300 °C, a structure of bainite with larger size of carbides was produced in both samples, which will lead to an unsatisfactory performance. This can be also noticed from the hardness result in Table 4.7, especially for the 0.94 wt% C alloy that has a much lower hardness of just above 500 HV.

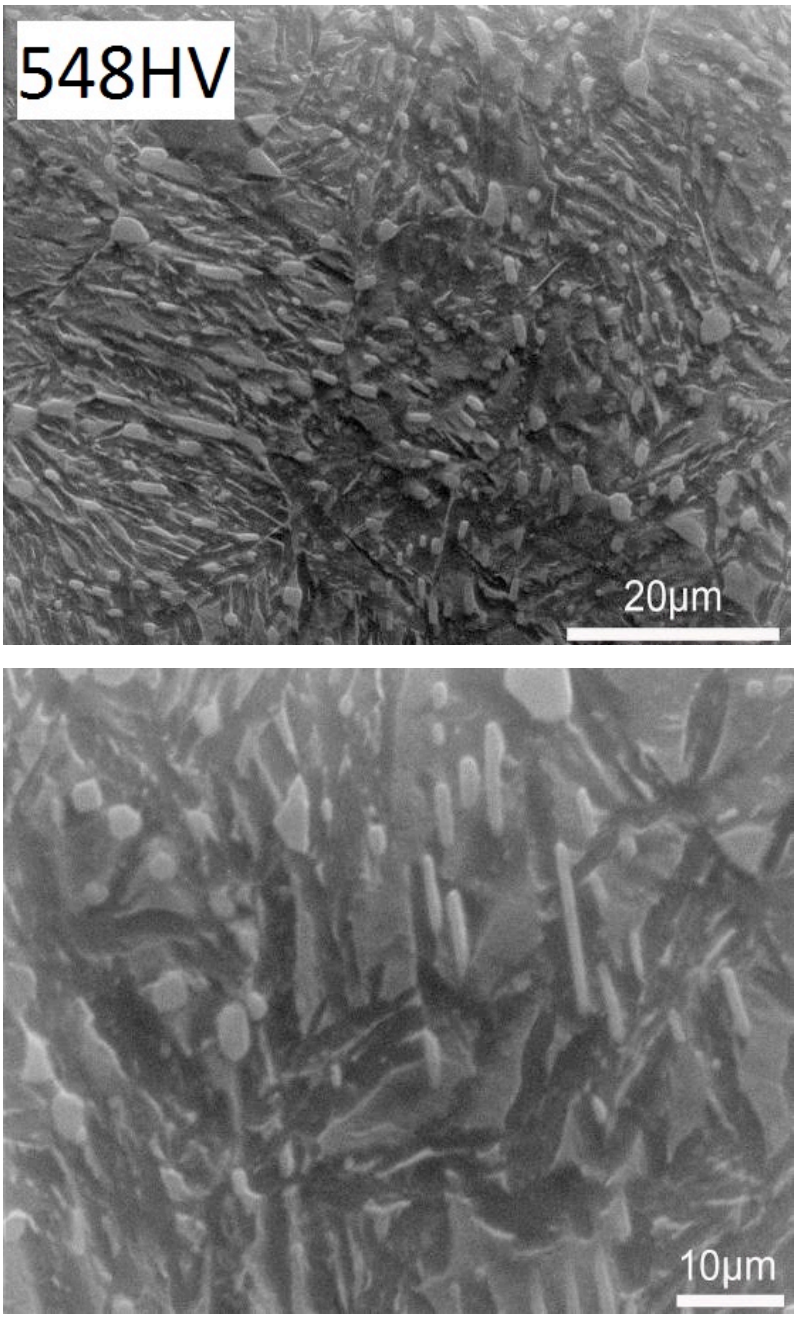

Figure 4.41: 0.85 wt% C, 300 °C, 10 h, quenched.

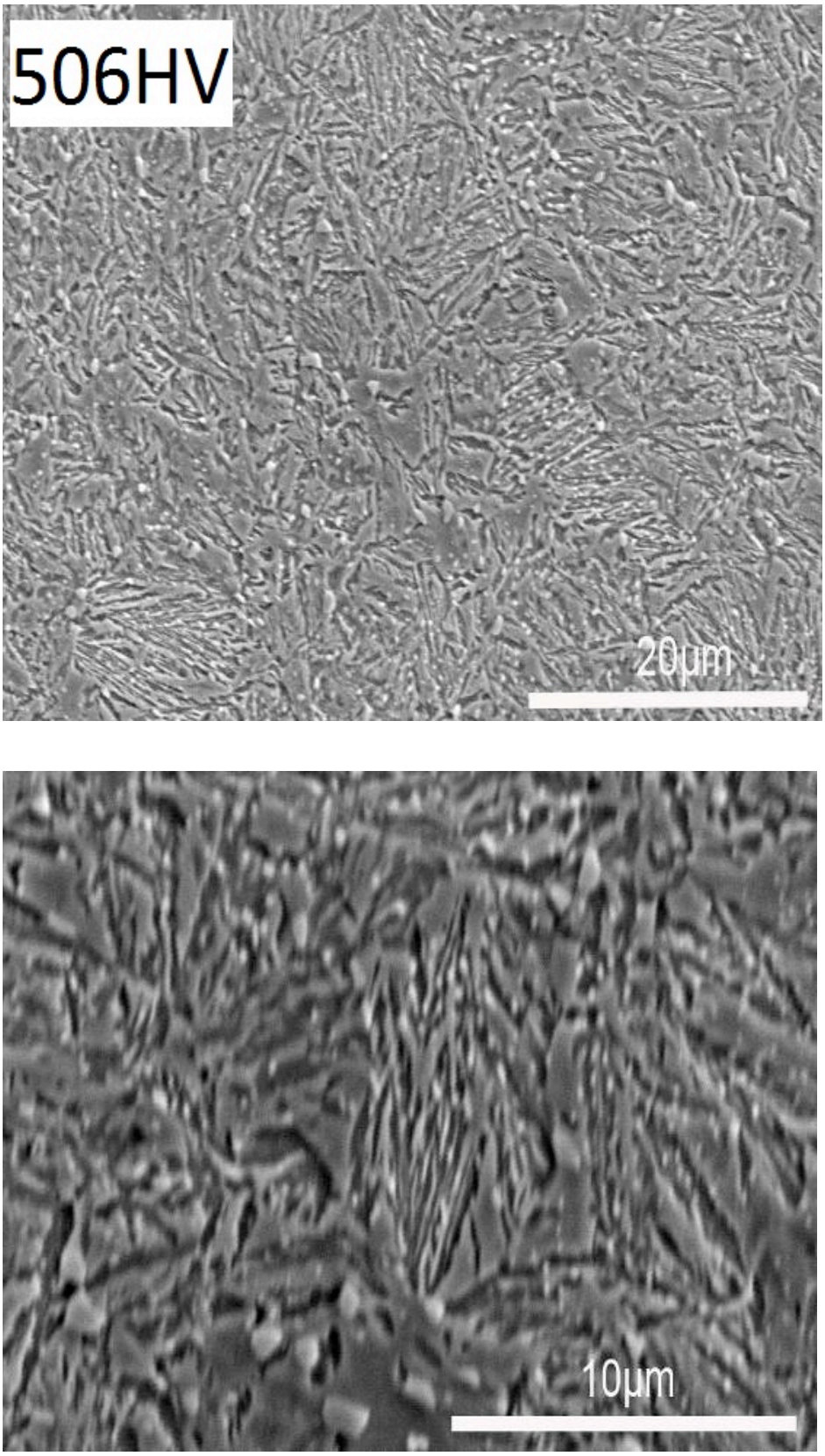

Figure 4.42: 0.94 wt% C, 300 °C, 10 h, quenched.

The hardness obtained after the different heat treatments are shown in Table 4.7. To compare the results from 10 h isothermal transformation, the hardness increases as the transformation temperature is reduced. This is because the thickness of the bainite plates deceases as the temperature is lowered. When the temperature rises up to 300 °C, the hardness of both samples drop significantly below 550 HV.

Table 4.7
The hardness results

Carbon content	Hardness (HV)			
(wt%)	200 °C, 10 days	200 °C, 10 h	250 °C, 10 h	300 °C, 10 h
0.85	657±9	760±19	668±18	548±11
0.94	649±5	786±21	771±21	506±28

Chapter 5
General Conclusions

The work presented in this thesis had the primary object of investigating a variety of spheriodisation processes and isothermal transformations for superbainitic steels. Two superbainitic steels with added carbon have been studied, in which the carbon contents in both steels produced were closed to that predicted by MTDATA software.

After much investigation of factors such as austenitisation temperature, time and cooling rate, spheroidisation of both steels was successfully achieved by retaining about 4 wt% of undissolved cementite particles. The optimal spheroidisation heat treatment condition was determined to be austenitising the steels at 840 °C for 1 h, cool to 750 °C at 25 °C h^{-1}, further cool to 690 °C at 10 °C h^{-1} followed by air cool from 680 °C to room temperature. The average carbide size and hardness value of the two steels after this heat treatment were about 1.4 μm and 250 HV, respectively. There was no significant difference in carbide size and hardness between the two steels after spheriodisation. However, simulations using quenching from different temperatures during the spheroidisation method reported above provided further observation on the distinction between two steels. It has been discovered that DET occurred faster for the 0.94 wt% C steel evident in the notable hardness drop at 740 °C. This may be useful on achieving a more rapid spheroidsation heat treatment in the future studies.

In addition, attempts were made therefore to select an optimal isothermal transformation temperature and time aimed at producing the bainite for both steels. Stimulations indicated a dilatational strain changes with increasing temperature for the two sample steels and the simulation results were used to determine the heat treatment. It has been concluded that the holding period of 10 h at 200 °C is inadequate for both steels to incur the bainitic transformation, but 10 days is sufficient. Isothermal transformation at 300 °C was found to be too high since a coarser bainite was generated. It seems that the combination of bainite and spheroidised cementite particles can be obtained for both steels under the following conditions:

austenitisation at 840 °C for 1 h followed by rapid cooling to 200 °C for 10 days or alternatively to 250 °C for 10 h. However, further analysis such as diffraction need to be done to prove the existence of the lower bainite. The average hardness value was 760 HV for the 0.85 wt% C steel and 786 HV for the 0.94 wt% C steel, respectively.

References

[1] H. K. D. H. Bhadeshia, "Steels for Bearing,"*Progress in Materials Science,* vol. 57, pp. 268-435, 2012.

[2] W. Li, Y. Wang, and X. Z. Yang, "Frictional Hardening and Softening of Steel 52100 during Dry Slidng," *Tribology letters,* vol. 18, pp. 353-357, 2005.

[3] N. Capatina and M. Teodorescu, "Research on the Machinability of Bearing Steels," pp. 39-44, 1979.

[4] V. Lyasheimko, V. Klimova, Y. Sokol, and B. Diomidov, "Optimization of Annealing Practice for Rapidly Cooled ShKhl 5 steel," *Steel in the USSR,* vol. 16, pp. 289-291, 1986.

[5] W. Hewitt, "The Spheroidise Annealing of High Carbon Steel and Its Effect on Subsequent Heat Treatment," pp. 56-62, 1982.

[6] D. Verhoeven, "The Role of Divorced Eutectoid Transformation in the Spheroidization of 52100 Steel," 2000.

[7] N. Gupta and S. Sen, "Spheroidisation Treatment for Steels," *Defence Science Journal,* vol. 56, pp. 665-676, 2006.

[8] T. R. McNelley, M. R. Edwards, A. Doig, D. H. Boone, and C. W. Schultz, "The effect of prior heat treatments on the structure and properties of warm-rolled AlSl 52100 steel," *Metallurgical & Materials Transactions A,* vol. 14, pp. 1427-1433, 1983.

[9] L. Heron, "Spheroidise Annealing of Steel Tube for Bearings," *Metallurgica,* vol. 1, pp. 53-58, 1969.

[10] J. V. Lyons and M. J. Hudson, "Machining properties of high- carbon chromium bearing steels," Iron and Steel Institute, London, U.K1967.

[11] K. Ryttberg, "The Effect of Cold Ring Rolling on the Evolution of Microstructure and Texture in 100Cr6 Steel," 2010.

[12] I. E. Dolzhenikov, A. F. Grinev, I. N. Lotsmanova, I. I. Andrianova, D. A. Shevchak, and G. I. Mirtoshkina, "Influence of Spheroidizing Treatment on Structure and Properties of Bearing Tubes, Rings, and Roller Bearings," *Stal,* vol. 6, pp. 552-554, 1978.

[13] J. O'Brien and W. Hosford, "Spheroidization of Medium-Carbon Steels,"*Journal of Materials Engineering and Performance,* vol. 6, pp. 69-72, 1997.

[14] H. K. D. H. Bhadeshia. (2012. Last accessed: 26 May 2011.). *Spheroidisation of Pearlite*. *Available: http://www.msm.cam.ac.uk/phase-trans/2006/spheroidisation/spheroidisation.html*.

[15] K. Z. Shepelyakovskii, A. G. Spektor, A. N. Kuznetsov, V. T. Gubenko, and V. S. Zdanovskii, "Rapid Spheroidizing Annealing of Roller Bearings with Induction Heating," *Metal Science and Heat Treatment,* vol. 18, pp. 78-80, 1976.

[16] N. V. Luzginova, L. Zhao, and J. Sietsma, "Metall,"*Mater. Trans. A,* vol. 39A, p. 513, 2008.

[17] J. H. Hong and Y. H. Lee, "Study for the behaviors of carbide on mechanical properties of bearing steel" vol. 17, pp. 19-27, 1979.

[18] W. Hagel, G. Pound, and R. Mehl, "Calorimetric Study of the Austenite: Pearlite Transformation," *Acta Metallurgica,* vol. 4, pp. 37-48, 1956.

[19] J. M. Beswick, "The Effect of Chromium in High Carbon Bearing Steels," *Metallurgical & Materials Transactions A,* vol. 18, pp. 1897-1906, 1987.

[20] J. M. Beswick, "The Effects of Alloying Elements in High Carbon Bearing Steels," *Ball Bearing Journal,* vol. 231, pp. 2-11, 1988.

[21] K. H. Kim, J. S. Lee, and D. L. Lee, "Effect of Silicon on the Spheroidization of Cemen-tite in Hypereutectoid High Carbon Chromium Bearing Steels," *Metals and Materials International,* vol. 16, pp. 871-876, 2010.

[22] E. Brown and G. Krauss, "Retained Carbide Distribution in Intercritically Austenitized 52100 Steel " *Metallurgical Transsactions,* vol. 17 (A), pp. 31-36, 1986.

[23] S. L. Gertsman, "Research and Special Projects Report for 1965," Canadian Department of Mines and Technical Surveys, Otawa, Canada1966.

[24] T. Oyama, O. Sherby, J. Wadsworth, and S. Waleer, "Application of the Divorced Eutectoid Transformation to Tee Development of Fine-Grained, Spheroidized Structures in Ultrahigh Carbon Steels," *Metallurgica,* vol. 18, pp. 799-804, 1984.

[25] K. Honda and S. Saito, "On the Formation of Spheroidal Cementite," *Journal of the Iron and Steel Institute,* vol. 102, pp. 261-267, 1920.

[26] J. Verhoeven and E. Gibson, "The Divorced Eutectoid Transformation in Steel," *Metallurgical and Materials Transactions A,* vol. 29 (A), pp. 1181-1189, 1998.

[27] J. H. Whitley, "The Formation of Globular Pearlite," *Journal of the Iron and Steel Institute,* vol. 105, pp. 339-357, 1922.

[28] R. F. Mehl and W. C. Hagel, "The Austenite: Pearlite Reaction," *Progress in Metal Physics,* vol. 6, pp. 74-134, 1956.

[29] N. V. Luzginova, L. Zhao, and J. Sietsma, "Bainite Formation Kinetics in High Carbon Alloyed Steel " *Materials Science and Engineering: A,* vol. 481-482, pp. 766-769, 2008.

[30] G. E. Hollox, R. A. Hobbs, and J. M. Hampshire, "Lower Bainite Bearings for Adverse Environments," *Wear,* vol. 68, pp. 229-240, 1981.

[31] H. K. D. H. Bhadeshia, *Bainite in Steels*. Cambridge: The university press, 2001.

[32] H. Lan, X. Liu, and L. Du, "Ultra-Hard Bainitic Steels Processed through Low Temperature Heat Treatment," *Advanced Materials Research* vol. 156-157, pp. 1708-1712, 2010.

[33] H. Bhadeshia and D. Edmonds, "The Mechanism of Bainite Formation in Steels," *Acta Metallurgica,* vol. 28, pp. 1265-1273, 1980.

[34] H. K. D. H. Bhadeshia and M. T. D. V. Edmonds, A, 10, 895 (1979), "The Bainite Transformation in a Silicon Steel," *Metallurgical and Materials Transactions A* vol. 10 (7), pp. 895-907, 1979.

[35] H. K. D. H. Bhadeshia and R. W. K. Honeycombe, *Steels: Microstructure and Properties*, Third ed., 2006.

[36] C. Garcia-mateo, F. G. Caballero, and H. K. D. H. Bhadeshia, *Development of Hard Bainite*, 2003.

[37] H. K. D. H. Bhadeshia, *Bulk Nanocrystalline Steel*, 2005.

[38] C. Garcia-mateo, F. G. Caballero, and H. K. D. H. Bhadeshia, "Acceleration of Low Temperature Bainite," 2003.

[39] S. Curtze, M. Kundu, and S.Datta, "Dynamic Properties of New Gerneration High-strength Steels for Armoring Applications," 2008.

[40] P. M. Brown and D. P.Baxter, "Hyper-strength Bainitic Steels."

[41] H. S. Hasan, M. J. Peet and H. K. D. H. Bhadeshia, "Severe Tempering of Bainite Generated at Low Transformation Temperatures," *International Journal of Materials Research (e-first),* May 2012.

[42] C. A. Stickels, "Carbide Refining Heat Treatment for 52100 Bearing Steels," *Metall trans,* vol. 5, pp. 865-874, 1974.

[43] *MTDATA Handbook: http://www.msm.cam.ac.uk/phase-trans/mtdata/*.

[44] H. Yang and H. K. D. H. Bhadeshina, "Uncertainties in Dilatometric Determination of Martensite Start Temperature," *Materials Science and Technology,* vol. 23, pp. 556-560, 2007.

[45] P. Payson, W. L. Hodapp, and J. Leeder, "Trans," *ASM,* vol. 28, pp. 306-326, 1940.

[46] T. Oyama, O. D. Sherby, J. Wadsworth, and B. Walser, "ScriptaMetall," vol. 18, pp. 799-804, 1984.

[47] J. Wadsworth and O. D. Sherby, "Influence of Chromium on Superplasticity in Ultra-high Carbon Steels," *Journal of Materials Science,* vol. 13, pp. 2645-2649, 1978.

[48] A. Ray, S. Ray, and S. R. Mediratta, "Effect of Carbides on The Austenite Grain Growth Characteristics in 1Cr-1C and 6Cr-1Mo-1C Steels," *Journal of Material Science,* vol. 25, pp. 5070-5076, 1990.

[49] K. Hase, C. Garcia-Mateo, and H. K. D. H. Bhadeshia, "Bainite Formation Influenced by Large Stress," 2004.

[50] H. K. D. H. Bhadeshia, S. A. David, J. M. Vitek, and R. W. Reed, *Mater. Sci. Technol.,* vol. 7, pp. 686-698, 1991.

[51] A. Matsuzaki, H. K. D. H. Bhadeshia, and H. Harada, "Acta Metall," *Mater.,* vol. 42, pp. 1081-1090, 1994.